Minnesota Department of Transportation

RESEARCH SERVICES & LIBRARY

Office of Transportation System Management

Field Implementation, Testing, and Refinement of Density Based Coordinated Ramp Control Strategy

John Hourdos, Principal Investigator
Minnesota Traffic Observatory
Department of Civil, Environmental, and Geo- Engineering
University of Minnesota

June 2015

Research Project
Final Report 2015-37

To request this document in an alternative format call 651-366-4718 or 1-800-657-3774 (Greater Minnesota) or email your request to ADArequest.dot@state.mn.us. Please request at least one week in advance.

Technical Report Documentation Page

1. Report No. MN/RC 2015-37	2.	3. Recipients Accession No.	
4. Title and Subtitle Field Implementation, Testing, and Refinement of Density Based Coordinated Ramp Control Strategy		5. Report Date June 2015 6.	
7. Author(s) John Hourdos, Nikolas Geroliminis, Stephen Zitzow, and Ypatia Stefania Limniati		8. Performing Organization Report No.	
9. Performing Organization Name and Address Minnesota Traffic Observatory Department of Civil, Environmental, and Geo- Engineering University of Minnesota 500 Pillsbury Drive SE Minneapolis, MN 55455-0220		10. Project/Task/Work Unit No. CTS # 2012059 11. Contract (C) or Grant (G) No. (c) 99008 (wo) 57	
12. Sponsoring Organization Name and Address Minnesota Department of Transportation Research Services & Library 395 John Ireland Boulevard, MS 330 St. Paul, Minnesota 55155-1899		13. Type of Report and Period Covered Final Report 14. Sponsoring Agency Code	
15. Supplementary Notes http://www.lrrb.org/pdf/201537.pdf			

16. Abstract (Limit: 250 words)

In the Twin Cities metropolitan area, freeway ramp metering goes back as early as 1969, when the Minnesota Department of Transportation (MnDOT) first tested ramp metering in an I-35E pilot project. To date, the Twin Cities ramp metering system has grown to include more than 433 ramp meters. Research on better, improved ramp control strategies has continued over the years and MnDOT has implemented minor and major changes in the control logic. Two independent studies both aimed at developing the next generation in ramp metering by focusing on density. Based on these efforts, two new algorithms were developed: the UMN Density and the UMD KAdaptive, named based on the campus at which they were developed. The goal of this project was to implement both algorithms and test them under real conditions. Priorities and technical problems prevented the evaluation of the UMN algorithms, so this report focuses on the evaluation of the UMD KAdaptive algorithm on two freeway corridors in the Twin Cities, MN. The first site, a section of TH-100 northbound between 50th Street and I-394, was selected to compare the then current logic, the Stratified Zone algorithm, with the new one. During the course of this project, the UMD algorithm eventually replaced the Stratified Zone algorithm and was implemented in the entire system. This full deployment also included corridors that were not controlled before. The second evaluation site on eastbound TH-212 was a site that allowed for a with/without control evaluation of the UMD algorithm. This report describes the experiments conducted at both sites and includes a comprehensive review of the state of ramp metering strategies around the world to date.

17. Document Analysis/Descriptors Ramp metering, Freeway management systems, Interrupted flow, Traffic density		18. Availability Statement No restrictions. Document available from: National Technical Information Services, Alexandria, Virginia 22312	
19. Security Class (this report) Unclassified	20. Security Class (this page) Unclassified	21. No. of Pages 142	22. Price

Field Implementation, Testing, and Refinement of Density Based Coordinated Ramp Control Strategy

Final Report

Prepared by:

John Hourdos
Stephen Zitzow
Minnesota Traffic Observatory
Department of Civil Environmental and Geo- Engineering
University of Minnesota

Nikolas Geroliminis
Ypatia Stefania Limniati
Ecole Polytechnique Federale de Lausanne (EPFL)

June 2015

Published by:

Minnesota Department of Transportation
Research Services & Library
395 John Ireland Boulevard, MS 330
St. Paul, Minnesota 55155-1899

Acknowledgments

We would like to thank the Minnesota Department of Transportation for supporting this project. We would like to acknowledge the help, support, and cooperation of Brian Kary and Jesse Larson at the RTMC. We also would like to acknowledge the help received from the staff of the Minnesota Traffic Observatory in collecting the data used in this research, and the undergraduate students who helped extract the information from the video recordings.

Table of Contents

List of Figures

List of Tables

EXECUTIVE SUMMARY

In the Twin Cities metropolitan area, freeway ramp metering goes back as early as 1969, when the Minnesota Department of Transportation (MnDOT) first tested ramp metering in an I-35E pilot project. To date, the Twin Cities ramp metering system has grown to include more than 433 ramp meters. Some operate only in the morning peak (5:30 a.m.–9:00 a.m.), some only during the afternoon peak (2:00 p.m.–6:30 p.m.), and others during both peaks. The ramp metering strategy employed by MnDOT has evolved over the years with some notable changes. Prior to year 2000, the deployed control strategy—the ZONE Metering strategy (Lau, 1996)—focused on maximizing freeway capacity utilization without handling ramp queue spillbacks and controlling ramp waiting times. By 2003, MnDOT had developed a new strategy aiming to strike a balance between freeway efficiency and reduced ramp delays. This new strategy, termed Stratified Zone Metering (SZM), took into account not only freeway conditions but also real-time ramp demand and queue size information (Xin et al.,2004).

Research on better, improved ramp control strategies has continued. More algorithms were implemented by other DOTs in the U.S. and abroad and a similar increase took place on the number of new algorithms proposed by researchers. A review of the most well-known cases is included in this report. While the aforementioned MnDOT control strategies primarily work with volume/capacity information, a different family of algorithms utilizes mainline density as the control variable. Specifically, two independent studies were performed in Minnesota, both aimed at developing the next generation in ramp metering by focusing on density. First, the "Development of the Next Generation Stratified Ramp Metering Algorithm Based on Freeway Density" project was performed by Geroliminis et al. (2011) at the U of M Twin Cities. The second, "Development of Freeway Operational Strategies with IRIS-in-Loop Simulation," was performed at the U of M- Duluth by Kwon et al. (2012). In both projects, the proposed density-based algorithms—termed the UMN Density and UMD KAdaptive algorithms—were tested through simulation and found superior to the SZM algorithm. Based on these preliminary results, MnDOT decided to test and evaluate the two algorithms in the field.

The project presented in this report was performed by the Minnesota Traffic Observatory (MTO), which was called to assist in the deployment of the two density-based ramp control strategies and to design and execute a field test involving all three ramp metering strategies: Stratified Zone Metering, serving as base conditions, and the two new density-based algorithms. A section of TH-100 northbound between 50th Street and I-394 was selected as the first study site. During the course of this project, multiple problems, operational issues, and unfortunate timing altered the original project goals and priorities. Although great effort was spent to integrate the UMN algorithm with the IRIS traffic operations system and deploy it in the field, an analysis of its performance based on the collected data was not completed because it was later discovered that the geometry of TH-100 did not allow for proper operation of the control algorithm. Although all three algorithms were affected by the peculiar geometry and detector layout of this section of TH-100, the UMN algorithm was the one most affected. Unfortunately, when this issue was discovered it was too late to switch test sites, and it was decided that the TH-

100 evaluation would only include the UMD algorithm. In addition, separately from this project MnDOT also run tests of the UMN algorithms on sections of Hwy-77 and I-35W with also poor results.

Later, during 2013 and 2014, the UMD algorithm underwent adjustments and was implemented on most of the ramp metering system. One specific location involves a recently reconstructed section of TH-212 in the southwest corner of the metro area. TH-212 was not controlled in the past and started being controlled by the UMD KAdaptive algorithm in the summer of 2014. MnDOT modified the scope of this project to include a before–after evaluation of the ramp metering system on TH-212.

Two types of analysis were performed for the evaluation of the new density ramp metering on TH-100: an analysis based on travel time data and an analysis based on loop detector data. Both methodologies compared traffic measurements between pairs of days with similar traffic and environmental conditions. The manually collected travel times show that during the PM period under the SZM control a shorter congested period developed in terms of time compared to the PM period under the UMD algorithm. Regardless, the congestion under the SZM seems to be stable with no evidence of recovery while the congestion under the UMD algorithm shows evidence of recovery, supporting the assumption that the control managed to recover from the heavy congestion, albeit briefly. Focusing on more detail, it can be noted that the congestion under the UMD algorithm seems to be more stable while the congestion under the SZM has great fluctuations for the entire length of the site, indicating the presence of shockwaves. This can indicate that the UMD algorithm, although handling more demand, was able to meter steadily while the SZM was closer to the tipping point and got trapped in a series of restrict and dump cycles. Both algorithms show greater instability closer to the bottleneck with the UMD algorithm keeping conditions in the mainline more fluid upstream compared to the SZM. The UMD algorithm seems to handle the large demand ramp of TH-7 better, and conditions immediately upstream of it are less congested. One other observation is that the UMD algorithm shows some sharp spikes of very large travel time, which could represent short-lived heavy congestion conditions from which the control is able to recover.

The loop detector data analysis on TH-100 show that the UMD KAdaptive metering strategy performs better than the SZM when conditions on TH-100 are not extremely congested. The UMD algorithm allows on average more vehicles to flow into the mainline and keeps the on-ramp occupancy relatively low. In the mainline, the flows are also higher with the UMD algorithm and in 3 out of 5 day-pairs investigated the speeds are also higher. In general, for the same occupancy, the flows are less when the SZM algorithm is applied. The main reason is that the UMD algorithm is more protective in the morning and queue detector occupancies are lower. Thus, the queue violation is not activated as often and the ramp metering is active (and successful) for longer time periods.

In the before–after analysis of the UMD KAdaptive algorithm on TH-212, we see that in terms of total travel time there are small gains from ramp metering. Focusing on the delays, which represent the gains to the traveling public from avoiding congestion, we see that an approximate 12% reduction in delay and a 3% increase in VMT is observed when considering only the

metered part of TH-212. These gains are reduced when the entire corridor is considered because the metering seems to spread lower speeds farther upstream but no severe congestion. When the ramp delays are included, we see an overall increase in delay with ramp metering indicating that with the present strategy (only four meters active), the gains on the mainline are not big enough to offset the delays accumulated in the ramps.

1 INTRODUCTION

Continuous urban sprawl and reliance on automobiles as a primary mode of transportation has led to a national increase in traffic congestion; from 1980 to 2010, there was a 77% increase in vehicle miles traveled nationally, compared to only a 6% increase in road mileage (Office of Highway Policy Information, 2013). This issue has been particularly noticeable in Minnesota, where only 20% of the Minneapolis-St. Paul metropolitan area population lives in one of the core cities (United States Census Bureau, 2014). In addition, travel per licensed driver and vehicles per person are 21% and 17% higher in Minnesota than the national averages, respectively (Office of Highway Policy Information, 2013).

Freeways by design are expected to be free-flowing and provide the desired level of service. In recent years, however, it is not uncommon for freeway traffic to become highly congested, even reach a stop-and-go state during peak periods. Of the various measures intended to alleviate freeway congestion, ramp control has been increasingly recognized as one of the most effective and viable strategies since its first deployment in the 1960s. In effect, the function of ramp control is (1) to limit the entering traffic from exceeding the operational freeway capacity and (2) to provide more efficient and safer merging at the freeway entrance by breaking up vehicle platoons. The benefits of ramp control reported in the literature include improved use of freeway capacity, increased throughput and freeway average speed, alleviated congestion, reduced system travel time as well as environmental benefits (Arnold, 1998; Cambridge Systematics, 2001; Elefteriadou, 1997; Papageorgiou et al., 1997; Taylor et al., 1996; Zhang and Levinson, 2003).

In the Twin Cities metropolitan area, freeway ramp metering goes back as early as 1969, when the Minnesota Department of Transportation (MnDOT) first tested ramp metering in a I-35E pilot project. To date, the Twin Cities ramp metering system has grown to include 433 ramp meters. Some operate only in the morning peak (5:30 a.m. - 9:00 a.m.), some only during the afternoon peak (2:00 p.m. - 6:30 p.m.), and others during both peaks. The ramp metering strategy employed by MnDOT has evolved over the years with some notable changes. Prior to year 2000, the deployed control strategy, i.e., the ZONE Metering strategy (Lau, 1996), focused on maximizing freeway capacity utilization without handling ramp queue spillbacks and controlling ramp waiting times. With this strategy, breakdowns at freeway bottlenecks can be effectively prevented; yet ramp delays and queues were often excessive. (Cambridge Systematics, 2001; Hourdakis and Michalopoulos, 2002). The latter resulted in public concerns, leading to a six-week system-wide shutdown study in late 2000. The study confirmed the overall benefits of the ZONE strategy; however, it also "highlighted the need for modifications towards an efficient but more equitable ramp control algorithm" (Cambridge Systematics, 2001). In response, MnDOT developed a new one aiming to strike a balance between freeway efficiency and reduced ramp delays. This new strategy, termed Stratified Zone Metering (SZM), took into account not only freeway conditions but also real time ramp demand and queue size information (Xin et al.,2004). Implementation of the new strategy with the Twin Cities freeway system began in early 2002; full deployment was completed in 2003.

Research on better, improved ramp control strategies has continued. While the aforementioned control strategies primarily work with volume/capacity information, a different family of algorithms utilize mainline density as the control variable. Two independent studies, both aimed in developing the next generation in ramp metering by focusing on density, were performed. The first by Geroliminis et al. 2011 in the "Development of the Next Generation Stratified Ramp Metering Algorithm Based on Freeway Density" project performed at the U of M- Twin Cities and the second by Kwon et al., 2012 in the "Development of Freeway Operational Strategies with IRIS-in-Loop Simulation" project performed at the U of M- Duluth. In both projects the proposed Density based algorithms, for short termed the UMN Density and UMD KAdaptive algorithms, were tested through simulation and found superior to the Stratified Zone metering algorithm. Based on these preliminary results, MnDOT decided to test and evaluate the two algorithms in the field.

The project presented in this report was performed by the Minnesota Traffic Observatory (MTO) which was called to assist in the deployment of the UMN algorithm, oversee the deployment of the UMD algorithm, and design and execute a field test involving all three ramp metering strategies, the Stratified, serving as base conditions vs the two density based algorithms. A section of TH-100 northbound between 50th Street and I-394 was selected as the deployment site. During the course of this project a lot of problems, operational issues, and simple bad timing had altered the project original goals and priorities. Although the UMN algorithm was integrated with the IRIS traffic operations system and was deployed in the field, analysis of its performance based on the collected data was not completed because it was later discovered that the geometry of TH-100 did not allow the correct operation of the control algorithm. Although all three algorithms were affected by the peculiar geometry and detector layout of this section of TH-100, the UMN algorithm was the one affected the most. Unfortunately, when this issue was discovered it was too late to switch test sites and it was decided to press on and only include the UMD algorithm in the evaluation. In addition, separately from this project MnDOT also run tests of the UMN algorithms on sections of Hwy-77 and I-35W with also poor results. During 2013 and 2014 the UMD algorithm underwent adjustments and has been implemented on most of the ramp metering system. One specific location involves a recently reconstructed section of TH-212 in the Southwest corner of the metro area. TH-212 was not controlled in the past and started been controlled by the UMD KAdaptive algorithm the summer of 2014. MnDOT modified the scope of this project to include a before/after evaluation of the ramp metering system on TH-212.

In summary, this report first covers a comprehensive review of the state of ramp metering strategies to date. It continues with a description of the selected site in TH-100 and the data collection layout deployed as well as with a description of the conducted field deployment of the two new density based algorithms. The results and comparison of the performance of the UMD KAdaptive based algorithm against the Stratified control are presented next followed by a before/after study of the UMD control on TH-212. Finally some overall conclusions are presented highlighting the lessons learned both during the implementation of the control algorithms as well as during the field test on TH-100.

2 AN OVERVIEW OF RAMP METERING OPERATIONS AND RESEARCH

The first task in the project presented in this report was to conduct a thorough review of the state-of-practice as well as state-of-the-art in ramp metering. The chapter starts with a description of the different ramp metering families and representative algorithms followed by the status of ramp metering in the United States and Europe.

2.1 RAMP METERING ALGORITHMS

Ramp metering algorithms can be mainly divided into three categories; fixed-time strategies (local and system-wide), local traffic responsive strategies and system-wide traffic responsive strategies.

1. Fixed-time control: Fixed time control strategies are implemented based on historical demand for particular times of day. They do not consider real-time measurements, and they are not adaptive systems. The objective criterion in the fixed time control case is to maximize number of served vehicles or total traveled distance considering the capacity constraints on the freeway and on the ramp. Nevertheless, as the metering rates are based on historical data, these systems are not able to produce efficient strategies in case of varying demands due to special events or incidents, and they are not able to adapt to traffic conditions on the freeway. Note that fixed-time control can be applied in either local or system-wide level, although system-wide fixed-time control is very rarely used.
2. Local traffic responsive control: Local control strategies compute ramp metering rate based on traffic conditions at the adjacent freeway section only. In contrast to fixed time control strategy, reactive ramp metering considers real-time measurements and computes metering rate based on downstream capacity. The primary reactive ramp control is demand-capacity strategy, which is described as follows:

$$r(k) = \begin{cases} q_{cap} - q_{in}(k-1) & if\ o(k-1) \le o_{cr} \\ r_{min} & otherwise \end{cases} \qquad \text{Eq. 2-1}$$

where q_{cap} is freeway capacity at downstream of ramp, $q_{in}(k-1)$ is the flow measurement at the previous time interval, $o(k-1)$ is freeway occupancy measurement at downstream of the ramp, o_{cr} is the critical occupancy value where freeway flow at downstream of ramp reaches its maximum, and r_{min} is the minimum allowed ramp metering rate. Basically, this strategy computes as high metering rates as necessary to reach capacity flow at the freeway section downstream of ramp. However, if $o(k-1)$ exceeds o_{cr}, ramp metering rate is reduced to the minimum allowed level to dissipate the congestion. This open-loop strategy is converted to a closed-loop policy, known as ALINEA, by Papageorgiou et al. (1991). The new feedback control law reads as follows:

$$r(k) = r(k-1) + K\big(o_{cr} - o(k-1)\big) \qquad \text{Eq. 2-2}$$

where K is a regulator parameter, and ALINEA's performance is not very sensitive to its choice. Other local ramp metering strategies are reviewed in Papageorgiou and Kotsialos (2002).

3. System-wide (area-wide) traffic responsive algorithm: This refers to the control of a series of ramps in conjunction considering the interdependency between them. The aim of area-wide ramp control is to optimize the traffic flow over a freeway stretch, rather than a specific location. They can be divided into three groups regarding the way they are implemented (Zhang et al., 2001).
    - *Cooperative algorithms:* The ramp metering rate computed by local strategies is further adjusted in this method to avoid congestion at the freeway stretch. The adjustment of metering rates is mainly done using heuristics in an ad hoc way. Examples of these algorithms are HELPER (Lipp et al., 1991) and Linked-Ramp (Banks, 1993).
    - *Competitive algorithms:* In these algorithms, ramp metering rate is calculated using both local and area-wide strategies, and the most restrictive one is implemented. This rate can also be further adjusted using some heuristics. Examples of competitive algorithm are Zone (Stephanedes, 1994), Bottleneck (Jacobson et al., 1989) and SWARM (Paesani et al., 1997) algorithms.
    - *Integral algorithms:* In these algorithms, metering rates at multiple ramp locations are computed to optimize the objective function (e.g. total travel time, throughput of the section) which represents the performance of the whole freeway stretch. They can also consider system constraints such as maximum allowable ramp queue, bottleneck capacity, etc. This group of algorithms is the most appealing regarding the problem design. However, they call for a sophisticated design procedure which is more demanding in computation. These algorithms can be implemented in a reactive way, considering the measurements from the previous time interval, or in a proactive way, considering demand predictions. Examples of integral algorithms are METALINE (Papageorgiou et al., 1990), fuzzy logic (Meldrum and Taylor, 1995) and MILOS (Ciarallo and Mirchandani, 2002).

Zhang et al. (2001) developed a ramp metering evaluation framework using microscopic simulation environment and compared the performances of 4 important ramp metering algorithms; ALINEA, Bottleneck, SWARM and Zone algorithms. Following findings are reported as the result of the analysis.

- *"Ramp metering reduces the total vehicle travel time up to 7% compared with no metering. The effectiveness of a ramp control algorithm depends on the level of traffic demand. As traffic demand increases, ramp metering tends to be more effective in reducing system travel time.*
- *No significant performance differences exist among ALINEA, modified Bottleneck, modified SWARM with 1 time-step-ahead prediction, and Zone algorithms under the tested scenarios.*

- *Modified SWARM with five-step-ahead prediction has the poorest performance among all tested algorithms due to the inaccuracy of the five-step-ahead prediction model. This indicates a good traffic prediction is the key to SWARM's performance.*
- *Coordinated ramp metering algorithms do not necessarily perform better than local control algorithms if some of their key parameters are not well calibrated. Well-tuned parameters are critical for the good ramp metering performance.*
- *Ramp metering performance and parameter values are non-linearly related. There is a broad range of parameter values over which ramp metering performance does not change significantly. Outside of this range, however, ramp metering performance deteriorates quickly.*
- *Ramp metering seems to be more effective under certain demand patterns than others."*

Zhang et al. (2001) provides a classification tree for algorithms, displayed in Figure 2-1. Note that although zone algorithm is classified as an isolated control method in Figure 2-1, it is considered as a coordinated strategy in this study, as it considers traffic conditions in a freeway stretch rather than a specific location. The algorithms presented in Figure 2-1 are reviewed in Zhang et al. (2001).

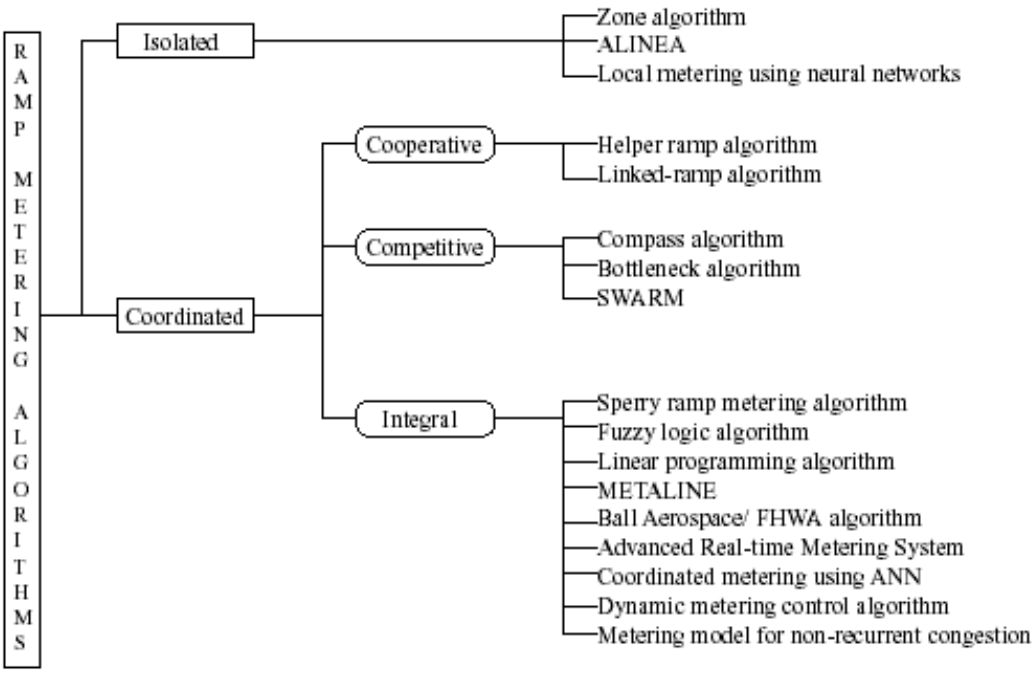

Figure 2-1. Ramp metering algorithms [Zhang et al., 2001].

An extension to the above proposed control methods is the incorporation of breakdown probability models into the ramp metering strategy proposed by Elefteriadou et al. (2011). They develop a breakdown probability model for the merge areas as a function of freeway flow and ramp flow. This model is, then, incorporated in an existing ramp metering algorithm (e.g. COMPASS, stratified zone algorithm). Breakdown probability models can be used with current or predicted traffic volumes, depending on the type of the algorithm used. Elefteriadou et al. (2011) tested this approach in a microscopic simulation environment and concluded that the new

approach has the potential to improve the performance of existing ramp metering algorithms by delaying or preventing flow breakdown and by increasing freeway throughput.

Although ramp metering algorithms have, in general, compact structures, a real-world ramp metering system consists of a combination of algorithms designed to handle various conditions. For instance, Highways Agency (2007) lists seven algorithms needed for their ramp metering operation system.

- *Ramp metering algorithm:* The core algorithm that produces ramp metering rates based on local or area-wide traffic conditions on the freeway.
- *Data filtering algorithm:* Filtering algorithm detects and removes outlier flow, speed and occupancy observations from raw data collected by detectors. The success of filtering algorithm is critical to the performance of ramp metering system.
- *Switch on-off algorithm:* This algorithm basically switches the ramp metering system on or off based on traffic conditions on the freeway and a pre-defined flow, occupancy or speed threshold.
- *Queue override algorithm:* It monitors the queue size on the ramp and releases the vehicles from the ramp to clear the queue that may spillback to the arterials.
- *Queue management algorithm:* This algorithm attempts to keep queue length on the ramp at a pre-defined desired level by monitoring proportional occupancy measurements. This algorithm is implemented to minimize the action of queue override function.
- *Arbitration algorithm:* This algorithm collects the output from ramp metering, queue management, queue override and switch on-off modules, and determines the final allowed inflow rate from the on-ramp to the freeway. Arbitration algorithm always selects the highest allowed inflow rate and passes it to the release algorithm.
- *Release algorithm:* This algorithm sets traffic signal durations based on the allowed flow rate computed by the controller. There are various signal policies that can be implemented in this step: one-car per green, two-cars per green or traffic-cycle realizations.

2.2 RAMP METERING STATUS IN THE US

Benefits of ramp metering reported in literature include system-wide travel time savings, improved safety, and reduction of fuel consumptions and vehicle emissions. However, there are no standard evaluation criteria to quantify these benefits. In addition, it is difficult to evaluate certain changes in particular (e.g. diversion of travelers to the arterials). Early ramp metering applications in Illinois, Michigan, California, Minnesota, and Washington have been very successful and have led to the extension of ramp metering systems to other metropolitan areas in US. There is no recent study that describes the current status of ramp metering systems in US, but Table 2-1 lists most of the ramp metering sites as of 1995 (ITSA, 1995).

Table 2-1. Ramp metering systems in the United States as of 1995 [ITSA, 1995].

State	Area	No. of Meters
Arizona	Phoenix	65
California	Fresno	15
	Los Angeles	808
	Orange County	278
	Sacramento	19
	San Bernardino	51
	San Diego	134
	San Francisco	96
Illinois	Chicago	109
Michigan	Detroit	49
Minnesota	Minneapolis	367
New York	Long Island	75
Virginia	Arlington	26
Washington	Seattle	54
Wisconsin	Milwaukee	43

Ramp Metering Development plan (RMDP) 2011 prepared by California Department of Transportation reports that there are 2460 existing ramp meters throughout the state, which accounts for 60% of all existing ramp meters in the US. RMDP 2011 indicates that state of California plans to implement 1715 new ramp meters within the next 10 years.

The ramp metering system in Minneapolis / St. Paul area has been first implemented in 1970s as a fixed-time control strategy by Minnesota Department of Transportation (MnDOT). This system is first converted to a local traffic responsive system and, later, to an area-wide traffic responsive control system using Zone algorithm. In 2000, an empirical experiment on ramp metering is conducted in Minneapolis-St. Paul area (Cambridge Systematics, 2001). Traffic flow and safety impacts are investigated by disabling 430 ramp meters for six weeks. The results indicated 9% reduction in freeway throughput, 22% increase in travel time, 7% decrease in freeway speed and 26% increase in the number of crashes. MnDOT implemented stratified zone metering strategy (Xin et al., 2004) in 2002 to dissolve the congestion on the freeway but also to minimize the waiting times on the ramps. Michalopoulos et al. (2005) evaluated the stratified zone algorithm in a microscopic simulation environment, and concluded that the algorithm produced less on-ramp delays compared to the previous zone metering algorithm, while the freeway delays increased with the implementation of the new algorithm. However, the algorithm presented clear improvements over the no-control case regarding freeway delay, freeway speed and number of stops.

Washington State Department of Transportation (WsDOT) developed Bottleneck algorithm (Jacobsen et al., 1989), a competitive area-wide ramp control strategy, and implemented it in Seattle central business district starting from 1981. WsDOT conducted a six-year evaluation study, which indicates that travel time decreased by 48%, mainline flow increased by 62-86%,

and crash rate decreased by 39%. WsDOT implemented fuzzy logic control (Meldrum and Taylor, 1995) later in 1999, considering the improvements over the existing Bottleneck algorithm. However, there is no study, to the authors' knowledge, that discusses the evaluation results of the fuzzy logic algorithm in details.

SWARM (Paesani et al., 1997) was first developed by the National Engineering Technology Corporation under a contract with the California Department of Transportation. The first field implementation of the algorithm was in Orange County for 6 weeks with no quantitative evaluation. Moreover, the system did not appear to operate properly. Later the implementation and evaluation of SWARM was more successful in Los Angeles and Ventura Counties, California, in the late 1990s. The benefits of the new SWARM algorithm compared with the previous ramp-metering operations were evaluated during the morning peak periods on a freeway corridor that contains 20 controlled on-ramps. The evaluation revealed an 11% increase of the main-line speed, a 14% decrease of the travel time, and a 17% decrease of the freeway delay. Moreover, the queue lengths at the nine busiest on-ramps increased by more than 40%.

The global mode of SWARM operates on an entire freeway stretch based on forecast densities at the bottleneck location. The density prediction is done by performing a linear regression on a set of short term historical data and applying a Kalman filtering process. A parameter, T_{crit}, denotes the forecasting time span, which is usually several minutes. The excess density is then the difference between the predicted density at T_{crit} and a predetermined threshold density representing the saturation level at the bottleneck. This excess density is converted to the (current) required density to avoid congestion at T_{crit} by reduction in volume at each detector station:

required density = current density – (excess density/T_{crit})
volume reduction = (local density − required density) * (no. of lanes) * (distance to next station).

SWARM algorithm has also been tested in Portland metropolitan area by Oregon Department of Transportation (ODOT). Ahn et al. (2007) study the implementation during a 2-week pilot study on a 7 mile long freeway corridor and report the benefit of the new SWARM system as compared with the fixed-time algorithm regarding the savings in delay, emissions and fuel consumption, and safety improvements on and off the freeway. The analysis shows that the percentage of communication failures was below 2% at most locations with the fixed-time strategy, whereas the failure percentages with SWARM were much larger, such as exceeded 10%. In addition, the VMT increased marginally (0.8%) with the SWARM operation, which indicates that the demand remained nearly independent of the ramp metering control deployed in the field (at least for the short term). However, surprisingly, SWARM increased the VHT and the average travel time by 6.0% and 5.1%, respectively, corresponding to a significant increase of 34.7% in total freeway delay. Empirical evidence suggests that this deterioration resulted from high metering rates at most of the on-ramps, resulting in lower travel times on on-ramps and increase in freeway delays. Currently, SWARM is under development and refinement by Delcan, the company which first developed the algorithm (Chu et al., 2009).

Chu et al. (2009) reports that there are three major real-world ramp control systems deployed in California:

- San Diego Ramp Metering System (SDRMS), deployed in Sacramento, Fresno, San Bernardino and Riverside, and San Diego areas
- Semi-Actuated Traffic Management System (SATMS), deployed in Los Angeles and Orange County
- Traffic Operations System (TOS), deployed in the Bay Area

These systems can be operated under traffic responsive metering control or pre-timed metering control. SATMS is based on demand capacity control, while SDRMS and TOS are based on occupancy control. Even though ramp metering algorithms have simple structures, these real-world ramp metering systems are complicated because of the necessity to handle various conditions.

There are various studies that evaluate ramp metering implementations in the state of California. The evaluation study on I-580 indicates that installation of ramp meters over an 18 mile long section of freeway led to 30% reduction in travel time (Kimley-Horn and Associates, 2008). Metropolitan Transportation Commission published the fact sheet that presents the benefits of ramp metering implementations; 80% of evaluated freeway segments exhibit 30% or greater delay reduction (MTC, 2011).

Ramp metering system, along with an isolated control strategy, has been installed in Denver (Colorado) on I-25 freeway in 1981. HELPER (Lipp et al., 1991) algorithm was first introduced in 1984 in the same area. Evaluation results indicated that if isolated ramp control is able prevent the breakdown, HELPER has little benefit. However, if not, cooperative control was found to be very effective in dissolving congestion.

METALINE (Papageorgiou et al., 1990) was tested in Milwaukee (Wisconsin) area, in 1997. Although the field results indicated improvements over local ramp control strategies, its deployment has been stopped (Bogenberger and May, 1999).

COMPASS algorithm was first implemented on the Queen Elizabeth Way in Toronto, Canada, in 1975. Ramp metering system can be operated under automated competitive control strategy or can be manually regulated from traffic control center. Local metering rates are computed using an ad hoc look-up table with various levels for each ramp, while global rates are computed using off-line optimization procedure based on area-wide traffic conditions. No evaluation study, to the authors' knowledge, exists related to the implementation of COMPASS algorithm.

In overall, ramp metering reduces congestion, decreases travel time and increases freeway throughput by managing the ramp flow and improving the efficiency of the merging area. This results also in fewer accidents, which in turn may cause significant delays in the freeways. As there are no standard evaluation criteria to assess the benefits of ramp metering systems, it is extremely difficult to compare performance of various algorithms described above, unless one develops an evaluation platform using a simulation environment (Zhang et al., 2001; Chu et al., 2009). In addition, there are few studies in the literature that attempt to put evaluation results

together for numerous field implementations. Table 2-2 summarizes such an evaluation study from six locations in the US (Piotrowicz and Robinson, 1995).

Table 2-2. Benefits of ramp meters [Piotrowicz and Robinson, 1995].

		Speed (mph)		Changes in (%)		
State	**Area**	**Before**	**After**	**Travel Time**	**Accidents**	**Flow**
Colorado	Denver	43	50	-37	-50	19
Michigan	Detroit	-	-	-	-50	14
New York	Long Island	29	35	-20	-	-
Minnesota	Minneapolis	34	46	-	-27	32
Oregon	Portland	16	41	-156	-43	-
Washington	Seattle	-	-	-91	-39	62

Kang and Gillen (1999) also reviewed numerous ramp metering implementations and summarized the impacts of ramp metering strategies on system performance. A part of this review is presented in Table 2-3.

2.3 RAMP METERING STATUS IN EUROPE

Despite the accelerated ramp metering deployment in Europe in the last decades, only few hundred of on-ramps in few European countries are equipped with ramp metering technology where all installations employ only local algorithms. Furthermore, there is no freeway in Europe with ramp metering installation in most of its on-ramps. In addition, motorway-to-motorway metering is non-existent in Europe. Thus, there is a huge potential for motorway traffic flow improvements, if available state-of-the-art ramp metering strategies would be applied in a coordinated way (Nearctis deliverable report 8, 2010).

A European Union funded research project, European Ramp Metering Project (EURAMP) has been conducted and completed in 2007. The first step of the project is the design and simulation testing of various ramp metering algorithms. The second step is the field implementation of different ramp metering strategies. Demonstration sites are A6 motorway (Paris, France), A28 and A2 motorways (Utrecht, Netherlands), A94 motorway (Munich, Germany) and Ayalon Highway (Tel Aviv, Israel). Evaluation results indicate that all test sites, except Utrecht, indicate travel time benefits. However, in Utrecht, ramp delays are more significant than travel time improvements achieved on the mainline. Among several control strategies used, coordinated ramp metering provided the best results. On the other hand, 1-car per green or 2-car per green strategy is used in Utrecht, which may lead to significant ramp delays.

Table 2-3. Evaluations of ramp metering systems [Kang and Gillen, 1999].

Location and Agency	*Site Description*	*Results*
Austin, Texas		
Texas Department of Transportation	Three ramp meters installed in 1997 on I-35 northbound	- Throughput increased by 7.9% - Speeds increased by 60%
Houston, Texas		
Texas Department of Transportation	I-10 freeway in 1996	- Total daily estimated travel time savings of 2,875 veh.h
Denver, Colorado		
Colorado Department of Highways	5 ramp meters on I -25 Evaluated in 1981-1982 HELPER algorithm	- Speeds increased by 58%. - Emissions dropped by 24% - Accidents dropped by 5% - Flows on area arterials increased from 100vph to 400vph, no degradation on surface street conditions
Detroit, Michigan		
Michigan Department of Transportation	Six ramp meters installed in 1982 on I-94 eastbound	- Speeds increased by 8%. - Accident dropped by 50%
Long Island, New York		
New York Department of Transportation	Sixty ramp meters installed in eastbound Long Island Expressway Evaluated between 1987-1990	- Travel times dropped from 26 min to 22 min - A motorist using a metered ramp saved 13% in travel time on average. - No significant change in throughput
Portland, Oregon		
Oregon Department of Transportation	I-5 freeway in 1981 16 meters in fixed-time are evaluated	- Speeds increased from 16-40 mph to 41-43 mph - Fuel consumption reduced by 540 gallons/day - Accidents dropped by 43%

2.3.1 Ramp Metering Status in the UK

The first ramp metering system in England has been installed on M6 J10 roadway in 1986 (Highways Agency, 2007). The first widespread deployment of ramp metering on the highway network was started in 2005 with the aim to deploy 30 ramp metering systems by the end of 2007. These ramp metering systems are implemented on the M1, M5, M6, M42, M56, M60, and M62 motorways located in the West Midlands and the North of England.

The operational evaluation of ramp metering installation has indicated benefits to the travelling vehicles on the mainline of the motorway in terms of travel time savings, increased speeds, increased flow, and more stable traffic conditions. The overall increase in peak period mainline flow and speed after the implementation of ramp metering are reported as between 1% and 8% and between 3.5% and 35%, respectively. In many cases, ramp metering has delayed the onset of flow breakdown and/or recovered earlier from the flow breakdown. The mainline travel time savings during peak periods is reported up to 40%. With daily 13% average travel time saving across all sites, the economic assessment indicates that ramp metering installation results to First Year Rate of Return of 48%. It is worth to note that ramp metering has not been successful at all sites. For instance, mixed results were obtained from ramp metering on the M27 and M3 motorways in Southern England, which has been stopped there. As of 2011, there are 88 ramp metering sites on England's motorway network (Nearctis deliverable report 7, 2010).

2.3.2 Ramp Metering Status in France

METALINE (Papageorgiou et al., 1990) and ALINEA (Papageorgiou et al., 1991) were introduced in Paris, in 1990 and early 1991. Both control strategies were tested during the morning peak period for 10 days, which resulted in higher mainline speeds for both. In the framework of the PDU (Plan de Déplacement Urbain) program and according to the results obtained in the EURAMP project, the authorities decided the renewal of the existing ramp metering system to consider the possibility of real-time control of several candidate on-ramps (Nearctis deliverable report 7, 2010). A field evaluation is done on the generalized ramp metering strategy on the East part of Ile-de-France motorway network using ALINEA strategy. The implementation started in February 2008 on 17 on-ramps with heavy peak period congestions. The obtained results indicated a positive impact of ALINEA on the traffic, which the total time spent (veh·h) on the mainstream plus the on- ramps and the total travel distance (veh·km) are between 3% to 15% and 1% to 8%, respectively. The overall collective benefit is evaluated to be equal to 13.5 M€/year for the 17 on-ramps field test.

Another field test was done to develop, test, and evaluate the traffic impact of four ramp metering strategies: No control, ALINEA, VC_ALINEA (Variable Cycle ALINEA), and Coordination (CORDIN). The field test site was located in the south of the Ile de France motorway network, 20 km-length A6W, which includes 5 consecutive on-ramps fully equipped with loop detectors and traffic signals. Each on-ramp is equipped with 2 detector loops, one at the signal stop line for on-ramp volume measurements, and the second one at the upstream of the on-ramp for the queue override strategy. In addition, the freeway is equipped with detectors stations (each 500 m) for traffic volume, occupancy and speed measurements. In the following, two ramp metering strategies (VC_ALINEA and CORDIN) are introduced.

The basic formula of VC_ALINEA requires computing the split ratio as the control variable instead of the green duration. The split is defined as $\alpha = G/C$, where G is the green time and C is the cycle time. The VC_ALINEA control law is:

$$\alpha(k) = \alpha(k-1) + K\,[\hat{o} - o_{out}(k-1)] \qquad \text{Eq. 2-3}$$

where K is a predefined parameter, $\hat{o}$, and o_{out} denote the desired and current occupancies. Similar to ALINEA, the split (α) is constrained by the minimum and maximum cycle durations. Similarly, the CORDIN strategy is based on ALINEA, in which the coordination is coded to a systematic manner to find first the location of an active congestion (Master on-ramp) and second to modify all upstream control values of ALINEA. The correction of ALINEA control values can be done by adjusting a few parameters.

The aforementioned strategies have been applied over the period from the mid-September 2006, until the end of January 2007. By scrutinizing the collected data, days with major detector failures, uncommon traffic patterns, and significant incidents or accidents are discarded. It was reported that ALINEA in comparison with the no control case decreases the total time spent by 10%, decreases the total travel distance by 2%, and increases the mean speed by 5%. Further, VC_ALINEA decreases the travel time spent and total travel distance by 12% and 5%, respectively. In addition, the CORDIN strategy resulted to 12%, 0% and 11% decrease of travel time spent, total travel distance and mean speed, respectively. For environmental analysis, fuel consumption of vehicles during activation of each ramp metering method is studied. In comparison with the no control case, the changes of -8 %, -5%, -8 % were reported for ALINEA, VC_ALINEA and CORDIN, respectively. The emission indices are also reduced for all strategies. For safety analysis, a risk model based on the traffic measurements (occupancy and flow) is considered, which was calibrated and validated both on the ring road of Paris and on A6W. The obtained results reveal improvement of 20% for all other strategies compared with the no control case. The results of the cost benefit analysis, with respect to the investments and the maintenance cost of the ramp metering system, indicated a collective benefit of 2.4 M€, 2.44 M€ and 3.5 M€ per year for ALINEA, VC_ALINEA and CORDIN, respectively (Nearctis deliverable report 7, 2010).

2.3.3 Ramp Metering Status in the Netherlands

In 1989, the first ramp metering system in the Netherlands was installed on the A10 motorway, with reported positive evaluations. There are 50 ramp meters operating as of 2006, with the implementation costs of 150000 euros for a one-lane onramp controller and 175000 euros for a two-lane controller including outside equipment. The A10 motorway is the ring road around Amsterdam with connections to the nation-wide motorway system of The Netherlands. The A10 is a busy motorway with up to 93.000 vehicles per day in 1994 and frequent congestion occurrences. In June 1994, three new local ramp metering systems have become operational. Taale and van Velzen (1996) report the analyses of two metering strategies on A10: Rijkswaterstaat and ALINEA. The former is a feed-forward strategy assigning the remaining

capacity of motorway to the onramp traffic. The Rijkswaterstaat (RWS) strategy can be summarized as follows.
The ramp control system switches on when i) the flow on the motorway or on the on-ramp or the sum of both flows exceed certain predefined values, ii) the speed upstream or downstream the onramp drops below a certain value. Afterwards, the number of vehicles allowed to enter the motorway is:

$$r_k = C - I_{k-1} \qquad \text{Eq. 2-4}$$

where r_k is the number of vehicles allowed to enter at time interval k, C is the capacity of the motorway downstream the on-ramp, and I_{k-1} is the measured flow upstream the on-ramp in the previous time interval. The cycle time of the metering system is then calculated:

$$t = \frac{n}{r_k} \times 3600 \qquad \text{Eq. 2-5}$$

where t is the cycle time (second) and n is the number of lanes on the on-ramp.

The evaluation results show no significant difference in flows. However, ALINEA increases speeds considerably such that during the peak periods the average minimum speed has increased approximately from 30 km/h to 50 km/h. Moreover, with the introduction of ramp metering a 19% reduction of delays has been achieved for both the motorway and the on-ramps. For the Rijkswaterstaat strategy, however, traffic conditions in terms of delays and speed have worsened with respect to the no ramp metering situation.

Taale et al. (1996) examined filed implementation of 3 different ramp metering strategies (RWS, ALINEA, and Fuzzy) at The A12 motorway from The Hague to Utrecht. The output of fuzzy strategy is the cycle time and the inputs are: speed upstream the on-ramp, speed downstream the on-ramp, and the existence of a queue on the onramp. The input variables are divided into a number of fuzzy sets, e.g. very low, low, medium, high and very high. In the first step (fuzzification), the measurement of an input variable is transferred to degrees of membership for those sets. Depending on the degrees of membership, some fuzzy rules are triggered (fuzzy reasoning). These rules have the form:

IF *speed upstream = medium* AND *speed downstream = low* THEN *cycle time = long*.

The switching on of the fuzzy strategy is when the calculated cycle time exceeds a certain threshold and switching off is when the cycle time drops below another threshold. The results of the assessment show that the fuzzy ramp metering strategy was performing better than the other strategies: the capacity of the bottleneck increased (RWS=4048 (veh/h), ALINEA=4000 (veh/h), and Fuzzy=4256 (veh/h)), giving a better throughput, higher speeds, and shorter travel time (RWS=6.0 (min), ALINEA=6.2 (min), and Fuzzy=3.9 (min)). However, fuzzy strategy shows a safety problem that it switches on and off too often.

Taale and Middelham (2000) investigate the manner of driver traffic law compliance at onramps. They report that in case of bottleneck occurrence, about 6% of the drivers ignores the red light, whereas in case of no bottleneck this increases to about 15%. However, where a traffic camera is

installed; only about 3% of drivers risk ignoring the red traffic signal. In addition, they state that with ramp metering the percentage of rerouting from the onramps to other roads is noteworthy.

2.3.4 Ramp Metering Status in Germany

Ramp metering has been implemented in Rhine-Ruhr area, Munich and Hamburg, in Germany. Germany has noted that ramp metering prevents significant speed drops at merge locations and leads to a reduction in accidents (German Ministry of Transportation, 2005). Moreover, the number of congestions is reduced by around 50%, the number of severe accidents (person injured or severe damage) is reduced by 25%, and particularly the speed on the through lanes is increased by 10 %. At September 2012, there are around 100 on-ramps at motorways in NRW, Germany equipped with ramp metering control.

2.4 RAMP METERING STATUS IN AUSTRALIA

A coordinated traffic responsive ramp control strategy, HERO (HEuristic Ramp metering coOrdination) (Papamichail and Papageorgiou, 2008), was implemented by VicRoads at 6 consecutive inbound on-ramps on the Monash freeway, in Melbourne, Australia. HERO objective is to target the critical occupancy for throughput maximization, which recent studies demonstrate that is more robust and effective than targeting a predefined capacity value. HERO adjusts local ramp metering rates computed by ALINEA based on real-time measurements of traffic conditions along the freeway stretch. HERO applies the coordination by appropriate setting of minimum ramp queue lengths that should be created and maintained at specific ramps. The principal methodology of HERO is summarized as follows:

i. HERO identifies potential active bottleneck of mainstream. The nearest ramp upstream of that bottleneck regarded as the master on-ramp.
ii. To delay or avoid the mainstream congestion and queue control of the master on-ramp, HERO increases the storage space by employing the upstream located slave on-ramps.
iii. The formed cluster of on-ramps (master and several slaves) is dissolved when the master on-ramp queue or the mainstream occupancy at the bottleneck become sufficiently low.

The Monash freeway is a six-lane dual roadway carrying more than 160,000 vehicles per day and experiences long periods of congestion between 3 to 8 hours a day. The evaluation undertaken by VicRoads for the pilot project shows a 4.7% increase in average flow (on top of the previous system) and a 35% increase in average speed at morning peak, and a 8.4% increase in average flow and a 58.6% increase in average speed at afternoon peak. Evaluation study also indicates that results produced by HERO are better than local ramp metering strategies and are close to sophisticated optimal control schemes, which require demand prediction. It is worth to mention that HERO was also field-implemented in a 20-km stretch of the A6 freeway in the south of Paris, France, in 2006, although in a simplified form due to the lack of real-time on-ramp data. Nevertheless, results indicated a clear improvement over the uncoordinated ALINEA case.

3 PREPARATION FOR THE FIELD DEPLOYMENT

3.1 IMPLEMENTATION OF THE UMN DENSITY ALGORITHM IN IRIS

The UMN Density algorithm was developed as part of an earlier, RITA funded, project. A later, now completed project, funded by MnDOT, ported the algorithm from its original C++ implementation to a JAVA implementation and was integrated with the IRIS operations system. This effort was completed in 2011. Between the end of the aforementioned project and the initiation of this one IRIS underwent several changes and upgrades. Unfortunately the UMN algorithm was not maintained during these upgrades and it was rendered non-operational by the time this project was initiated. As part of this project effort was aimed in the re-integration of the UMN algorithm into IRIS.

This effort mainly took place during summer of 2012 with testing taking place early fall. Specifically, in order to efficiently perform the required work and to minimize disruption of RTMC operations, the development took place under simulated conditions through the AIMSUN microsimulation interface with IRIS. The AIMSUN-IRIS interface was a low priority project of the MTO. Given the need for this project, priorities were adjusted to complete the interface development, funded by MTO operations funds, on time for it to be used for this project.

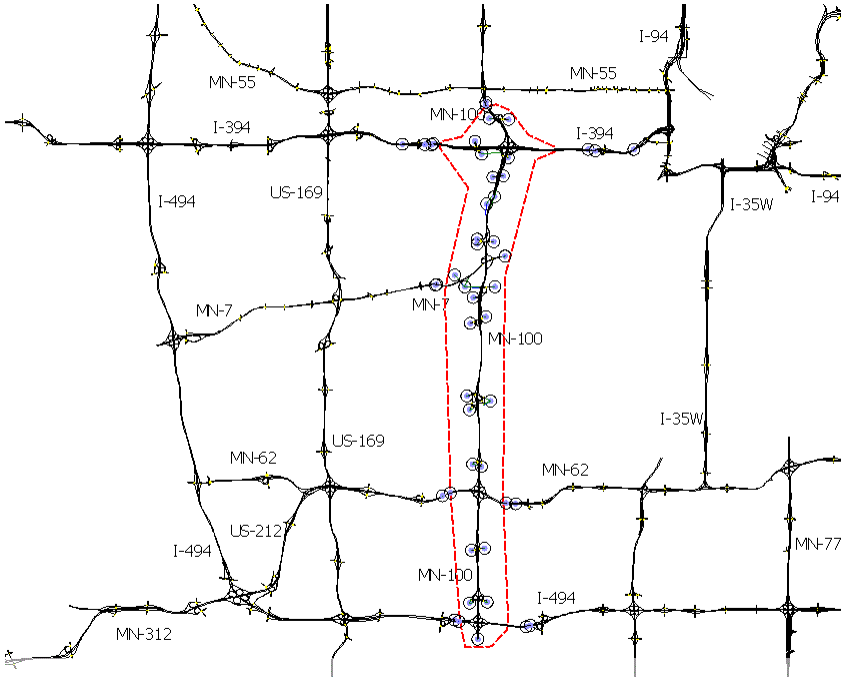

Figure 3-1. TH-100 simulated network for testing the UMN Density Algorithm.

The AIMSUN-IRIS Interface allowed the research team to contact all development and experiments in the MTO utilizing an off-line version of IRIS fueled with data provided by the microsimulation application for TH-100. The TH-100 model was the product of an earlier RITA funded project that modeled the entire Twin Cities freeway network. In Figure 3-1 the section of TH-100 used in the Simulated IRIS experiments is surrounded by the red dashed line. It is

important to note that the objective of this effort was to re-integrate the UMN algorithm so it is compatible with IRIS and not to make functional changes or improvements. The tasks with the simulated IRIS confirmed the successful operation of the UMN algorithm as part of IRIS but did not conduct any evaluations of its effectiveness and performance. Specifically, the tests were conducted under the following assumptions:

- No changes were made to IRIS outside of the two files containing the UMN Density algorithm. As far as the system was concerned it was communicating with the field.
- Time was manually changed in the IRIS server to match the time of the simulation.
- A Time Server running on the IRIS server computer handled the synchronization between the two machines.
- During the tests the afternoon period was implemented with ramp metering starting at 14:59:45 PM.
- Five ramps were tested from 50th Street to Minnetonka Blvd in the northbound direction.
- Data provided for all detectors in the area indicated in Figure 3-1.
- Only 10 records per controller are maintained in a circular buffer. This invalidated the archival function of IRIS but it is unrelated to the operation of the ramp metering system.
- Time to running the simulation did not cross 11:59 PM in the night. Longer period simulations became unstable and fixing this problem for the purposes of this project was not necessary.

Finally, it is important to note that, considering it was tested in a simulated TH-100, the UMN Density algorithm was not thoroughly tested for its robustness in view of incomplete or erroneous data which are possible during real operations.

The code of the reintegrated UMN Density algorithm was transmitted to the RTMC in July 2012 and the tests took place between that time and End of September 2012. It was after the research team secured the successful operation of the algorithm that the field tests were scheduled.

Although, no actual documentation regarding the UMD KAdaptive ramp metering algorithm was ever received by the research team a basic understanding of its operation was developed through information found a final project report (Kwon and Park, 2012). We also performed a cursory inspection of the code in IRIS to complete our understanding and the changes between theory and implementation.

3.2 Preparation of the MTO Traffic Surveillance and Detection Stations

The MTO traffic surveillance stations are modular machines and required modification in order to adapt to the chosen deployment locations on TH-100. The MTO surveillance stations were used to collect video of the freeway at multiple points along TH-100. This video was later processed to extract flow characteristics and specifically travel times. These locations of video collection will be augmented with 30-second loop detector data from existing MnDOT sensors.

The video was collected using observation equipment designed and built by the Minnesota Traffic Observatory. These units are made up of:

- A secure cabinet enclosure which houses the recording computer, timer, and battery power supply
- A telescoping pole which extends up to roughly 30 feet from the ground and transmits power and signal internally between the cabinet and the camera enclosure
- An enclosed dome housing a fixed lens camera

These units are designed to be securely attached to some existing piece of infrastructure or other rigid object (e.g., stop light, light pole, tree, etc.). The pole is braced at two locations to minimize sway of the camera when the mast is fully extended. Figure 3-2 shows one of these stations deployed on a light pole as part of a work-zone observation project.

Figure 3-2. MTO portable traffic observation station deployed along HW-280.

The MTO has 5 of these observation units ready for field implementation. To augment these five systems, two additional systems were assembled (financed by the MTO). These did not include the 30-foot telescoping pole. Instead, the camera enclosures were mounted directly to existing supports, in this case a tall tree and a fence along the freeway. Each of these portable stations has self-contained battery power and timing mechanisms and can record up to 48 total hours between recharges (roughly one week of recording AM and PM peak periods). The enclosures, both for the standard observation units and those without the telescoping pole, are weather resistant and can be secured against tampering. The standard as well as the mast-less units carried each a single camera each.

3.3 FIELD DEPLOYMENT REGION

Ramp meters have been implemented across the majority of the Twin Cities freeway network. To test the ramp metering algorithm in the field, a suitable freeway region was chosen based on the following criteria:

- Contains a bottleneck with reliable activity during peak period(s)
- Contains multiple entrance ramps upstream of the bottleneck that contribute similar amounts of volume to the mainline which can be controlled by the ramp metering algorithm
- Freeway elevation below the surrounding terrain and/or has sufficient overpasses to allow for clear observation and data collection

In evaluating these criteria, TH-100 northbound between 50th Street and Minnetonka Boulevard was selected. This region contains a several ramps which contribute significant traffic up to a bottleneck region at Minnetonka Boulevard/TH-7. The freeway is generally lower than the surrounding terrain and has multiple overpasses available for locating/mounting observation equipment. Figure 3-3 shows a map of the region of interest.

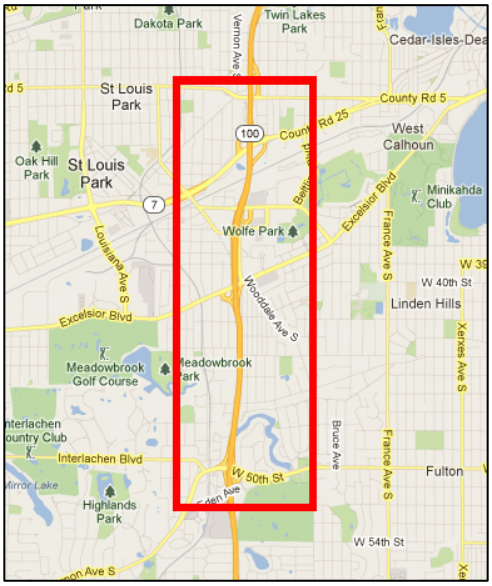

Figure 3-3. Region of interest for ramp metering field test.

It is unfortunate that at the time of site selection the research team was not informed and did not realize that the freeway geometry, and specifically the service road near Excelsior Blvd and 36th St was incompatible with all ramp metering strategies including the Stratified Zone control. Specifically, the way the detectors are deployed the exiting volume heading for 36th St may be overestimated, also counting traffic that use the service road to travel from Excelsior to 36th. This volume is not large but it prompts the control logic to release more vehicles from the downstream ramps and tip the conditions towards the breakdown sooner. Attempts to improve this issue were made during the field experiment but time and system stability issues prevented them from being implemented.

3.3.1 Specific Observation Locations

After in-person site visits, nine specific locations were identified as possible candidates for installation of observation stations. From these seven were finally selected for deployment. Permits were requested for all nine so the research team could have the ability to relocate the equipment during the experiment if problems arose. These locations are:

1. W 50th St Bridge luminary
2. Approximately, W 48th St sound wall (Backup)
3. Morningside Rd sound wall (Backup)
4. W 41st St pedestrian bridge or sound wall
5. Park Center Blvd luminary
6. W 36th St Bridge overpass.
7. Cedar Lake Trail Bridge overpass
8. Approximately between TH-7 and Co Rd 5 (Minnetonka Blvd).
9. Approximately at the TH-100 NB exit to Co Rd 5 (Minnetonka Blvd).

3.3.1.1 Site 1: W 50th St Bridge luminary

Figure 3-4. Site 1 overview images.

On the overpass at W 50th street. Station located on the sidewalk and secured to the light pole at the approximate center of the bridge. During the field experiment this station was relocated a few feet east so a better view of traffic on the freeway is achieved.

3.3.1.2 Site 2: Backup location on the 48th St sound wall

Figure 3-5. Site 2 overview images.

At approximately W 48th Street, a station would have been attached to the east face of the sound wall (away from the freeway) and the telescoping pole would be extended to allow the camera to view the freeway over the top of the sound wall. The station would have been screwed into the face of the sound wall for bracing.

3.3.1.3 Site 3: Backup location at Morningside Road sound wall

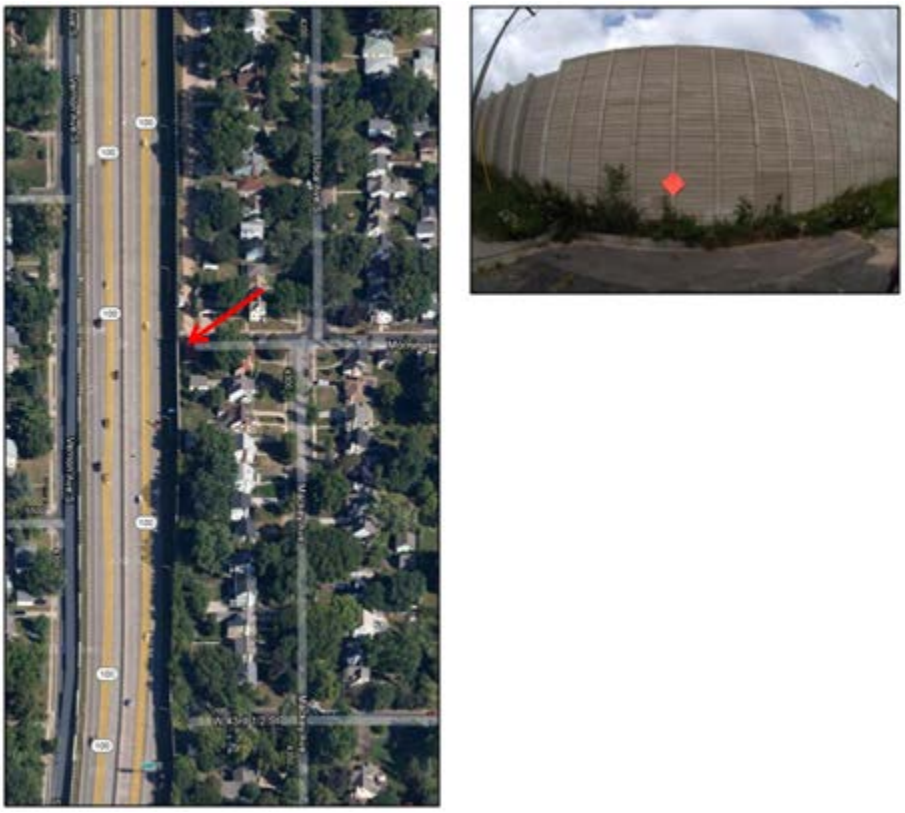

Figure 3-6. Site 3 overview images.

Similar to Site 2, at approximately Morningside Road, a station would have been attached to the east face of the sound wall with the camera observing the freeway from over the edge of the sound wall.

3.3.1.4 Site 4: W 41st St pedestrian bridge or sound wall

Figure 3-7. Site 4 overview images.

At approximately W 41st St a standard station was deployed along the east side of the sound wall as in Sites 2 and 3. Note that the location is just off to the side from the stairs as pictured in Figure 3-7.

3.3.1.5 Site 5: Park Center Blvd luminary

Figure 3-8. Site 5 overview images.

A station was attached to the light pole along Park Center Boulevard at approximately Auto Club Way. Initially it was planned that the pole for this station would only need to extend roughly 15 feet above the road surface of Park Center Boulevard. During the field experiment, taking into account the distance with the freeway mainline the full extent of the mast was utilized and modifications were made to safely secure it on the light pole.

3.3.1.6 Site 6: W 36th St Bridge overpass.

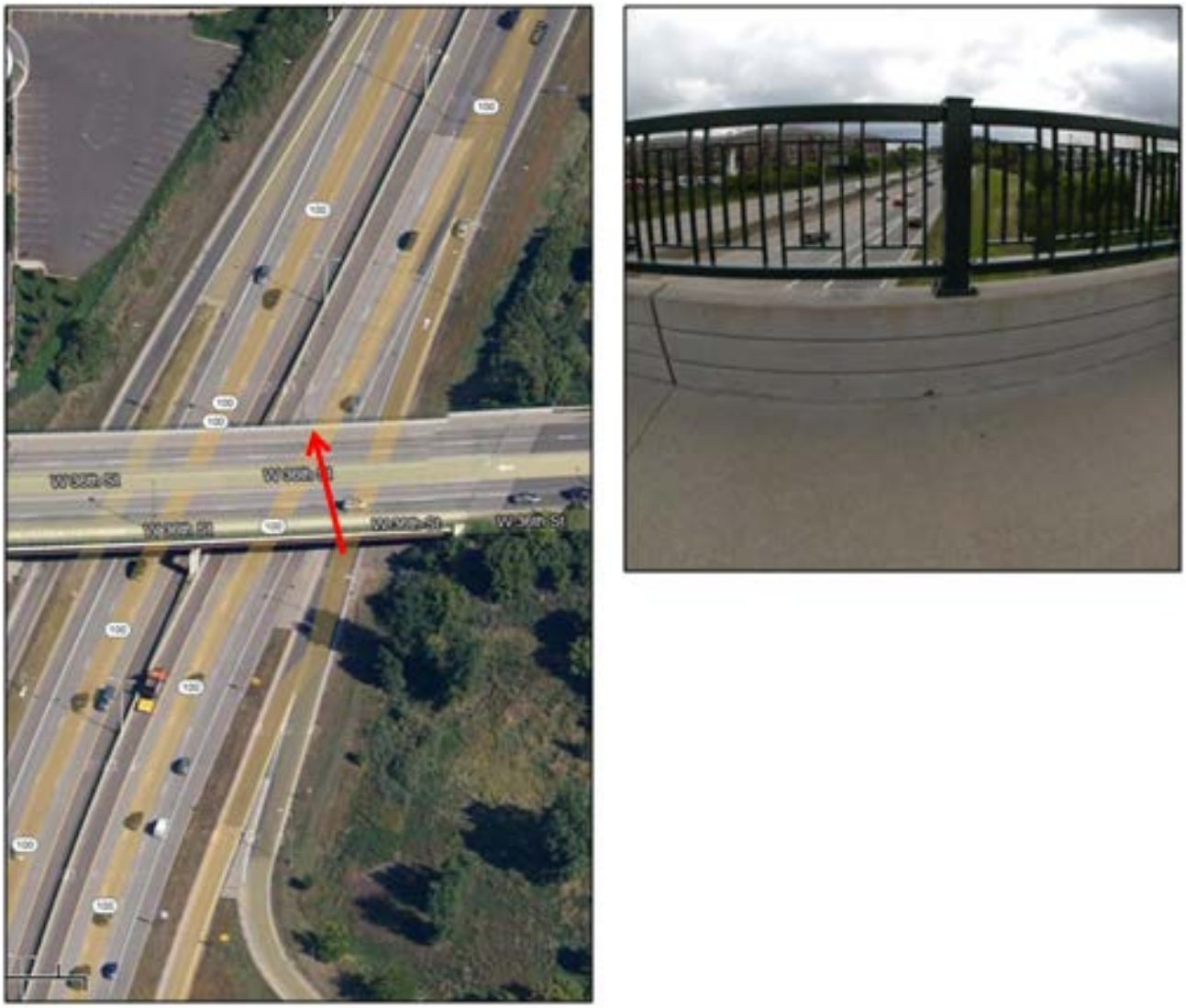

Figure 3-9. Site 6 overview images.

On the overpass at W 36th Street, a station was attached to the guard rail along the north sidewalk. Like on 50th Street the original location of the station was not directly over the freeway but later moved to the center for better data collection. The pole was extend up to 15 feet above the bridge deck.

3.3.1.7 Site 7: Cedar Lake Trail Bridge overpass.

Figure 3-10. Site 7 overview images.

On the Cedar Lake Trail Bridge, a station was secured to the fencing along the north side of the Greenway. For the purposes of this location a new, mast-less, version of the MTO station was developed. The camera is secured on the chain link fence and the recording equipment is on a waterproof box on the ground behind the wall. These modifications were necessary to increase the security of the station and reduce its visibility from the Greenway commuter trail.

3.3.1.8 Site 8: Between TH-7 and Co Rd 5 (Minnetonka Blvd).

Figure 3-11. Site 8 overview images.

Another mast-less version of the MTO surveillance station was developed with the camera enclosure mounted to the tree shown above approximately halfway between the bridges of TH-7 and County Road 5. The tree is on the outside of a fence along a walking path. The base unit was secured at the base of the tree.

3.3.1.9 Site 9: Approximately TH-100 NB exit to Co Rd 5 (Minnetonka Blvd)

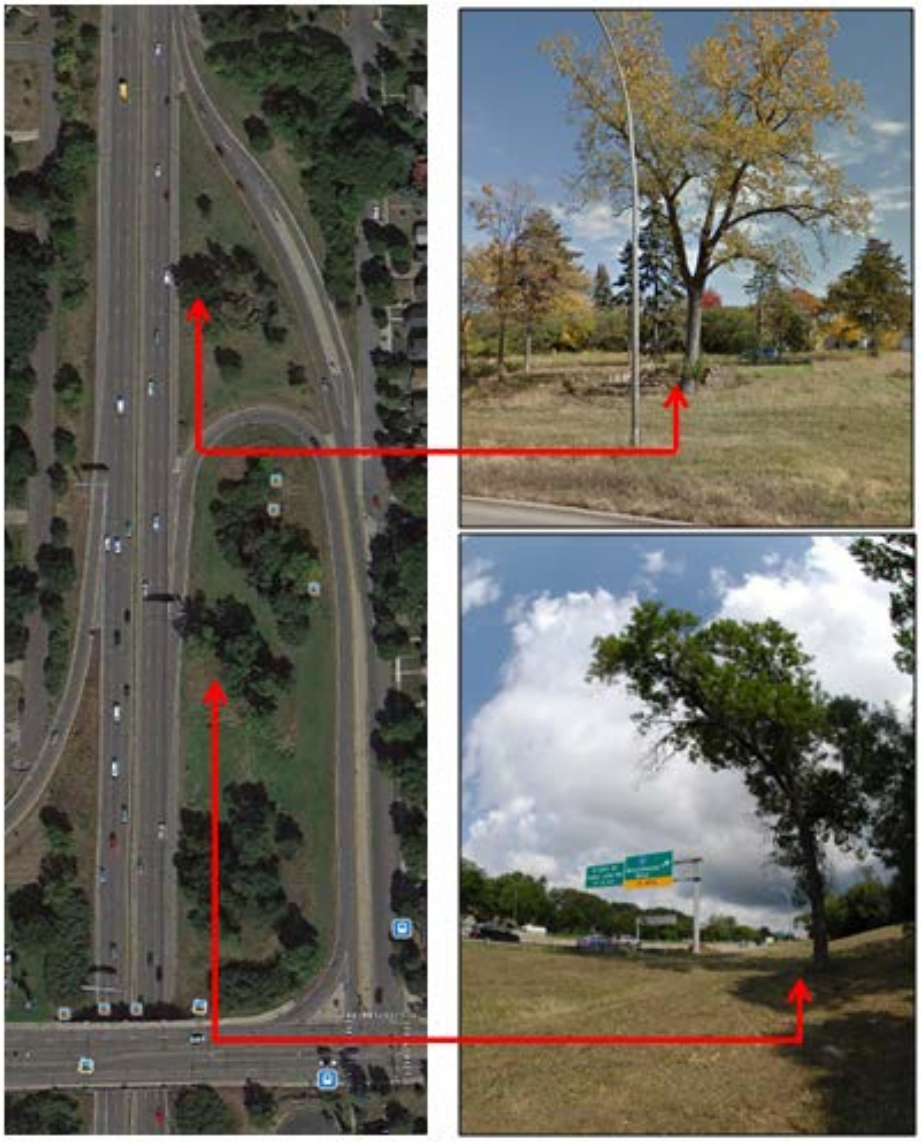

Figure 3-12. Site 9 overview images.

As with Site 8, a regular MTO surveillance station was mounted to a tree located approximately 70 feet from the freeway fog line just north of Minnetonka Boulevard. Almost immediately after the initial deployment the station was moved further north on a tree between the entrance and the exit to the freeway. The reason for the change was to improve the quality of the data collected. The

4 REDUCTION OF VIDEO DATA AND COLLECTION OF TRAFFIC MEASUREMENTS

Two methodologies were employed in reducing the video data collected into usable information for the evaluation of the ramp metering algorithms. Both methodologies required a lot of effort which retrospectively it did not reflect in the conclusions reached. Unfortunately this did not became known early enough to greatly affect the project progress which resulted in great delays and time extensions.

The first methodology involved the processing of the video data with the Autoscope machine vision sensor to extract better measurements of speeds as well as microscopic elements of traffic flow like time and space headways between vehicles. Details of this procedure will be presented in the next section.

The second methodology involving the collected video data involved the manual extraction of travel times from the days selected for the analysis. This involved a number of undergrad students watching the video and identifying vehicles at subsequent stations. Details of this procedure will be presented later in this chapter. Before proceeding in describing the two analysis methodologies and their results the amount and dates video was collected is presented.

4.1 VIDEO DATA COLLECTED ON TH-100

Views of the collected video can be seen in Figure 4-1. Some of these views changed a little during the field experiment to improve data collection but the locations remained the same. Data collection took place during the months of May and June of 2013. Specifically, video was collected during every week day from May 13 to June 21. Not all video collected was good enough to reduce by the Autoscope due to camera movement and rain. Table 4-1 shows the days video was collected and which part of the day and location was reduced with the Autoscope. The same table also shows which ramp metering strategy was active during each of the field test days. To be precise the ramp metering strategy was always changed midday the Monday of the week it was going to be active. This means that the AM of each Monday was under the control of the previous week strategy. During the first two weeks there was a mistake in switching the control of the ramp on 50th St and while the others were running the Stratified Zone Metering algorithm (SZM), that one was running the UMD KAdaptive algorithm (UMD). This issue was resolved when it was discovered and a full week of only the SZM in control was later executed.

For each view and view variation an Autoscope detector layout was developed and calibrated. An example of one such detector layout can be seen in Figure 4-2. In the figure, the three types of detectors are presented. Count detectors supply the counts for the Detector Stations and Speed detectors provide speed. The Stations aggregate the data every 30sec. Both the Count and Speed detectors also output individual vehicle presence and speed respectively. The later since it is time stamped it also provides time headways also. Calibrating the Autoscopes required great effort since the cameras were either moved intentionally, to improve capture performance, or unintentionally either by the wind or because the pole deflated/lowered overnight. In total,

instead of having only seven detector layouts it finally required to develop 45 layouts. This consumed a lot of the project time on top of the fact that each of these videos had to be played in real speed since the Autoscope is not designed to operate with video running faster than real time.

As was pointed out earlier, retrospectively the data extracted from the Autoscope did not offer much additional detail over the analysis of loop detector data and given the effort to utilize them their use did not go beyond verifying and adjusting the loop detector speed estimation by calibrating the effective vehicle length instead of using the default provided by IRIS.

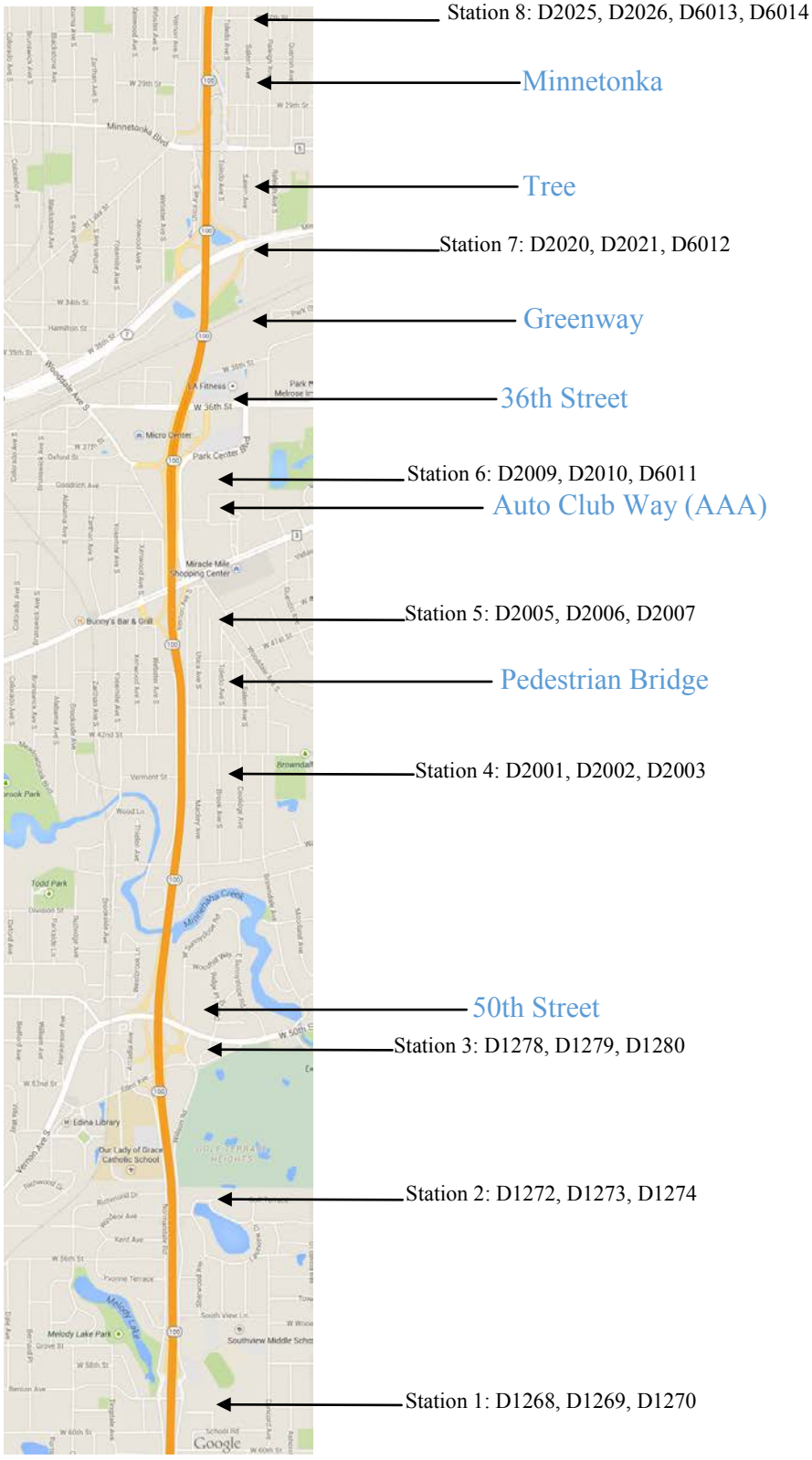

Figure 4-1. Data collection locations: (blue) is video, (black) loop stations.

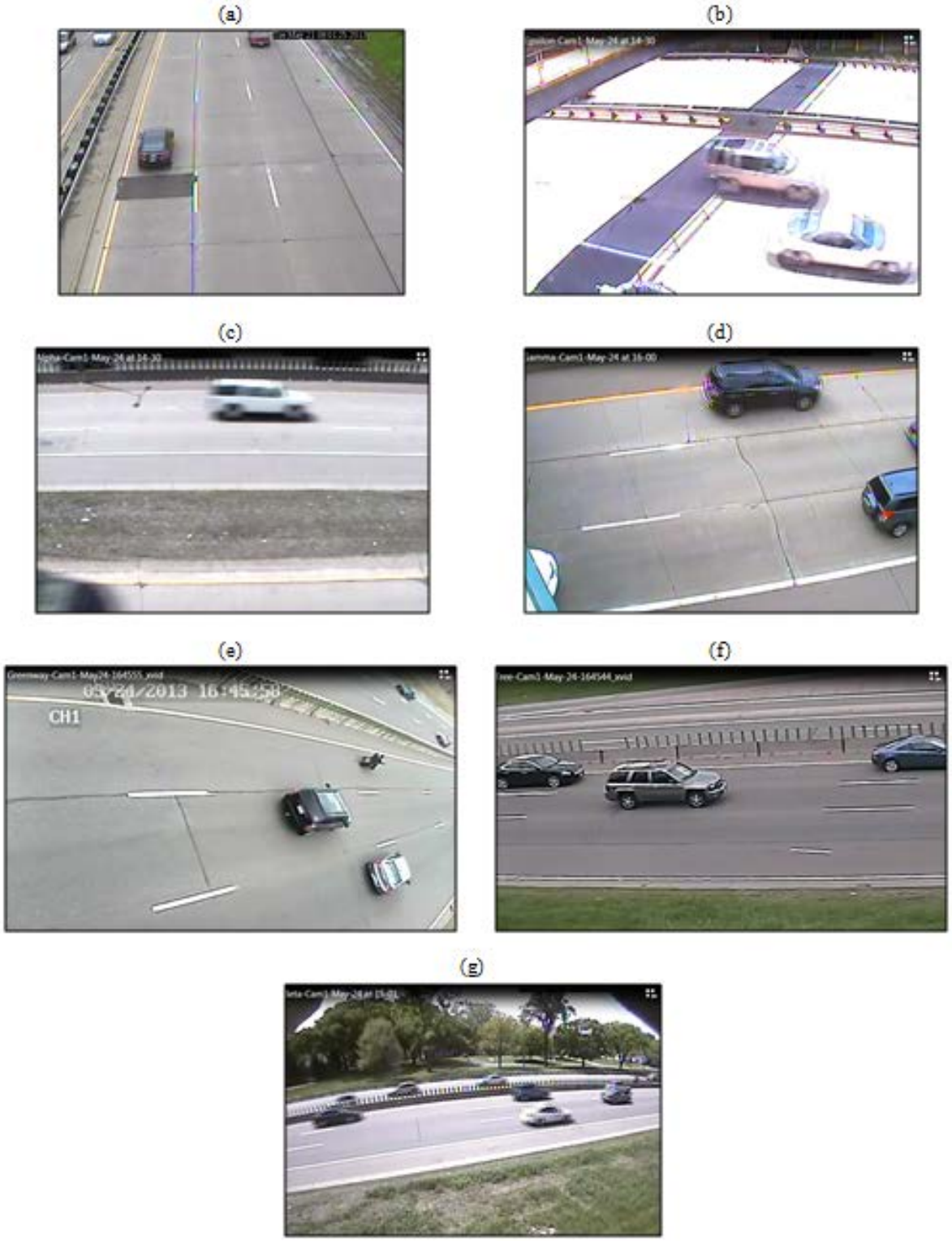

Figure 4-2. Sample images from each video collection location: (a) 50th Street, (b) Pedestrian Bridge, (c) Auto Club Way, (d) 36th Street, (e) Greenway, (f) Tree, (g) Minnetonka.

Table 4-1. Video reduced by Autoscope.

Dates	Ramp Strategy	50th Street	Ped Bridge	Auto Club	36th Street	Greenway	Tree	Minnetonka
May 13, 2013	SZM	AM+PM	x	AM+PM	AM+PM	x	x	x
May 14, 2013	SZM	AM+PM	x	AM+PM	AM	x	x	x
May 15, 2013	SZM	AM+PM	x	AM+PM	AM+PM	x	x	x
May 16, 2013	SZM	AM+PM	x	AM+PM	AM	x	x	x
May 17, 2013	SZM	AM+PM	x	AM+PM	AM+PM	x	x	x
May 20, 2013	SZM	AM+PM	AM+PM	AM+PM	AM+PM	AM+PM	AM+PM	AM+PM
May 21, 2013	SZM	AM+PM	PM	AM+PM	AM+PM	AM+PM	x	AM
May 22, 2013	SZM	x	AM+PM	AM+PM	AM+PM	AM+PM	x	PM
May 23, 2013	SZM	AM+PM	AM+PM	AM+PM	AM+PM	AM+PM	x	AM+PM
May 24, 2013	SZM	AM+PM	PM	AM+PM	AM+PM	AM+PM	AM+PM	AM+PM
May 27, 2013	UMD	AM	x	x	AM+PM	x	x	x
May 28, 2013	UMD	AM+PM	AM+PM	AM+PM	AM+PM	AM+PM	AM+PM	AM+PM
May 29, 2013	UMD	AM+PM	AM+PM	AM+PM	AM+PM	AM+PM	AM+PM	PM
May 30, 2013	UMD	AM+PM	AM+PM	AM+PM	AM+PM	AM+PM	AM+PM	AM+PM
May 31, 2013	UMD	AM+PM	AM+PM	AM+PM	AM+PM	AM+PM	AM+PM	AM+PM
June 3, 2013	SZM	AM+PM	x	AM+PM	AM+PM	AM+PM	AM+PM	AM+PM
June 4, 2013	SZM	AM	AM+PM	x	AM+PM	AM+PM	AM+PM	AM+PM
June 5, 2013	SZM	x	x	x	x	x	AM+PM	AM+PM
June 6, 2013	SZM	x	x	PM	AM+PM	AM+PM	AM+PM	AM
June 7, 2013	SZM	PM	x	AM+PM	AM+PM	AM+PM	x	x
June 10, 2013	UMD	AM+PM	PM	AM+PM	AM+PM	AM+PM	x	AM+PM
June 11, 2013	UMD	AM+PM	AM+PM	AM+PM	AM+PM	AM+PM	AM+PM	AM+PM
June 12, 2013	UMD	AM+PM	AM+PM	AM+PM	AM	AM+PM	x	AM+PM
June 13, 2013	UMD	AM+PM	AM+PM	AM+PM	x	AM+PM	x	AM+PM
June 14, 2013	UMD	AM+PM	AM+PM	x	x	AM+PM	x	AM+PM
June 17, 2013	UMN	PM	x	x	AM+PM	x	x	x
June 18, 2013	UMN	AM+PM	AM+PM	AM+PM	AM+PM	AM+PM	AM+PM	AM+PM
June 19, 2013	UMN	AM+PM	AM+PM	AM+PM	x	AM+PM	x	AM+PM
June 20, 2013	UMN	AM+PM	x	AM+PM	AM+PM	AM+PM	x	AM+PM
June 21, 2013	UMN	AM+PM	x	x	AM+PM	x	x	x

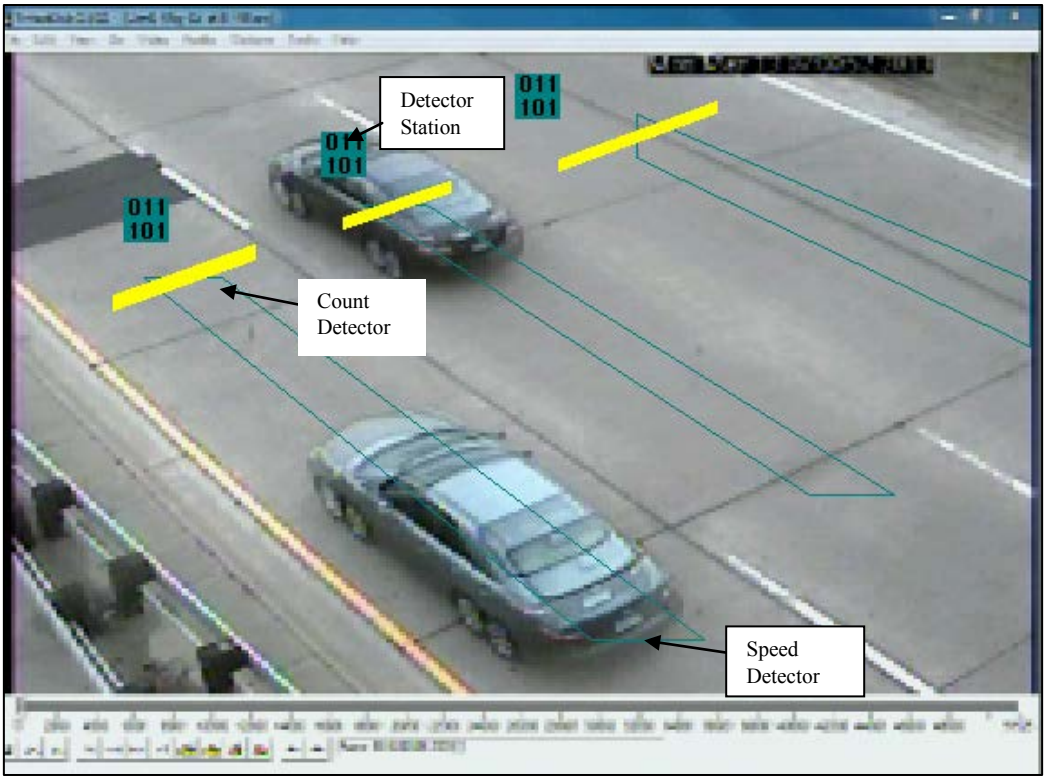

Figure 4-3. Example of one Autoscope detector layout for 50th Street.

An additional problem that was detected later was the fact that the video recorder clocks did not keep accurate time and drifted during the times the system power was off. This resulted in spending a lot of time and effort to develop correction factors for each day and station. The correction factors were determined manually by watching video from uncongested parts of the day, selecting vehicles that stand out, finding them and their speed in the Autoscope data, and then locating them on each subsequent station. The speed was used to determine an average travel time under free flow conditions and since we know the distance between stations it was possible to calculate the time difference between stations. All station times were adjusted by taking the clock of the 50th Street station as the base. The time correction was necessary for both the Autoscope data collection as well as the manual extraction of travel times explained in the next section.

4.2 TRAVEL TIME MEASUREMENT COLLECTION AND ANALYSIS METHODOLOGY

The video records allowed the research team to collect actual vehicle travel times for most of the days of the field deployment. These measurements are the most accurate data because they do not depend on any particular sensing technology and they were not based on aggregated raw measurements which is the case with loop detectors. A particular sampling methodology was developed in order to balance the measurement of travel times and effort/time available. Specifically, for all available video records, starting at the station at 50th St, one vehicle was selected on each lane at random. These three vehicles were then identified on all subsequent stations and their time of arrival was recorded. If a vehicle exited before the last station in

Minnetonka Ave, it was noted and another vehicle was selected to replace it for the rest of the distance. This process was repeated every 5 minutes for the whole length of the available video. Not all days of the field experiment were utilized, since discussions with the MnDOT technical liaisons, produced a priority list of day pairs selected from SZM and UMD weeks. Several days were excluded because of heavy rains that affected traffic speeds. The collection of the travel times allowed the research team to measure the travel time for the whole trip as well as the travel times from station to station. The latter is used later to track the extent of the congestion. This depiction of congestion is more accurate and informative than the traditional based on spot measurement of speeds since it takes into account short length slowdowns between stations due to shockwaves.

The analysis of the travel time data takes place by comparing pairs of days with similar traffic and environmental conditions. The analysis of loop detector data also follows the same methodology and uses the same day pairs. Because of video outages and other factors related with the reduction of the data, there were discontinuities in the travel time samples. To deal with this an interpolation methodology in space and time was developed to cover the gaps with the best possible estimates of travel time. The graphs in Figure 4-4 show the travel time measurements in space and time. The top graph is before the interpolation while the bottom one is after the data were filtered through the interpolation method. The graphs on Figure 4-5 show the travel times between stations. Essentially they are slices of the surface in Figure 4-4.

4.3 LOOP DETECTOR TRAFFIC MEASUREMENTS AND ANALYSIS METHODOLOGY

For the comparison of metering algorithm performance on TH-100 through loop detector data, a 6.5 kilometers congested segment of the TH-100 freeway was selected starting almost 2 kilometers before 50th Street with direction north, up until Minnetonka Blvd. On the map in Figure 4-1, the detector station locations are displayed along with the ones where video was collected. For this part of the analysis, only the loop detector data in the mainline and on the ramps are utilized.

In the mainline, there are 25 loop detectors at 8 different location (1 detector per lane). These were aggregated in 8 new detectors with code numbers 1 to 8. At the ramps, 7 passage detectors, 8 queue detectors, as well as 5 off-ramp detectors were included in the study. The details of the detectors used are shown in Table 4-2 and Table 4-3. The loop detector data from several days and day pairs were used to construct Flow and Occupancy graphs and contour plots, as well as Macroscopic Fundamental Diagrams (MFDs). The distances are measured from the location of the first upstream station to approximately 6.5 kilometers downstream. The location where the active bottleneck most of the times is located approximately 200m upstream of the TH-7 entrance ramp.

In the analysis, 10 days in 2013 are utilized. More specifically, the days representing the SZM metering algorithm are May 22, May 23, May24, June 3 and June 4 whereas May29, May30, May 31, June 10 and June 11 provide data measured with the UMD algorithm . Please note that Mondays (June 3 and June 10) were the switching points, meaning that a different algorithm is applied in the morning and in the afternoon (in the morning the UMD algorithm was used on the

3rd of June and the SZM on the 10th of June, whereas the opposite happens in the afternoon). Five pairs derived from this data set. These pairs include the same weekday with the SZM algorithm and the respective weekday the following week with the UMD algorithm. In particular the pairs of days are May 22 and 29, May23 and 30, May24 and 31, June 3 and 10 as well as June 4 and 11.

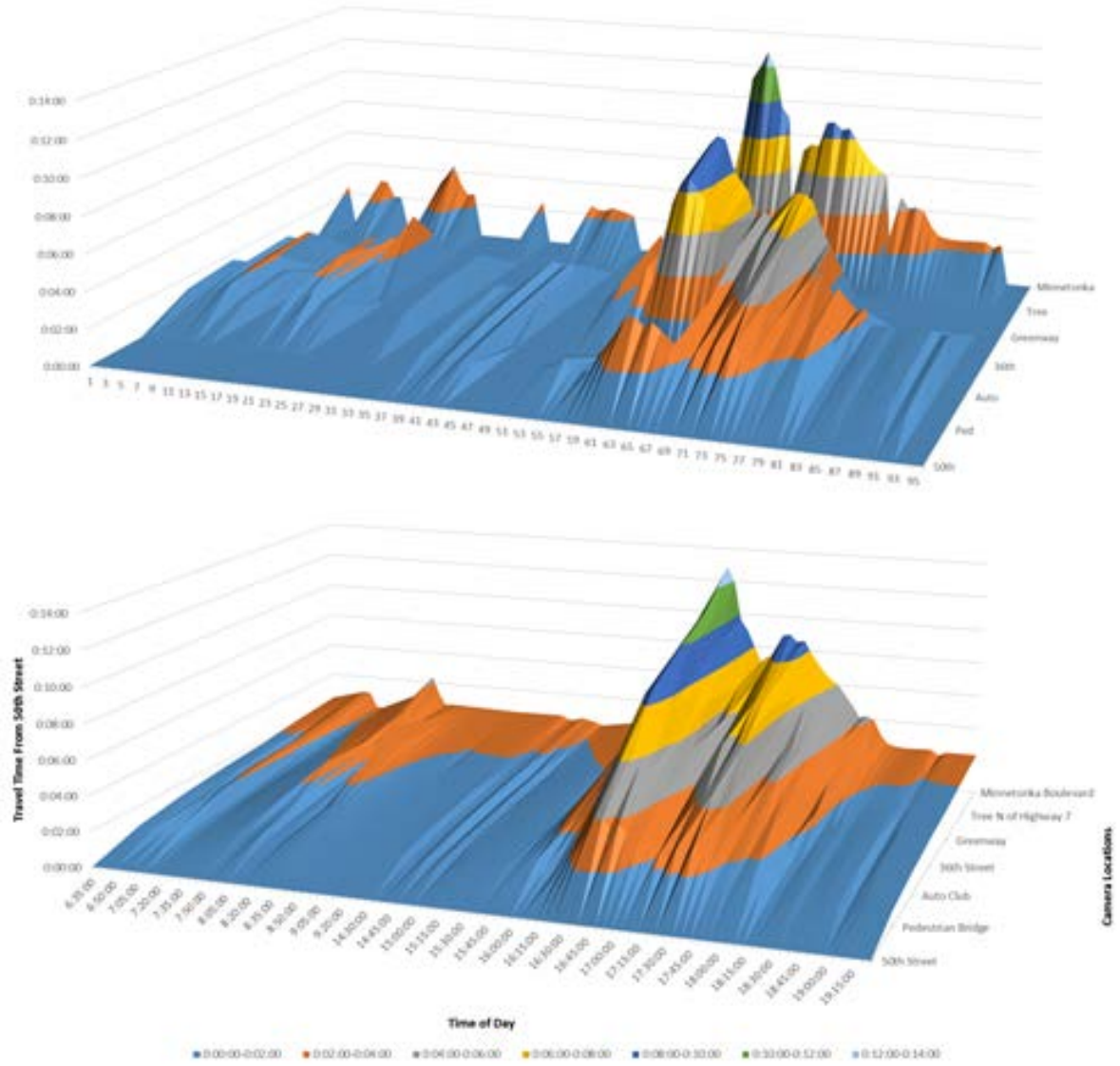

Figure 4-4. Travel time graphs before and after interpolation.

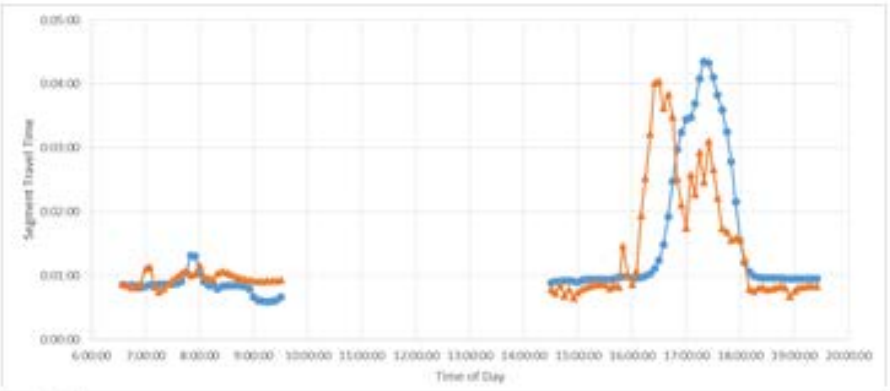

50th St to Pedestrian bridge

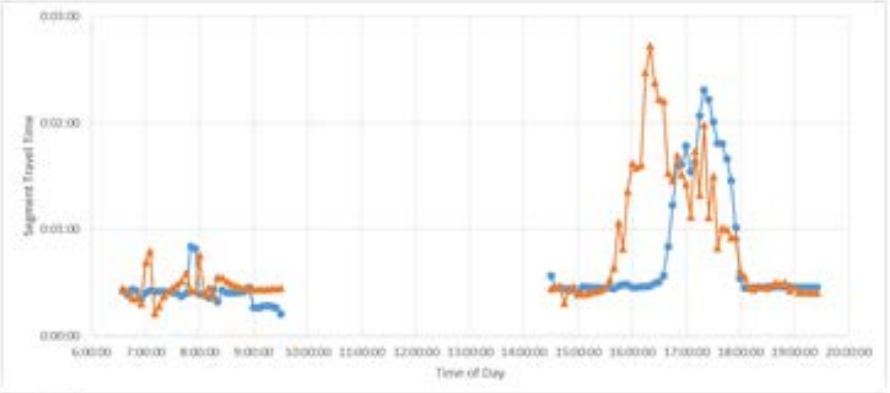

Pedestrian bridge to AAA

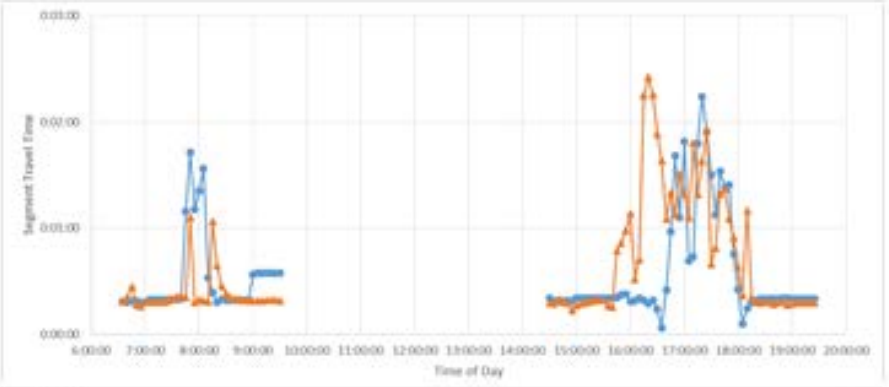

AAA to 36th St.

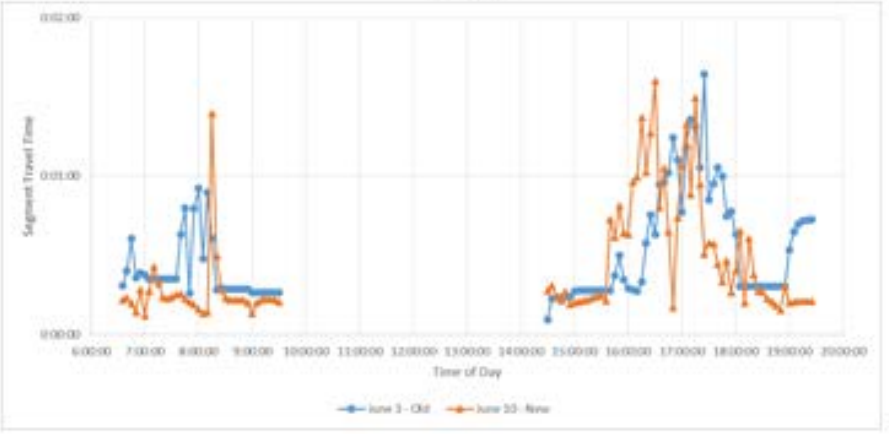

36th St to Greenway

Figure 4-5. Station to station travel time graphs.

Table 4-2. Detector IDs, types, and distances expressed in meters.

Category	ID	Milepost		Category	ID	Milepost
L1	1268	0		L1	2009	4370
L2	1269	0		L2	2010	4370
L3	1270	0		L3	6011	4370
Passage	1271	315		Exit	2008	4415
L1	1272	1005		Queue	3649	4540
L2	1273	1005		Passage	2012	4540
L3	1274	1005		Queue	3650	4655
Exit	1275	1565		Passage	2013	4655
L1	1278	1735		36th str		4775
L2	1279	1735		Greenway		5160
L3	1280	1735		Exit	2017	5170
Passage	1276	1795		L1	2020	5435
Queue	3775	1795		L2	2021	5435
Queue	3626	1795		L3	6012	5435
50th Street		1915		Queue	6010	5635
Queue	3645	2090		Queue	3652	5635
Passage	1277	2090		Passage	2022	5635
L1	2001	3080		Tree		5725
L2	2002	3080		Exit	2023	6010
L3	2003	3080		Minnetonka		6220
Pedestrian Bridge		3475		Passage	2024	6435
Exit	2004	3675		Queue	2011	6435
L1	2005	3725		L0	2025	6575
L2	2006	3725		L1	2026	6575
L3	2007	3725		L2	6013	6575
Auto club		4225		L3	6014	6575

Table 4-3. Relabeled mainline detectors.

New Detectors	IDs of detectors included				mileposts
1	1268	1269	1270	-	0
2	1272	1273	1274	-	1005
3	1278	1279	1280	-	1735
4	2001	2002	2003	-	3080
5	2005	2006	2007	-	3725
6	2009	2010	6011	-	4370
7	2020	2021	6012	-	5435
8	2025	2026	6013	6014	6575

The information provided from the loop detectors contain flow, occupancy, and speed data for 30 second time periods from 6 am to 6 pm. Nevertheless, morning and afternoon peak periods are identified to be more or less between 7-9 am and 3-6 pm respectively. For each of the days above, performance indicators are measured for both the morning and the evening peak periods.

4.3.1 Description of Methodology

To have a clear view of the demand and congestion in the freeway segment analyzed as well as to evaluate the contribution of the compared ramp metering strategies to the improvement of the mainline and ramp performance, the following performance indicator methods are chosen:

- Contour plots of flow and occupancy from the mainline loop detectors.
- Performance of queues at on-ramps.
- Investigation of capacities through the Fundamental Diagrams (FD)
- Derivation of network level Macroscopic Fundamental Diagrams (MFD).

After the source of the active bottleneck is identified from the contour plots, flow and occupancy time series of the closest detectors can help in a more careful look at the bottleneck (like a zoom in) and more accurate computations of the active bottlenecks durations. In the resulted time periods some additional time should be prudently added that includes some uncongested time periods before and after the congested duration so as to verify that demand instead of supply is depicted for the analysis.

Regarding the ramps' performance, equity of traffic management schemes in freeways is a high priority. Violations of queue constraint and activation of higher metering rates create additional congestion both in the freeway and the ramps and decrease the efficiency of ramp metering. These types of violations are identified by high values of occupancy in the ramps at the queue detectors and were monitored with the time of day for the various strategies. Flow and occupancy time series of the passage (at the intersection with the mainline) and queue (at the beginning of the on-ramp) detectors respectively facilitates this type of investigation. It is known that a coordinated strategy has as an objective to equalize queues at ramps in the proximity of the bottleneck and avoid queue violations.

Last, the capacities on the Fundamental Diagrams (FD) are considered. The capacity of freeway sections is most commonly defined as the maximum flow possible at a specific location under the current circumstances. Active bottlenecks can influence the maximum flow upstream or downstream and cause congestion on networks. The performance at one location thus can bring down the performance of the entire system. While this maximum possible flow was traditionally considered a fixed value for a given location, many studies have revealed that there is a stochastic nature of bottleneck capacities and strong capacity drops (see for example Srivastava and Geroliminis, 2013 or Zhang and Levinson, 2004 for Twin Cities analysis). Plotting flow-density fundamental diagrams for different locations will help identify (i) the value(s) of capacity, (ii) its fluctuations across time and space and (iii) if ramp metering strategies succeed in retaining such values for long times. Given that loop detectors are usually located upstream of the merge, a correct estimation of capacity and the relationship with the level of congestion in the mainline has to be contacted by plotting mainline detector occupancy vs. throughput flow.

Throughput has to be estimated as the sum of volumes at the upstream mainline detector station and volumes at the on ramp merge. For a more concrete explanation, the reader could refer to Srivastava and Geroliminis (2013). FDs will be constructed for the 3 locations of the merges in the study site (data will be aggregated in 3 minute intervals to avoid dispersed plots). Figure 4-6 shows an example of such an FD. Note the strong variations of capacities and the highly congested points for densities more than 40 veh/m.

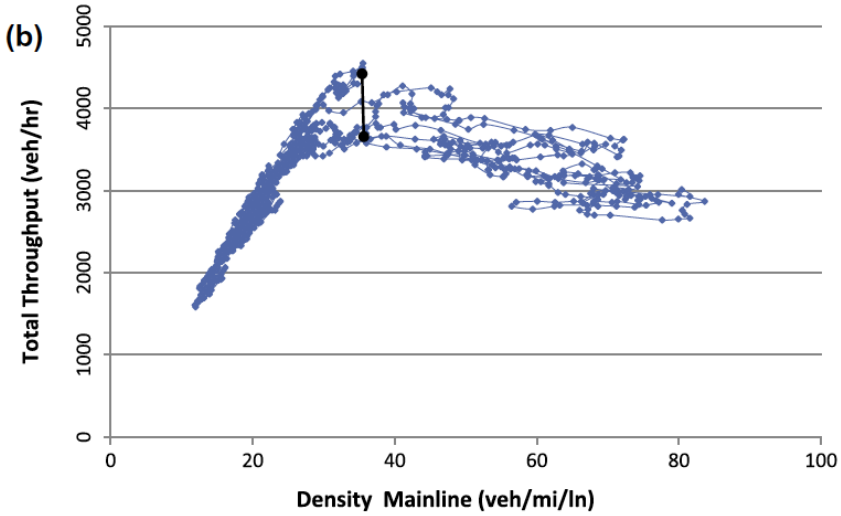

Figure 4-6. Example fundamental diagram in a merge location.

Finally, Macroscopic Fundamental Diagrams (MFD) are plotted for the whole mainline freeway. MFD estimates in short time intervals (e.g. every 3 minutes) the space-mean (average across space) flow vs. the space-mean occupancy from all the mainline detectors. This plot can provide a rough estimate of the average network density and identify how the active bottlenecks breakdown and their severity influence the overall performance of the freeway. If locations with various levels of congestion are aggregated (both congested and uncongested locations) then hysteresis loops might be identified in the MFD (usually clockwise). These hysteresis loops show that the performance of the freeway is worse in the offset of congestion for the same space-mean occupancy.

The performance measures presented herein have strong transferability and can be integrated at a future project in MnDOT framework of performance measures. They can be streamlined for the whole freeway network to provide a quick and reliable input for problematic locations that need intervention and advanced traffic management.

In addition to the visualization based methodologies, quantifiable traffic performance measures are available to assist in the algorithm comparison. More specifically for each of the 8 detectors the average flow during the morning (or evening) peak is estimated. The weighted average of flow with respect to the distance between detectors provides a good estimation of the Vehicle Kilometers Travelled (VKT) during the analysis period. This VKT estimation is a good proxy for the total demand occurred during this period of analysis (as it contains some uncongested periods before and after the peak period to guarantee that demand and not supply is calculated). VKT is a

measure of system productivity since the higher it is the more vehicles have used the corridor in the given time interval. Similarly, Vehicle Hours Traveled (VHT) is a measure of the service provided by the corridor since the higher it gets the more time vehicles spent in the corridor. Because demand is not the same from day to day the final performance measure is the overall speed of the network then $\overline{U} = VKT/VHT$ which is higher when more vehicles use the corridor and/or spending less time traversing it. The following section describes how to estimate these quantities from loop detector measurements of volume and occupancy.

Consider that the freeway is divided in N segments (N=8 for our case) with index i=1,2,..,N and length l_i (units in lane-km) and one detector per segment that provides flow and occupancy measurements averaged across lanes, q_{it} and o_{it} in each time interval t=1,2,…,T with duration τ (30 seconds in the case of MnDOT loop detectors). Assuming an effective vehicle length of L in meters, then density at segment i and interval t can be approximated as $k_{it} = \frac{o_{it}}{100}\frac{1000}{L}$ (units of density is veh/km/lane). From that and the fundamental relationship u=q/k we get that $u_{it} = \frac{V\,L}{10 o_{it}\,\tau}$ which is the average speed on segment i at time interval t serving a V vehicles. The travel time at that segment is $TT_{it} = \frac{l_i}{\frac{V\,L}{10 o_{it}\,\tau}}$ and the total travel time is TT_{it}*V which is the same as VHT. VKT and VHT for the time of analysis can be approximated as (VKT and VHT are estimated averaged across lane and can be easily multiplied by the number of lanes and have units for the whole freeway):

$$VKT = \tau \sum_{t=1}^{T}\sum_{i=1}^{N} q_{it} * l_i \qquad \text{Eq. 4-2}$$

$$VHT = \tau \sum_{t=1}^{T}\sum_{i=1}^{N} 10\, o_{it} * l_i / L$$

Eq. 4-1

Physically speaking, equation 1b states that to calculate VHT, we need to sum the number of vehicles in the network across all different time intervals. If a vehicle enters the network at time t_1 and exits at time t_2, then it contributes in the density of the freeway (in different segments possibly) at all intervals between enter and exit time. Note that vehicles should not travel more than one segment during duration τ, as equations might be slightly more complicated. These formulas are good approximations but with small estimation errors due to the fact that flow and occupancy are measured at a limited number of locations and these equations assume that similar conditions occur in the whole segment with the ones measured in the detectors. While more complicated approaches exist (e.g. integrating traffic flow models as in Srivastava and Geroliminis, 2013) previous research from many researchers and practitioners have shown that having one detector per segment between successive ramps, provides good approximations. The average flow and density can be estimated as:

$$\bar{Q} = \frac{\sum_{t=1}^{T}\sum_{i=1}^{N} q_{it} * l_i}{\sum_{i=1}^{N} l_i}$$

Eq. 4-3

$$\overline{K} = \frac{\tau \sum_{t=1}^{T}\sum_{i=1}^{N} 10\, o_{it} * l_i}{L * \sum_{i=1}^{N} l_i}$$

Eq. 4-3

The average speed is then $\overline{U} = VKT/VHT = \bar{Q}/\overline{K}$. While equations 1 and 2 provide the correct formula for estimation of average flows and densities with weighted averages, if segment length is not taken into account and unweighted averages are utilized, the values obtained are almost identical (error smaller than 1-2%). In the next chapter these measures are used to compare conditions between pairs of days controlled with the SZM and UMD algorithms.

5 TH-100 FIELD EXPERIMENT RESULTS

Two type of analysis were performed for the evaluation of the new Density ramp metering, an analysis based on travel time data and an analysis based on loop detector data. Both methodologies compare traffic measurements between pairs of days with similar traffic and environmental conditions. The total selected day-pairs are:

- May 22nd and May 29th
- May 23rd and May 30th
- May 24th and May 31st
- June 3rd and June 10th
- June 4th and June 11th

The loop based study used all these pairs but the quality of video and time available allowed only the days in June to be used for the travel time based analysis. The following sections present the results from the day pair comparisons first from the travel time based method and later from the loop detector based one.

5.1 TRAVEL TIME BASED COMPARISON

5.1.1 June 3rd and June 10

Figure 5-1 and Figure 5-2 present the comparison of station to station travel times for morning and afternoon peak periods while Figure 5-3 shows the two travel time surfaces for the two paired days. There is one important detail regarding this specific day pair. Both days were Mondays and as it was discussed in an earlier chapter Monday noon was when the control algorithm was switched. Therefore the graphs are a little misleading since their AM is reversed as compared to the PM. Under the UMD control the morning of June 3rd had a break down while the morning of June 10th under the SZM did not have a breakdown. It is not clear if the absence of a breakdown was because of the SZM so this point will not be expanded.

The daily volumes during the UMD trial were about 5% higher at 63,028 vehicles as compared to 60,114 during the SZM day. The PM of June 3rd under the SZM control developed a shorter congested period in terms of time as compared to the PM period of June 10th under the UMD. Regardless, the congestion under the SZM seems to be stable with no evidence of recovery while the congestion under the UMD presents two peaks supporting the assumption that the control managed to recover from the heavy congestion, albeit briefly. Both algorithms show greater instability closer to the bottleneck with the UMD keeping conditions in the mainline more fluid upstream as compared to the SZM. The UMD algorithm seems to handle better the large demand ramp of TH-7 and conditions immediately upstream of it are less congested. One other observation is that the UMD algorithm shows some sharp spikes of very large travel time which could represent short lived heavy congestion conditions from which the control is able to recover.

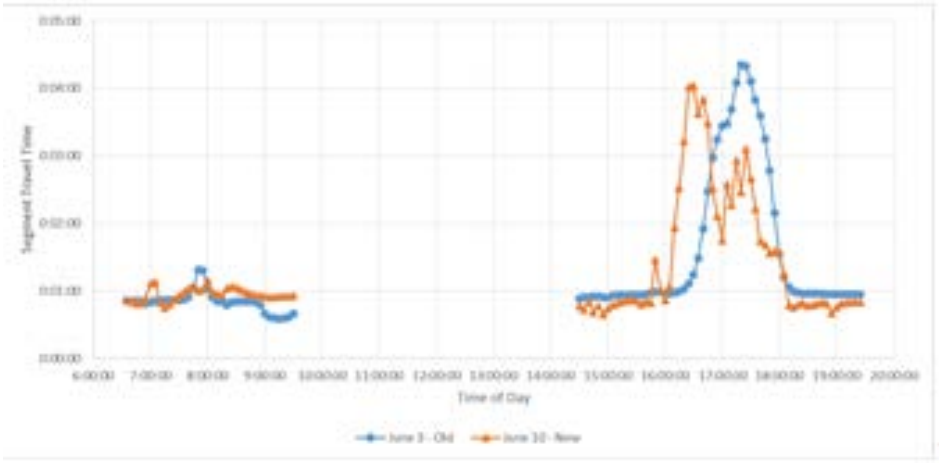

50th St to Pedestrian Bridge

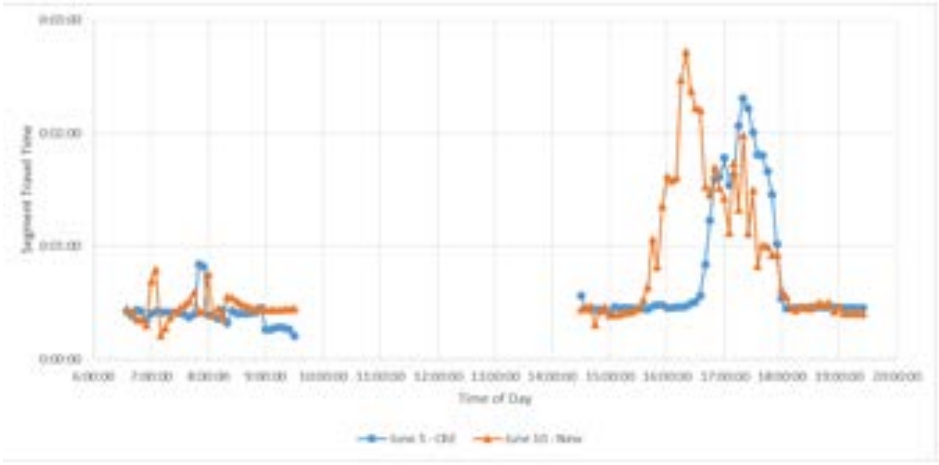

Pedestrian bridge to AAA

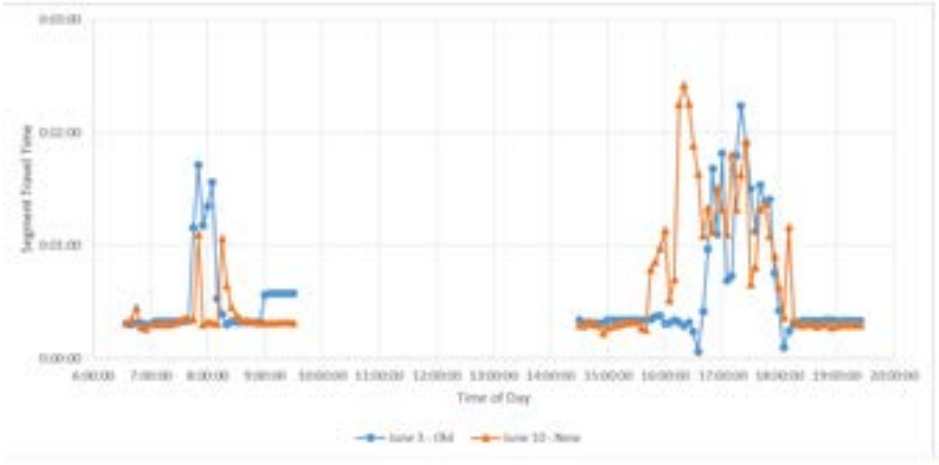

AAA to 36th St.

Figure 5-1. Station to station travel time graphs for June 3 (SZM) and June 10 (UMD).

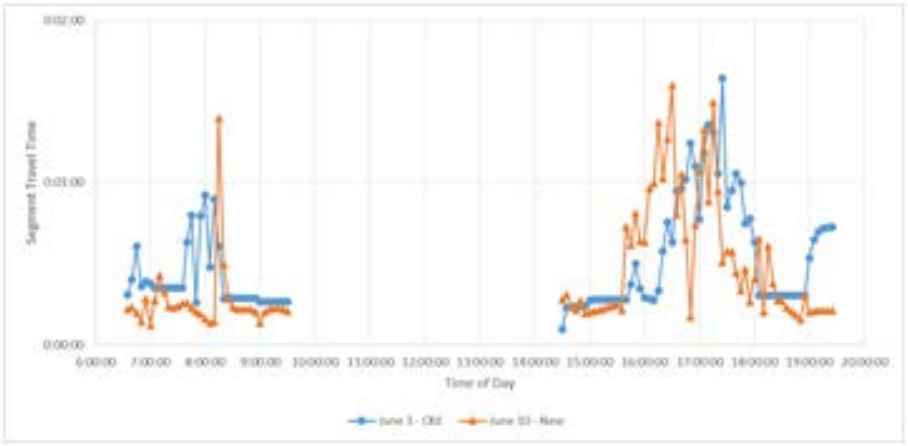

36th St to Greenway

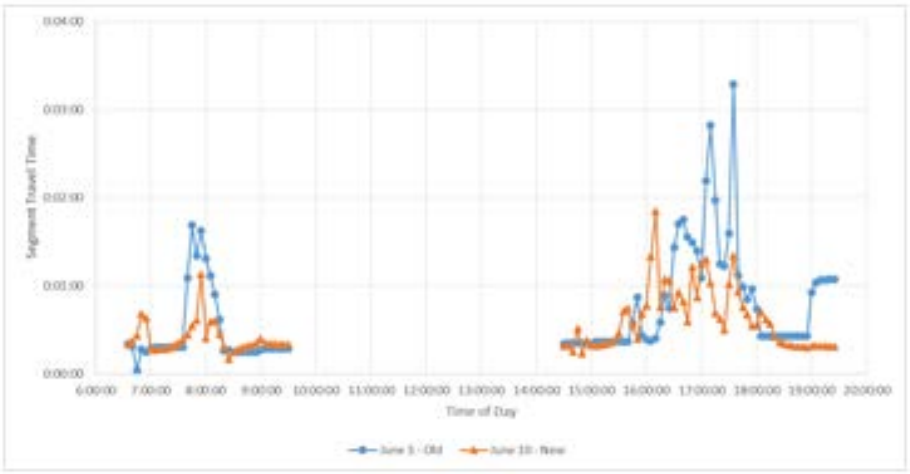

Greenway to Tree (TH-7)

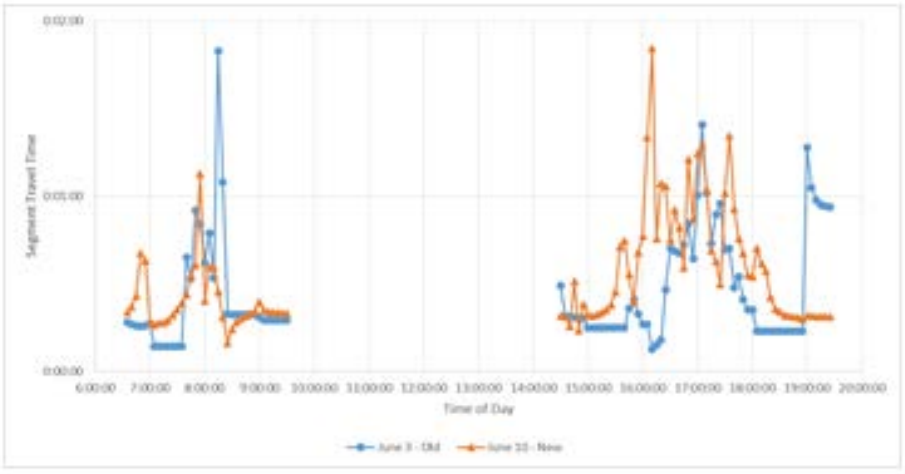

Tree to Minnetonka Ave

Figure 5-2. Station to station travel time graphs for June 3 and June 10 (continued).

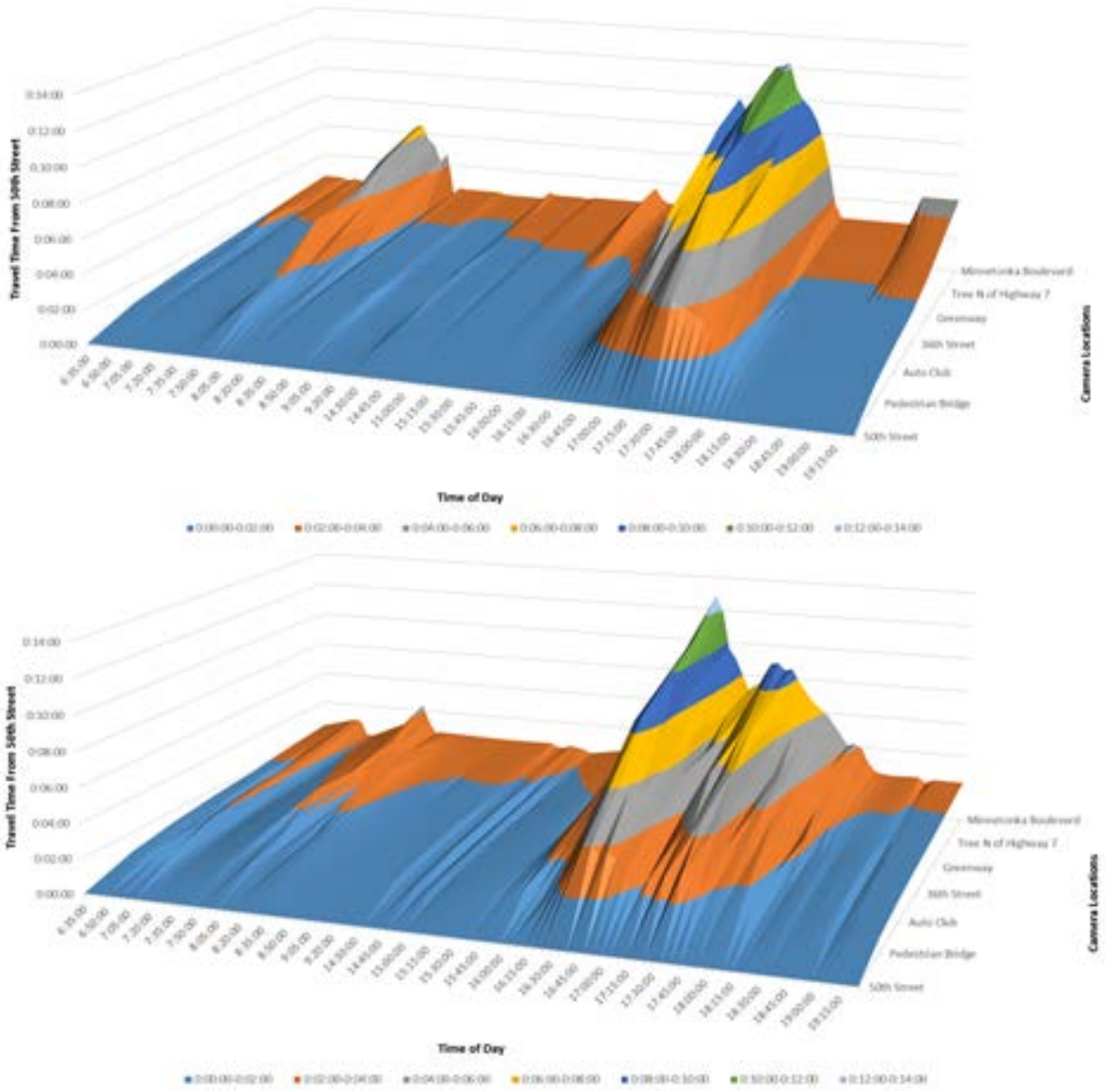

Figure 5-3. Travel time surface for June 3rd (SZM) and June 10th (UMD).

5.1.2 June 4th and June 11th

Figure 5-4 and Figure 5-5 present the comparison of station-to-station travel times for morning and afternoon peak periods. Figure 5-6 shows the two travel time surfaces for the two paired days.

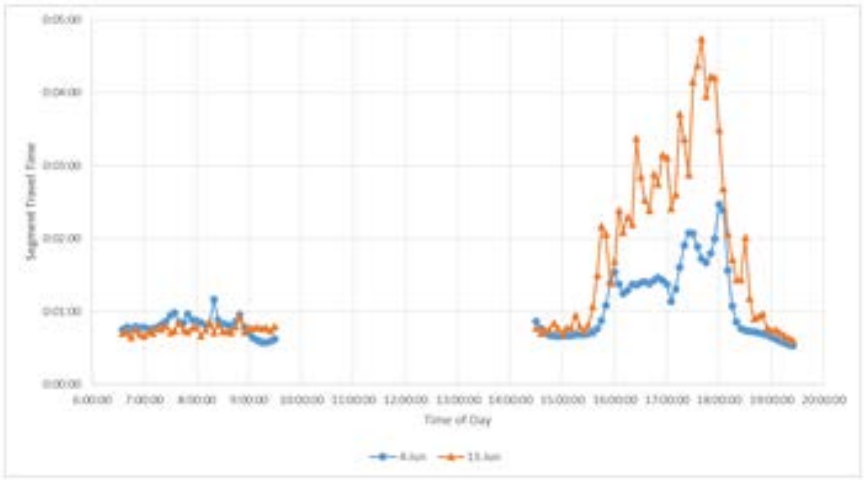

50th St to Pedestrian Bridge

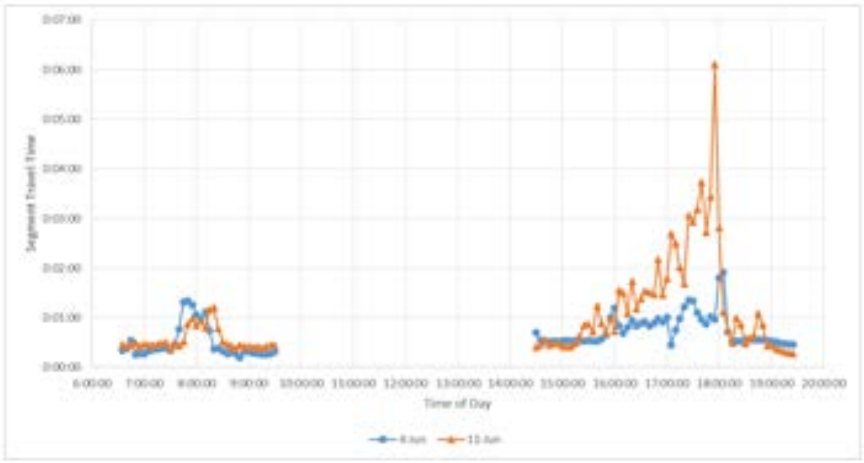

Pedestrian bridge to AAA

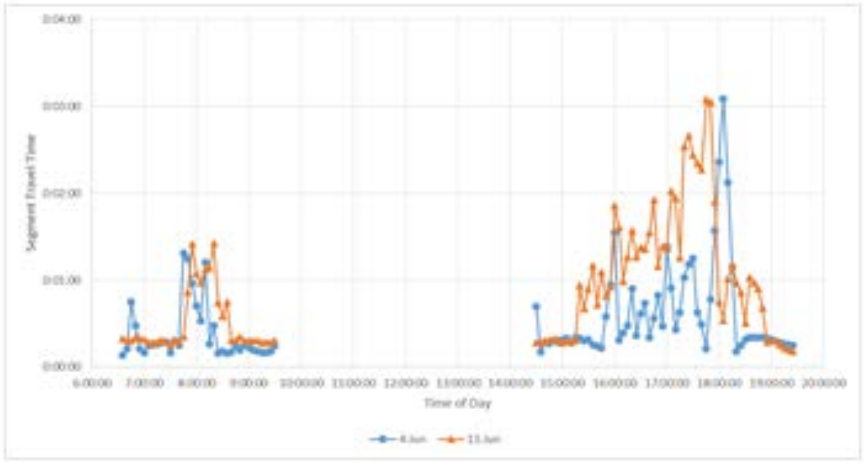

AAA to 36th St

Figure 5-4. Station to station travel time graphs for June 4 (SZM) and June 11 (UMD).

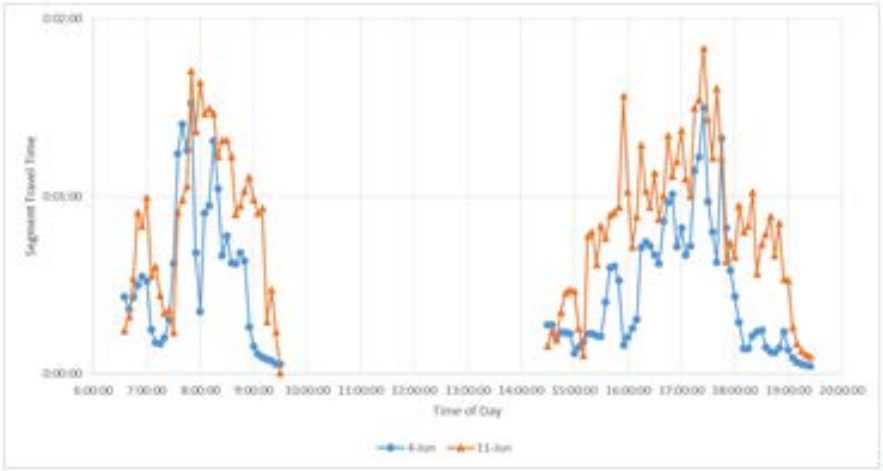

36th St to Greenway

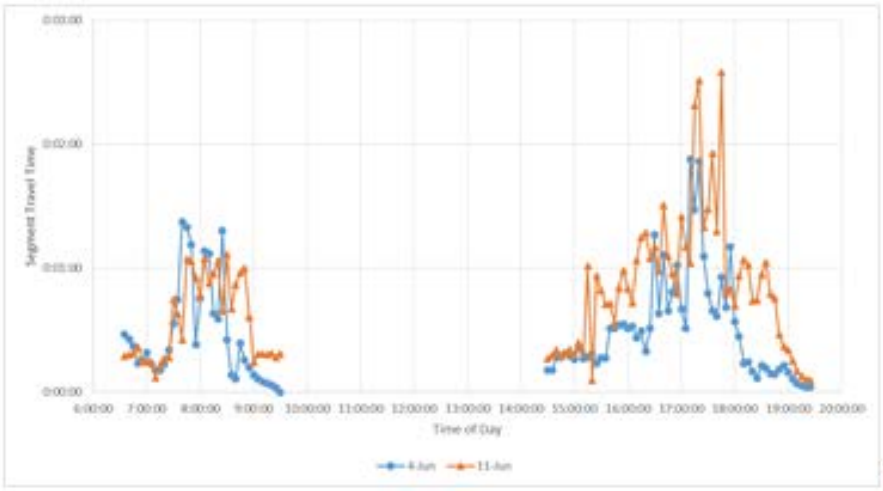

Greenway to Tree (TH-7)

Tree to Minnetonka Ave

Figure 5-5. Station to station travel time graphs for June 4 and June 11 (continued).

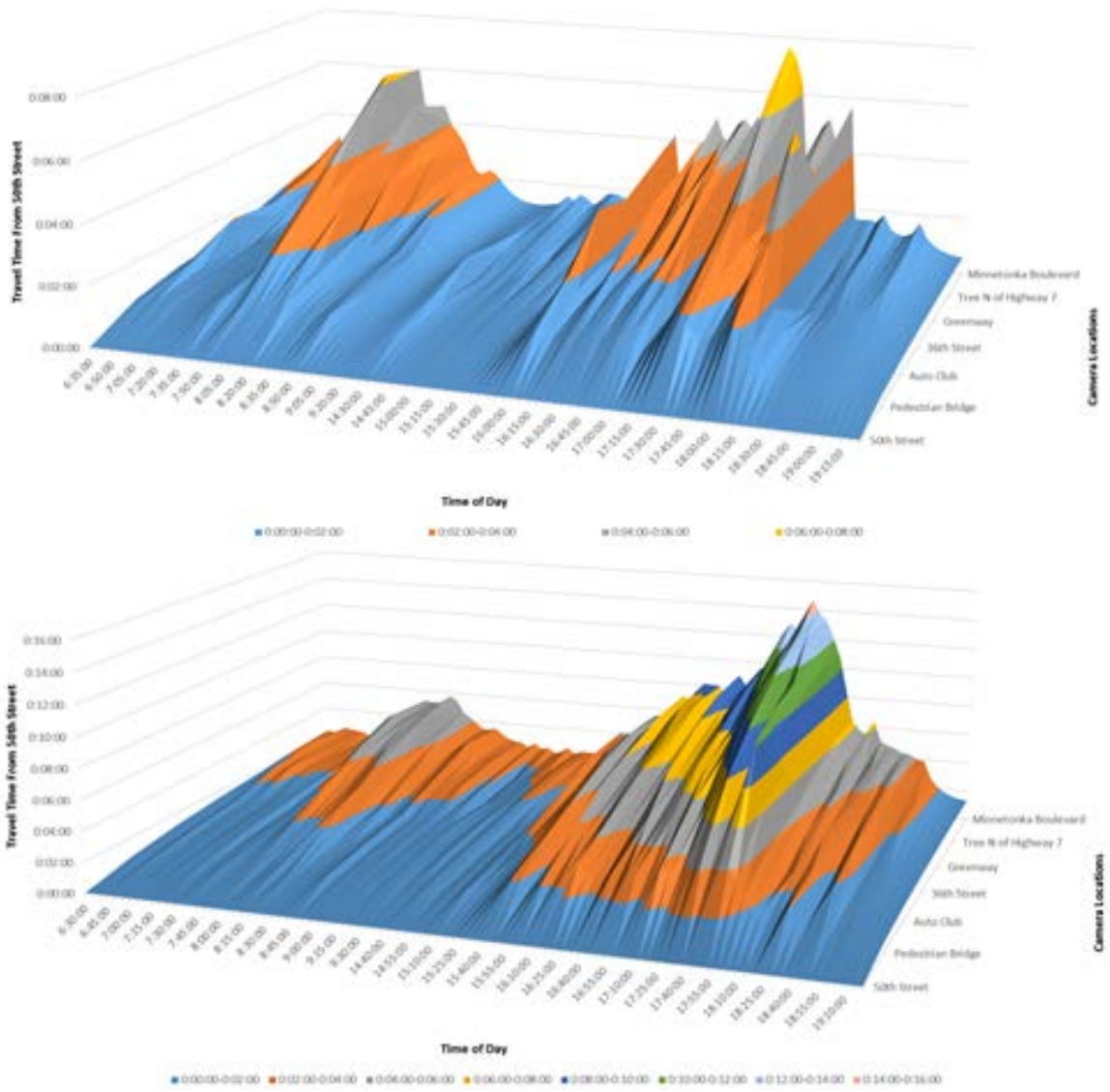

Figure 5-6. Travel time surface for June 4th (SZM) and June 11th (UMD).

Like in the earlier day pair analyzed. The daily volumes during the UMD trial were about 9% higher at 67,434 vehicles as compared to 62,637 during the SZM day. The PM of June 4th under the SZM control developed a shorter congested period in terms of time as compared to the PM period of June 11th under the UMD. In this particular day pair the Travel times under the UMD algorithm are much higher as compared to the SZM. It is possible that the extra volume tipped the balance against the UMD which was not capable to recover. Regardless, the congestion under the UMD seems to be more stable while the congestion under the SZM has great fluctuations for the entire length of the site indicating the presence of shockwaves. This can indicate that the UMD, although handling more demand, it was able to meter it steadily while the SZM being closer to the tipping point it got trapped in a series of restrict and dump cycles. Both algorithms show greater instability closer to the bottleneck with the UMD keeping conditions in the mainline more fluid upstream as compared to the SZM. The UMD algorithm seems to handle better the large demand ramp of TH-7 and conditions immediately upstream of it are less congested. The same observation that the UMD algorithm shows some sharp spikes of very large travel time which could represent short lived heavy congestion conditions from which the control is able to recover can be made also here.

5.2 LOOP DETECTOR BASED COMPARISON

In both ramp metering strategies, the occupancy at the queue detector identifies when long queues occur at the on-ramp, and activates the maximum waiting time ramp constraint and release more vehicles to the freeway. The ramp supply at the merge detector location (passage detector) shows at what rate vehicles are entering the freeway from the ramp. The results based on the quantifiable measures of VHT and VKT are presented first for all studied day pairs. These results are concentrated in Table 5-1 through Table 5-6. No computation has been done for Detector 5 as for most of the days no data are available for some or for all the time periods. The days are presented as pairs with the left of the pairs to represent the results from the current ramp metering strategy. Bold values indicate better performance.

Table 5-1 contains the average flow (units are vehicles per time period of 30 seconds) and occupancy (expressed in percentages representing each 30 seconds time period) plus aggregated performance measures. Specifically, for each of the 8 detectors the average flow during the morning peak is estimated. The weighted average of flow with respect to the distance between detectors provides a good estimation of the vehicle kilometers travelled (VKT) during the analysis period. This VKT estimation is a good proxy for the total demand occurred during this period of analysis (as it contains some uncongested periods before and after the peak period to guarantee that demand and not supply is calculated). Below the VKT estimate in the table and the average flow per detector (in vehicles per minute) is shown. Note that at each location the flow is the aggregated flow from all the lanes of the freeway.

Table 5-2 shows the average occupancy for the same five pairs of days. Detector 5 has values of zero for both flow and occupancy as it is not considered in the analysis (as stated before). In the same table the sum of the occupancies is estimated, which as explained in the methodology chapter leads to the vehicle hours travelled (VHT) in the whole mainline freeway during the

period of analysis. The average value of Density (units are vehicles per meter) and the average speed (estimated as VKT over VHT) is estimated for the period of analysis.

Table 5-1. Average flows of mainline loop detectors during morning peak.

	Average Flow (veh per 30 sec)									
	May-22	May-29	May-23	May-30	May-24	May-31	Jun-10	Jun-03	Jun-04	Jun-11
Det1	31.59	**33.34**	32.66	**33.51**	30.57	**34.66**	31.87	**32.44**	32.43	**37.10**
Det2	34.98	**36.93**	35.48	**36.46**	33.44	**38.34**	34.66	**35.57**	35.83	**39.50**
Det3	30.31	**31.92**	31.20	**31.42**	28.87	**33.21**	30.33	**30.92**	31.64	**34.88**
Det4	39.62	**41.87**	41.31	40.96	37.49	**41.90**	39.09	**41.02**	41.30	**43.68**
Det5	0.00	**0.00**	0.00	0.00	0.00	**0.00**	0.00	**0.00**	0.00	**0.00**
Det6	30.39	**32.44**	31.90	31.77	28.52	**32.57**	30.52	**31.08**	31.80	**33.54**
Det7	36.42	**38.89**	38.97	37.97	35.95	**39.44**	37.78	**37.92**	38.11	**39.24**
Det8	52.65	**55.80**	54.98	**55.72**	51.15	**55.77**	53.40	**54.74**	55.26	53.22
Veh-Km Travelled	255.95	**271.21**	266.50	**267.81**	246.00	**275.90**	257.65	**263.70**	266.36	**281.16**
Flow per det/min	73.13	**77.49**	76.14	**76.52**	70.29	**78.83**	73.61	**75.34**	76.10	**80.33**

Table 5-2. Average occupancies of mainline loop detectors during morning peak.

	Average Occupancy (% of 30sec)									
	May-22	May-29	May-23	May-30	May-24	May-31	Jun-10	Jun-03	Jun-04	Jun-11
Det1	**9.32**	9.51	**9.44**	9.75	**8.77**	10.00	**9.15**	9.36	**9.39**	10.92
Det2	**10.71**	11.00	**10.66**	10.97	**9.98**	11.56	**10.26**	10.70	**10.76**	12.01
Det3	10.34	**8.05**	**7.94**	8.01	**7.39**	8.50	**7.64**	7.96	**8.04**	8.99
Det4	18.94	**10.61**	11.02	**10.50**	**9.54**	10.90	**9.96**	10.57	**10.94**	11.55
Det5	0.00	**0.00**	0.00	**0.00**	**0.00**	0.00	**0.00**	0.00	**0.00**	0.00
Det6	26.10	**16.62**	18.52	**13.38**	**7.11**	8.19	**7.72**	22.35	23.94	**20.04**
Det7	37.27	**35.75**	34.37	**33.21**	**11.78**	24.49	**12.55**	35.07	35.74	**30.71**
Det8	17.00	**17.71**	17.38	**17.92**	**13.71**	17.16	**14.48**	17.43	**17.23**	17.37
Σ(average occupancy)	129.67	**109.24**	109.33	**103.74**	**68.28**	90.80	**71.76**	113.44	116.04	**111.59**
Average Density (veh/m)	0.031	**0.026**	0.026	**0.025**	**0.016**	0.022	**0.017**	0.027	0.028	**0.027**
AvgSpeed (km/hr)	47.37	**59.58**	58.50	**61.96**	**86.47**	72.93	**86.18**	55.79	55.09	**60.47**

Table 5-3. Average flows and occupancies on entrance ramp during morning peak.

Average Flow on Passage Detector from 7am to 9am

Detector ID	May-22	May-29	May-23	May-30	May-24	May-31	Jun-10	Jun-03	Jun-04	Jun-11
1276	4.12	**4.15**	4.10	**4.15**	3.51	**4.05**	3.39	**4.10**	**3.95**	3.64
1277	4.84	**5.10**	**4.98**	4.71	**4.19**	3.96	4.71	**4.74**	**4.91**	4.83
2012	4.55	**5.07**	**5.15**	4.86	4.66	**5.00**	4.79	**4.90**	4.62	4.84
2013	2.54	**2.81**	2.64	**2.75**	2.49	**2.84**	2.61	**2.72**	**2.74**	2.73
2024	6.97	**7.46**	6.60	**7.45**	6.33	**6.85**	6.43	**7.20**	**6.85**	6.60
2022	5.76	**6.56**	**6.49**	6.37	5.90	**6.43**	**6.45**	6.08	**6.36**	6.27

Average Occupancy on Queue Detector from 7am to 9am

Detector ID	May-22	May-29	May-23	May-30	May-24	May-31	Jun-10	Jun-03	Jun-04	Jun-11
3626	13.01	**8.79**	9.39	**7.80**	**6.37**	8.40	13.80	**7.91**	11.81	**10.12**
3645	10.62	**9.59**	9.38	**9.37**	7.75	**7.28**	14.65	**9.91**	13.05	**10.62**
3649	10.92	**6.02**	14.08	**5.65**	8.80	**5.51**	8.30	**7.12**	16.46	**5.98**
3650	**4.93**	5.28	**4.96**	5.22	**4.71**	5.25	6.50	**5.12**	6.62	**5.21**
3652	19.64	**14.57**	**15.00**	16.08	**12.07**	13.84	**11.90**	15.66	16.32	**11.26**
2011	26.20	**16.18**	30.39	**15.12**	17.95	**14.05**	26.89	**15.28**	27.34	**16.61**

From the morning measurements it appears that the UMD KAdaptive metering strategy performs better than the SZM when conditions are not extremely congested. The UMD KAdaptive algorithm allows on average more vehicles to flow into the mainline and keeps the on-ramp occupancy relatively low. In the mainline, the flows are also bigger with the UMD KAdaptive algorithm and 3 out of 5 times the speeds are higher too. In general, for the same occupancy the flows are less when the SZM algorithm is applied. The main reason is that the UMD KAdaptive algorithm is more protective in the morning and queue detector occupancies are lower. Thus, the queue violation is not activated as often and the ramp metering is active (and successful) for longer time periods. This will be discussed later together with the graphs of the ramp detectors.

On the other hand, the results seem to be worse in the afternoon when demand is higher for most of the days. However, is remarkable that the congestion is higher in terms of volumes, occupancies and duration. For almost the same level of average flow, commonly the average speed is lower and the average occupancy higher when the UMD KAdaptive ramp-metering strategy is implemented. In this case, it is not clear if the algorithm introduces by default bigger volume of vehicles in the mainline. Indeed, Figure 5-7 and Figure 5-8 implies that in the afternoon (bottom graph), unlike the morning (top graph), the UMD KAdaptive algorithm does not seem to successfully work proactively. In the figure, the data from Table 5-3 (top graph) and Table 5-6 (bottom graph) are utilized. The flow is measured in vehicles per time period of 30 seconds during each day's morning (or evening) peak and occupancy is expressed in percentages representing again each the 30 seconds time period. The flow and occupancy data are taken from the passage and queue detectors at the on-ramps respectively. Clearly, the steeper the line is the better as bigger flows are measured for the same occupancy level. The slope of the graph (which is a proxy for the speed at capacity) for the UMD KAdaptive algorithm is much steeper in the morning while it is almost the same with the one of the SZM algorithm in the afternoon. Thus, no conclusion can be drawn for which algorithm works better in the afternoon when bigger congestion is noticed. It should be highlighted that obviously the linear fit is not the best trend line option and this is confirmed by the R^2 parameter, but it is a simple way to overall compare

the occupancies measured at the same level of flow, which is directly influenced by the ramp metering strategy.

Table 5-4. Average flows of mainline loop detectors during afternoon peak.

	Average Flow (veh per 30 sec)									
	May-22	May-29	May-23	May-30	May-24	May-31	Jun-03	Jun-10	Jun-04	Jun-11
Det1	**34.68**	32.73	35.85	**38.05**	36.21	**36.60**	37.70	**37.74**	**39.05**	35.45
Det2	**36.33**	34.00	37.23	**40.12**	38.43	**38.87**	**39.44**	38.97	**40.74**	36.50
Det3	**31.57**	29.45	32.17	**34.72**	33.81	**34.12**	34.01	**34.30**	**35.13**	31.80
Det4	**38.36**	35.80	38.70	**41.13**	**41.17**	41.04	39.46	**40.68**	**41.22**	38.31
Det5	**0.00**	0.00	0.00	**0.00**	**0.00**	0.00	0.00	**0.00**	**0.00**	0.00
Det6	**29.81**	27.78	29.47	**31.16**	**32.29**	31.68	29.35	**31.15**	**31.16**	29.53
Det7	**34.87**	32.89	34.71	**36.17**	**38.07**	37.23	33.89	**36.33**	**35.81**	34.92
Det8	**49.24**	47.56	49.48	**51.58**	**51.88**	51.08	46.82	**49.03**	**48.54**	47.69
Veh-Km Travelled	**254.87**	240.21	257.60	**272.92**	**271.85**	270.63	260.67	**268.21**	**271.66**	254.19
Flow per det/min	**72.82**	68.63	73.60	**77.98**	**77.67**	77.32	74.48	**76.63**	**77.62**	72.62

Table 5-5. Average occupancies of mainline loop detectors during afternoon peak.

	Average Occupancy (% of 30sec)									
	May-22	May-29	May-23	May-30	May-24	May-31	Jun-03	Jun-10	Jun-04	Jun-11
Det1	**25.36**	35.83	30.93	**21.06**	**10.38**	10.51	**14.36**	31.15	**11.27**	35.15
Det2	**24.19**	33.16	28.29	**23.97**	**11.45**	11.81	**20.66**	28.80	**13.47**	31.94
Det3	**25.08**	32.76	28.23	**21.20**	**8.58**	10.94	**21.08**	27.79	**13.24**	30.65
Det4	**21.92**	27.98	25.78	**20.57**	**10.65**	18.79	**23.24**	24.61	**20.36**	26.00
Det5	**0.00**	0.00	0.00	**0.00**	**0.00**	0.00	**0.00**	0.00	**0.00**	0.00
Det6	**28.89**	30.18	35.56	**29.66**	**19.59**	27.00	**31.16**	32.76	**30.43**	35.71
Det7	**37.03**	38.09	39.52	**38.03**	**32.67**	34.49	40.85	**36.84**	**34.16**	36.92
Det8	**15.41**	16.21	18.78	**16.49**	**15.10**	16.07	21.60	**18.59**	**19.26**	18.41
Σ(average occupancy)	**177.87**	214.22	207.09	**170.98**	**108.42**	129.61	**172.94**	200.53	**142.19**	214.77
Average Density (veh/m)	**0.042**	0.051	0.049	**0.041**	**0.026**	0.031	**0.041**	0.048	**0.034**	0.051
AvgSpeed (km/hr)	**34.39**	26.91	29.85	**38.31**	**60.18**	50.11	**36.17**	32.10	**45.85**	28.40

Table 5-6. Average flows and occupancies on entrance ramp during afternoon peak.

Average Flow from 3pm to 6pm

Detector ID	May-22	May-29	May-23	May-30	May-24	May-31	Jun-03	Jun-10	Jun-04	Jun-11
1276	3.35	**3.43**	**3.52**	3.34	3.10	**3.48**	2.85	**3.43**	3.08	**3.32**
1277	**3.60**	3.42	**3.60**	3.55	3.42	**3.47**	2.96	**3.34**	3.15	**3.76**
2012	4.60	**4.82**	4.85	**4.90**	**5.29**	4.97	4.83	**5.03**	4.80	**4.84**
2013	2.76	**2.86**	2.75	**3.19**	**3.30**	3.11	**3.16**	2.88	**2.89**	2.82
2024	4.91	**5.39**	4.89	**5.61**	4.77	**5.11**	4.58	**4.66**	4.51	**4.63**
2022	**6.68**	5.54	6.22	**7.13**	7.01	**7.22**	6.88	**6.89**	**7.45**	6.62

Average Occupancy from 3pm to 6pm

Detector ID	May-22	May-29	May-23	May-30	May-24	May-31	Jun-03	Jun-10	Jun-04	Jun-11
3626	10.08	**8.67**	9.03	**8.10**	**6.02**	10.98	**9.00**	11.07	**6.87**	10.22
3645	**7.62**	8.13	7.49	**6.95**	**6.65**	6.70	**6.81**	8.28	**7.15**	9.90
3649	29.80	**26.57**	41.80	**12.34**	**16.68**	24.30	22.10	**15.50**	**9.30**	24.99
3650	**5.29**	5.58	**5.77**	6.03	6.83	**5.79**	8.72	**5.52**	6.11	**5.36**
3652	**35.48**	45.73	43.77	**33.20**	19.85	**18.52**	25.88	**17.20**	22.26	**22.09**
2011	20.66	**13.95**	23.03	**14.43**	18.89	**13.11**	22.35	**11.52**	23.39	**15.75**

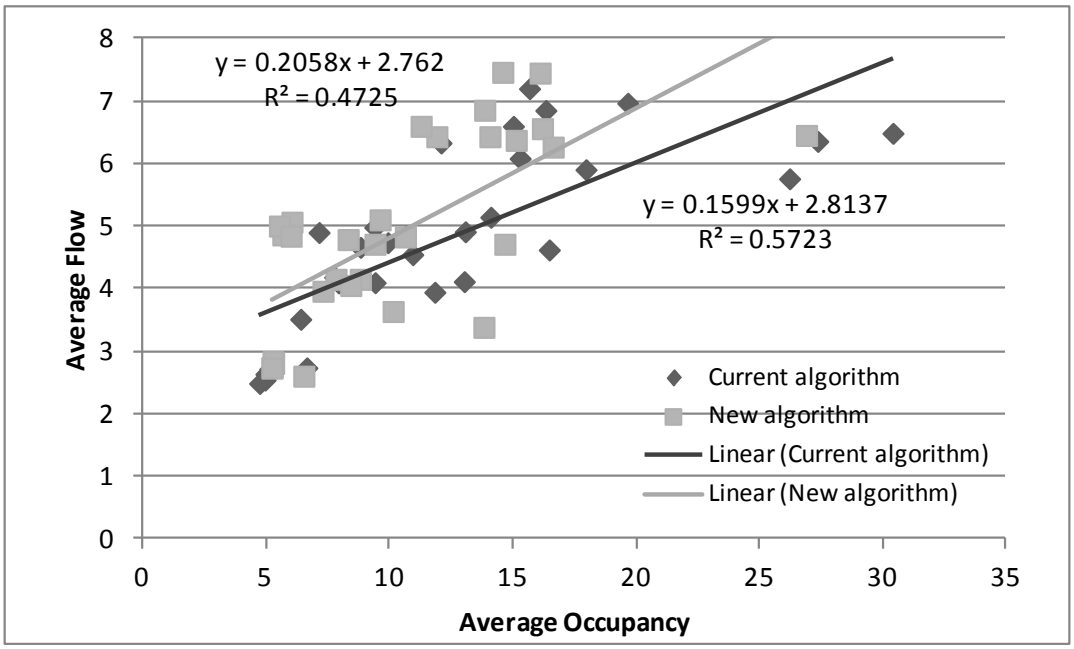

Figure 5-7. Average flow versus average occupancy measured at the ramps for each day in the morning.

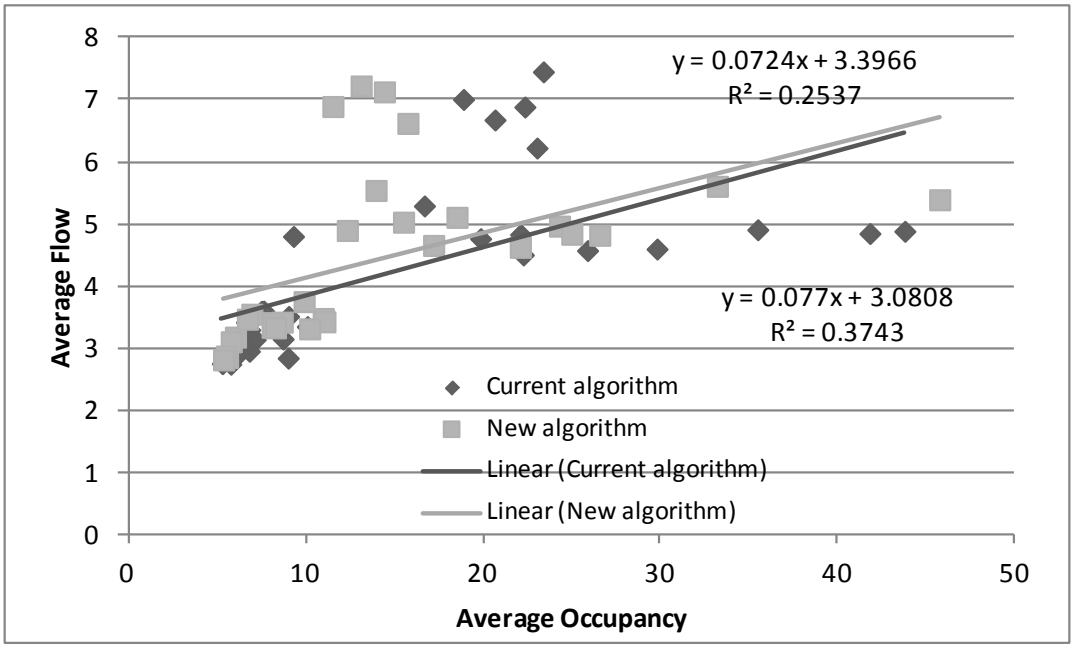

Figure 5-8. Average flow versus average occupancy measured at the ramps for each day in the afternoon.

In the following sections the results from each individual day-pair selected are presented. For efficiency not all figures will be discussed but the first few pairs will highlight the resulting interpretations.

5.2.1 Day Pair of May 22nd and May 29th

The flow and occupancy contour plots of the May 22nd and May 29th pair are shown in Figure 5-9 and Figure 5-10 (downstream is point 6000, upstream is point 0 in meters). The color map in the space – time graph show the magnitude of flow and occupancy. There is a white space on the 22nd of May approximately between the points 3000 and 4500 meters, as there are no measurements from detector 5 for this day. The occupancy contour plots help to identify the active bottleneck, which seems to be expanded in the whole freeway segment and last for a longer period in the afternoon. Overall, lower occupancies with higher flows are present in the morning with the UMD KAdaptive metering strategy while this behavior slightly reverse in the afternoon.

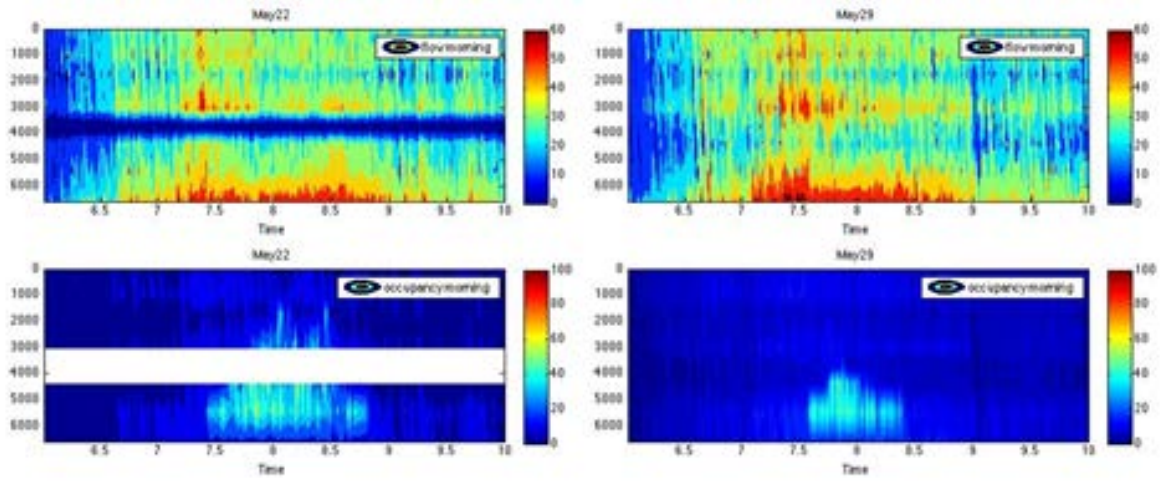

Figure 5-9. Flow and occupancy contour plots – mornings, May 22 and May 29.

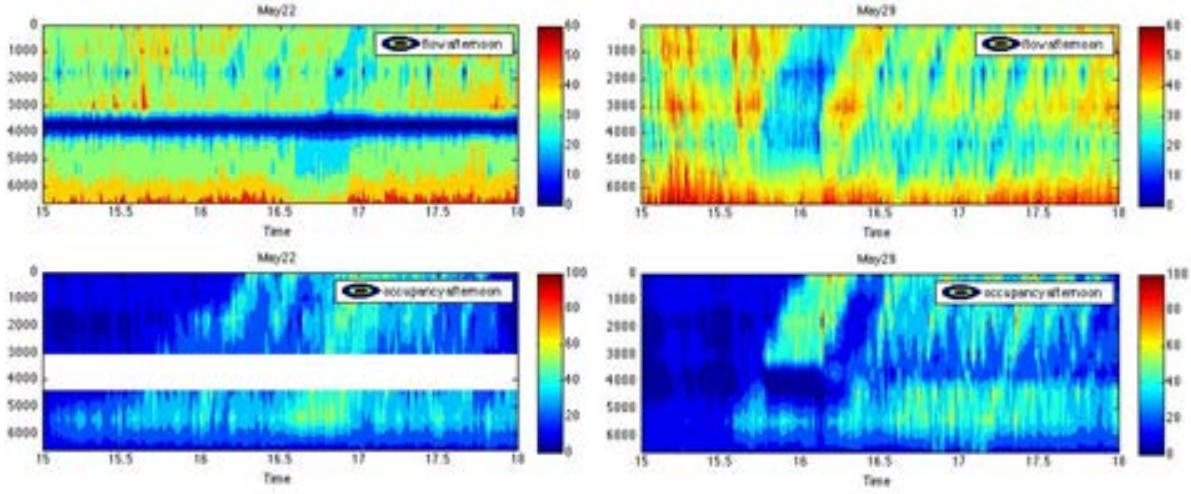

Figure 5-10. Flow and occupancy contour plots – afternoons, May 22 and May 29.

To accurately find the duration of the active bottleneck, the 30-seconds flow and occupancy time series at its nearest mainline loop-detector, detector 7, is plotted in Figure 5-11 and Figure 5-13 for the morning and afternoon time periods respectively. In the morning, even though the average flows of both days are similar (see Table 5-1), the day with the UMD KAdaptive algorithm performs better in terms of occupancies developed. The congestion lasts longer on May 22nd (1.5 hour instead of 1) and for many time periods the occupancy is above 50 percent.

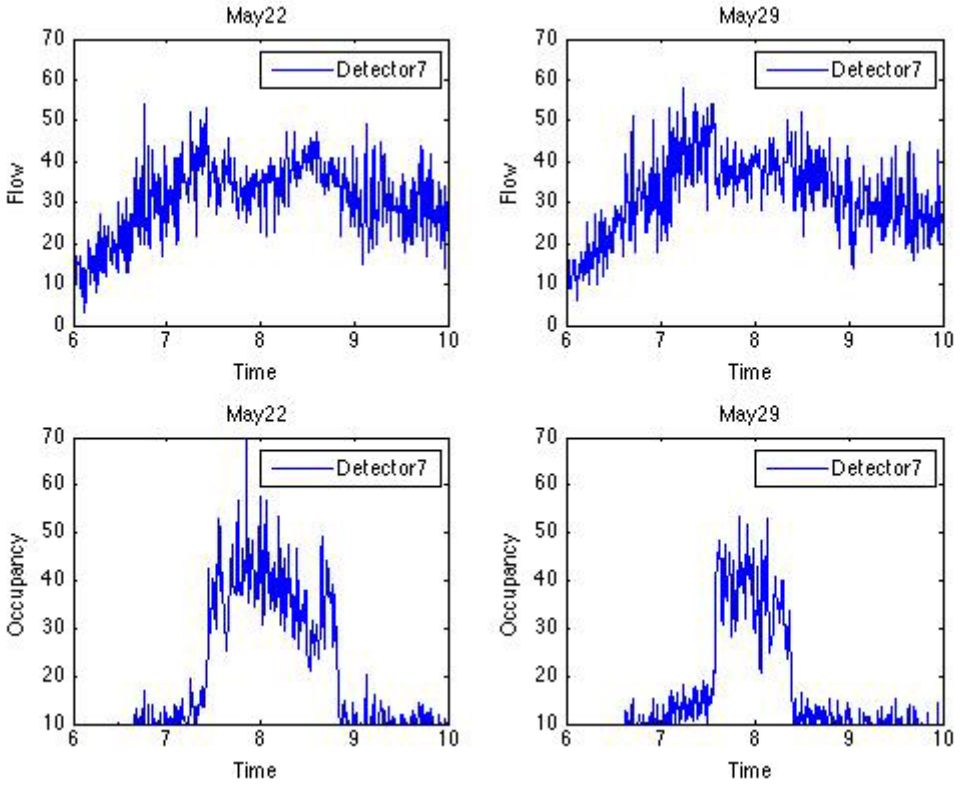

Figure 5-11. Mainline flow and occupancy at the active bottleneck - mornings, May 22 (SZM) and May 29 (UMD).

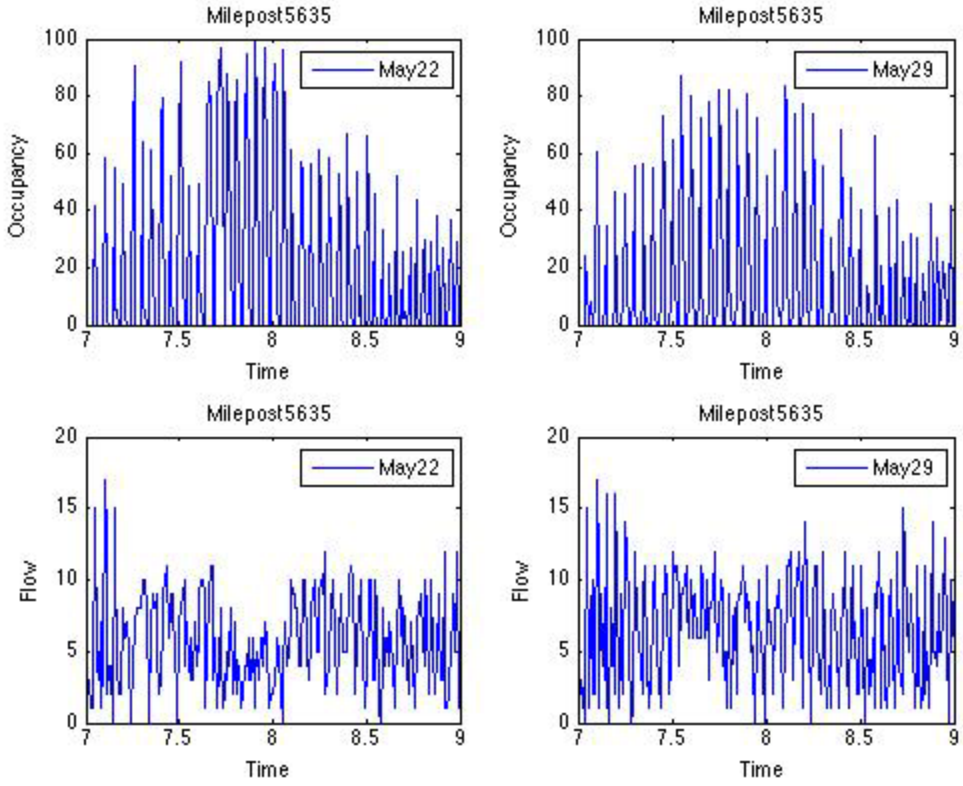

Figure 5-12. Flow (passage detector 2022) and occupancy (queue detector 3652) downstream of the active bottleneck – mornings, May 22 (SZM) and May 29 (UMD).

The direct cause of the increased occupancies in the mainline is the metering flow rates at the downstream on-ramp detector, measuring the actual ramp flow entering the mainline. In Figure 5-12 and Figure 5-14 the morning and the afternoon flow and occupancy time series of the downstream to the active bottleneck on-ramp are depicted. Obviously, in the morning, the UMD KAdaptive metering strategy achieves better results as it manages to keep the occupancies at lower level and provide a more stabilized in-flow to the mainline. Oppositely, the SZM algorithm generates more oscillations coming from the ramp-metering violation that slow down more suddenly the mainline vehicles and as a result increases the mainline but also the on-ramp occupancies.

With regard to the afternoon performance of the UMD KAdaptive metering strategy, it does not seem to follow the success experienced in the morning. Again the average flows in the mainline are comparable, but the average occupancy on the 29th of May is much higher. Despite the fact that the new algorithm attempts to avoid the violation of the metering, this goal is not attained. Thus, more vehicles flow on average towards the mainline and the mainline occupancies are elevated. Additionally, apart from larger occupancy values, on the 29th of May the active bottleneck lasts longer and for a lengthier segment of the freeway (see Figure 5-13).

The level of the occupancies can be also noticed in the Fundamental Diagram at the location where the active bottleneck is initiated. The flow versus occupancy plot for the bottleneck, using flow as the total output flow at the bottleneck (upstream mainline and on-ramp passage detectors, and occupancy at the upstream mainline detector, is shown in Figure 5-15 and Figure 5-16 for

the morning and the afternoon time periods. The plots are however smoothed out using 3 minutes time periods instead of 30 seconds used so far. This smoothing is done in order to observe the trend of volumes more clearly and to reduce the high disturbances in 30 seconds data that might reflect neither steady nor mean states (and thus not be representative of the capacity of bottleneck). This plot is useful to understand the value of capacity before and after the occurrence of the breakdown.

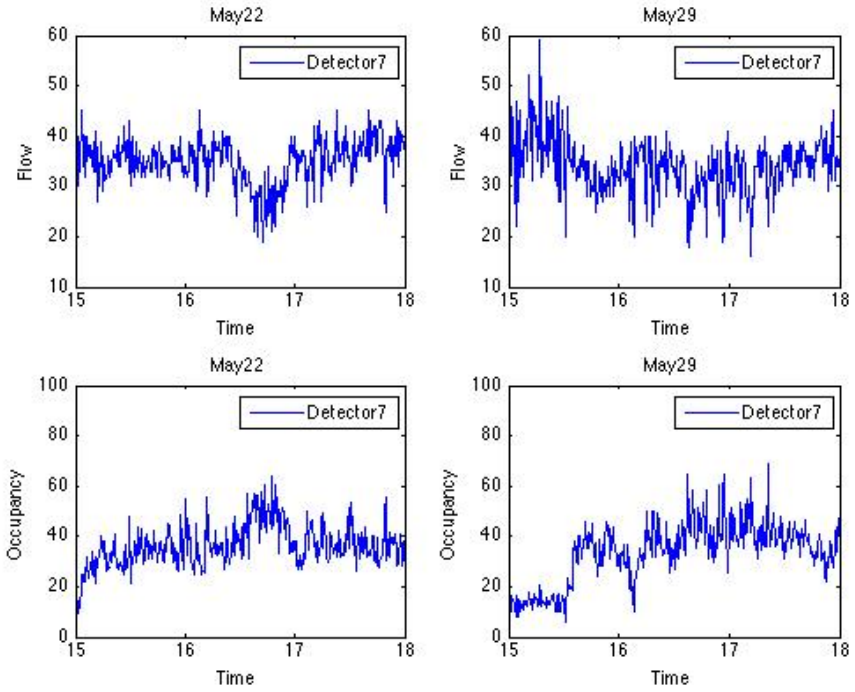

Figure 5-13. Mainline flow and occupancy at the active bottleneck – afternoons, May 22 (SZM) and May 29 (UMD).

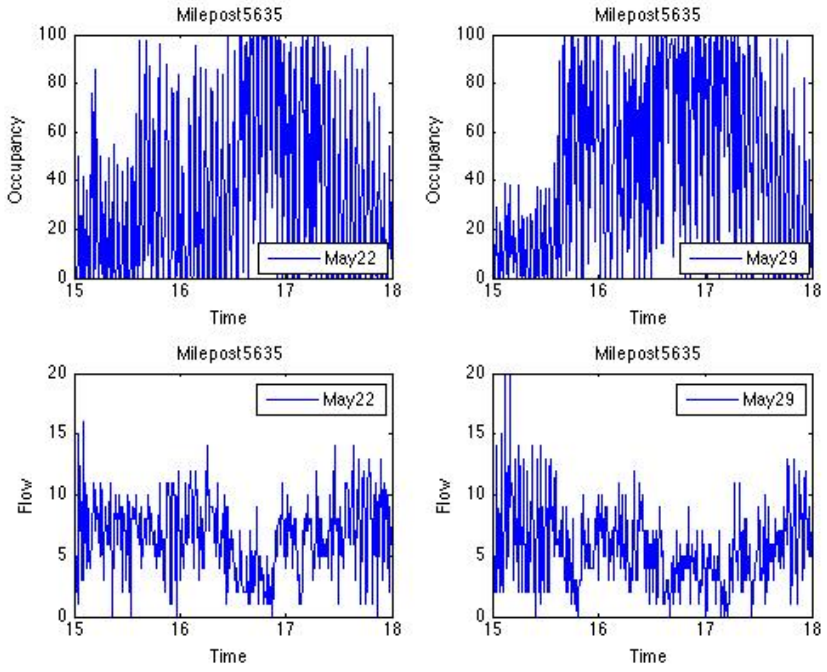

Figure 5-14. Flow (passage detector 2022) and occupancy (queue detector 3652) downstream of the active bottleneck – afternoons, May 22 (SZM) and May 29 (UMD).

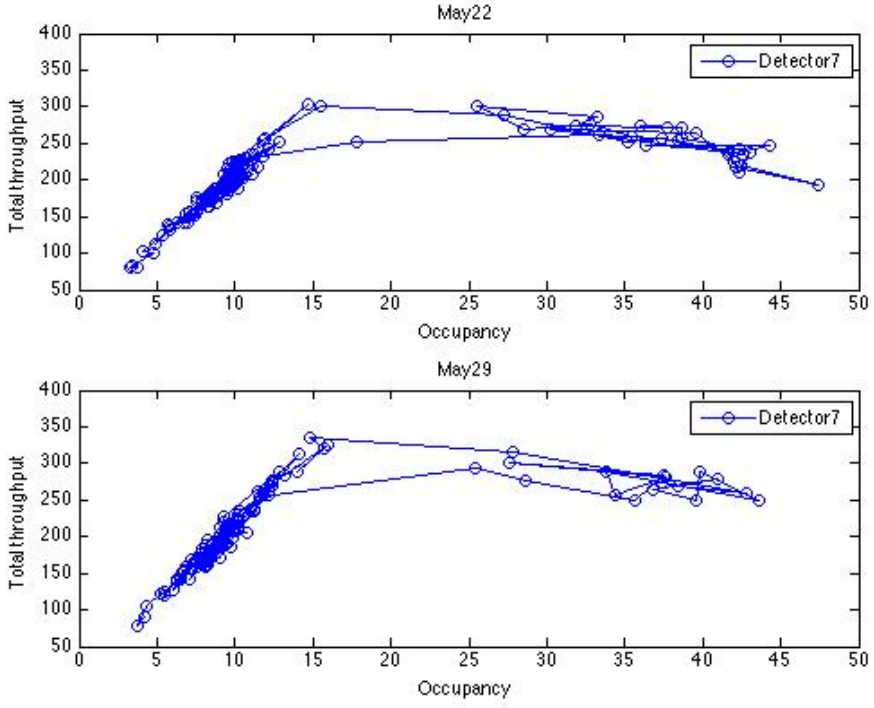

Figure 5-15. Total throughput (mainline upstream and ramp) versus occupancy (only mainline upstream) – mornings, May 22 (SZM) and May 29 (UMD).

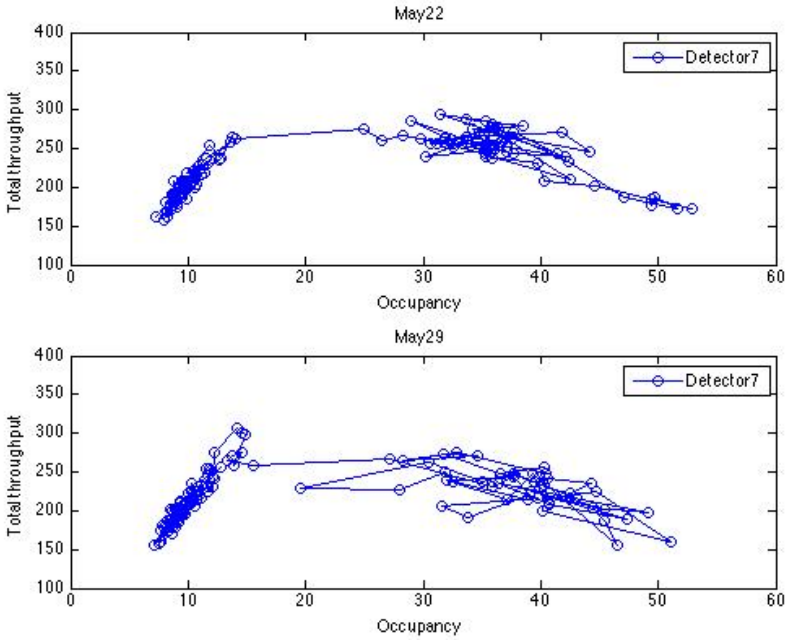

Figure 5-16. Total throughput (mainline upstream and ramp) versus occupancy (only mainline upstream) – afternoons, May 22 (SZM) and May 29 (UMD).

These graphs support the views expressed before that the UMD KAdaptive algorithm performs better in the morning but fails to have similar results in the afternoon when the demand and the congestion are higher. Reversely to the morning, in the afternoon, the descending part of the FD in denser as for more time periods the occupancies are higher. But, although the UMD KAdaptive metering strategy operates well in the morning, the capacity drop is almost similar with the one created on the 22nd of May. This fact is contradicting the main purpose of ramp metering which is to improve mainline conditions. Improved ramp metering strategies could be expected to create smaller capacity drops, when compared with the no control case. The high stop-and-go effect created due to an inadequately designed ramp metering suggests that an improved strategy could possibly decrease the magnitude of capacity drop.

The main reason for this high drop is the extremely high values of ramp flows a few minutes before the occurrence of the breakdown, due to the overreaction of the existing ramp metering strategy once long queues occur at the on ramps. Recent simulation findings (Geroliminis et al., 2011) show that a ramp metering strategy with a smoother reaction to long queues can significantly improve total travel times.

The detailed graphs from analysis of the remaining day pairs support the conclusions presented in the above sections. For brevity, those figures are not included here and can instead be found in Appendix A.

6 EVALUATION OF RAMP METERING IMPLEMENTATION ON TH-212

Ramp metering was implemented along the TH-212 corridor in 2014, giving the research team the opportunity to explore the impact of the UMD KAdaptive algorithm on traffic in that portion of the Twin Cities network. TH-212 has limited congestion which is concentrated at one bottleneck at the junction with I-494. This is not an ideal scenario for evaluating ramp metering, since the controlled volume is a relatively small fraction of the mainline total. However, the before-after approach enabled this analysis to isolate the impacts of the ramp metering strategy and hold physical and demand parameters nearly or completely constant.

This analysis focuses on the fall months of 2013 and 2014 (September through mid-December). Physical alterations to the corridor preclude using additional years prior to 2013, while adjustments to the ramp metering algorithm exclude spring/summer months from 2014. Only morning peak period was examined, between 6:00 AM and 10:00 AM, and only for the eastbound side of the corridor. The UMD KAdaptive algorithm was only active during those conditions.

Throughout this section, data from 2013 (the pre-ramp metering condition) will be referred to as "Before" data, while 2014 data will be referred to as "After" data.

6.1 ANALYSIS CORRIDOR AND DATA SOURCES

Ramp meters were installed on each entrance ramp starting from Great Plains Boulevard at the west end of the corridor, proceeding through each interchange until TH-212 merges with TH-62 at the east end of the corridor. During the study period, only a subset of ramp meters were actively using the UMD algorithm; the meters at Great Plains Boulevard, Valley View Road, and Shady Oak Road were unmetered during morning peak. Thus, four ramps were analyzed: Dell Road, Eden Prairie Road, Mitchell Road, and Prairie Center Drive. The selected corridor for analysis starts immediately upstream of Dell Road, includes each of the other UMD-governed ramps, and continues through the TH-212/TH-62 merge.

Along this portion of the network, loop detector stations are found at regular intervals. These stations include lane-by-lane detection and produce 30-second aggregated volume and occupancy. To ensure that loop measurements accurately represent the conditions on the roadway, the corridor was broken into 33 segments (see Figure 6-1). Each segment is bounded by either a loop station or an entrance or exit ramp. Thus, each segment represents a contiguous geometric element with no entrance or exit within its boundaries.

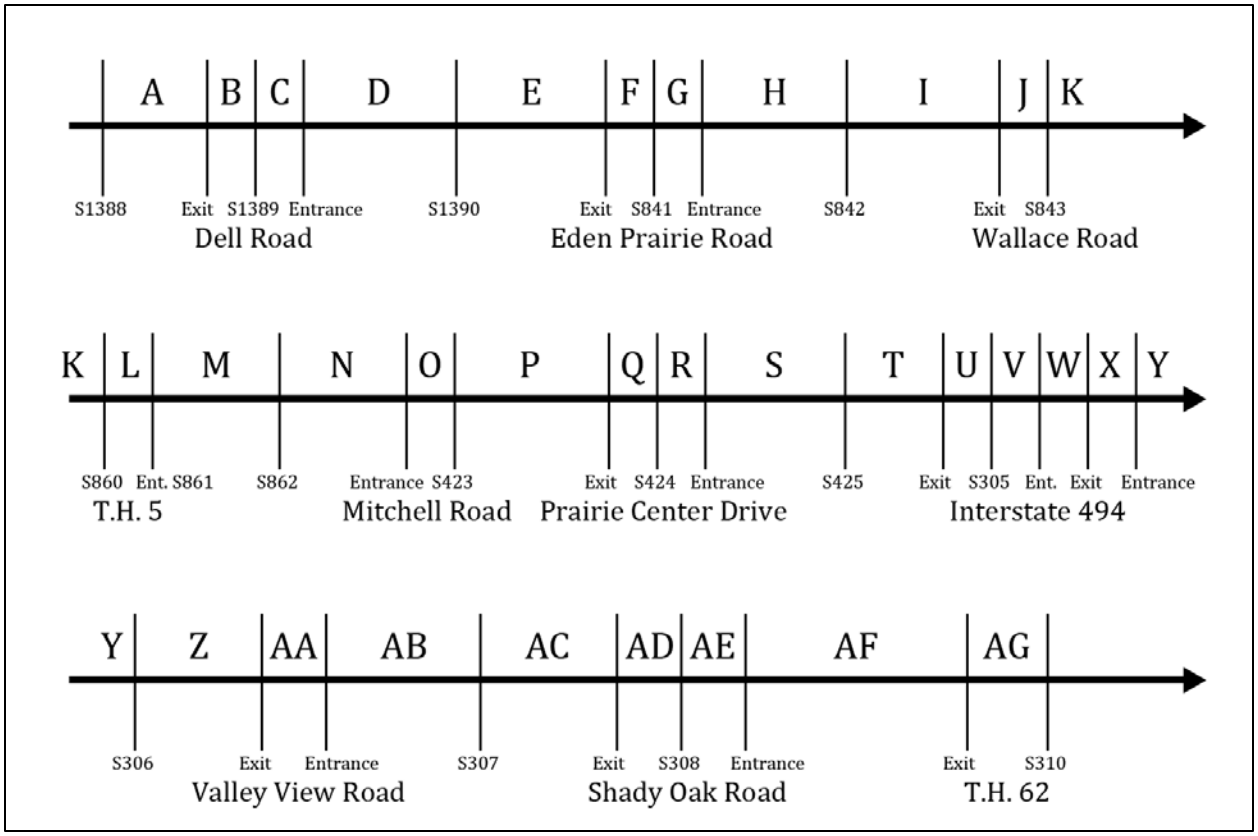

Figure 6-1. TH-212 corridor diagram indicating contiguous segments.

For each segment (labeled alphabetically from A to AG), loop detector data for all mainline detectors were gathered using the Highway Automated Reporting Tool (HART). HART retrieved all 30-second data for the dates within the selected range indicated above and performed a series of cleaning steps to remove small gaps in the data. HART produced volume, occupancy, and speed values for each location along the corridor. It is important to note that speed is not directly measured from these detectors, but is instead estimated using a calibrated vehicle effective length. Only small holes within the data (gaps of less than 3 minutes) were interpolated. For any larger gaps caused by detectors not operating properly, those dates were excluded from the analysis. In the course of this analysis, only a few days were excluded for this reason.

After HART produced cleaned 30-second data for all mainline detectors, this data was aggregated to 5-minute periods. All further analysis was based on 5-minute aggregate values, developed using the following formulae:

$$Vol_t^{5min} = \sum_{i=0}^{9} Vol_{t-(i*30sec)}^{30sec} \quad \text{Eq. 6-1}$$

$$Occ_t^{5min} = \frac{\sum_{i=0}^{9} Occ_{t-(i*30sec)}^{30sec}}{10} \quad \text{Eq. 6-2}$$

$$Spd_t^{5min} = \frac{\sum_{i=0}^{9} Spd_{t-(i*30sec)}^{30sec}}{10} \quad \text{Eq. 6-3}$$

where t is the time of the segment, indicated in the form HH:MM:SS. Thus, the volume is simply the sum of the 5-minute period ahead of the indicated time (e.g., 12:00:00 AM to 12:05:00 AM is marked as 12:05:00 AM). Occupancy and speed are the average across the ten 30-second values.

A similar procedure was performed on data for each of the entrance and exit detectors along the portion of TH-212 involved in this analysis. However, as HART was developed to only operate on mainline detectors, these other data were retrieved from MnDOT directly using the DataExtract program. This program produced a set of text files containing all necessary data. Data from HART and DataExtract were reformatted into a unified structure and placed into a PostgreSQL database.

6.2 TRAVEL TIME ANALYSIS

The ultimate goal of this analysis is to compare system performance before and after the implementation of the ramp metering system. One performance measure used to accomplish this was total system travel time. To produce total travel time, three components are necessary: mainline travel time and volume, and ramp delay incurred. Each of these was developed using 5-minute aggregation, as described below.

From the mainline data produced by HART, volume was aggregated separately for each detector. To generate volumes for each segment (as described by Figure 6-1), a simple arithmetic model was created using conservation of flow (assuming no storage). For each segment, the total volume which departed during the 5-minute period was calculated as the nearest downstream station's volume plus any exiting volume minus any entering volume. For example, Figure 6-2 and the following equations show the calculation for Segments Z, AA, and AB.

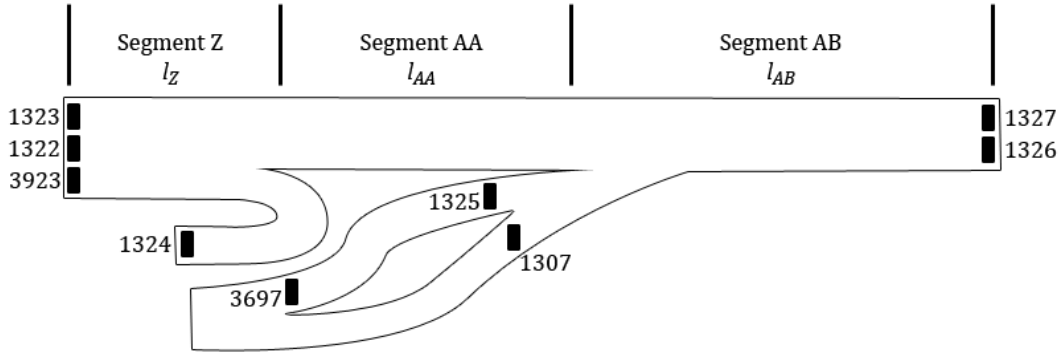

Figure 6-2. Sample calculation figure for Segment Z.

$$V_Z = (V_{1326} + V_{1327}) - (V_{1307} + V_{1325}) + (V_{1324}) \quad \text{Eq. 6-4}$$

$$V_{AA} = (V_{1326} + V_{1327}) - (V_{1307} + V_{1325}) \quad \text{Eq. 6-5}$$

$$V_{AB} = (V_{1326} + V_{1327}) \quad \text{Eq. 6-6}$$

where $V_{\#\#\#\#}$ is the volume at the given detector number.

Mainline travel times were estimated based on the length of each segment and speeds as produced by Equation 3, above. Lengths were measured along the roadway centerline using aerial imagery of the corridor and the locations of detector stations and entrance/exit points within a GIS framework. Since speeds could only be estimated at the station location, each segment's center point was used to interpolate a speed. Using the same figure above, the following equations show the estimation of speed for Segments Z, AA, and AB.

$$S_Z = \frac{S_{down} - S_{up}}{l_Z + l_{AA} + l_{AB}} * \left(\frac{l_Z}{2}\right) + S_{up} \quad \text{Eq. 6-7}$$

$$S_{AA} = \frac{S_{down} - S_{up}}{l_Z + l_{AA} + l_{AB}} * \left(l_Z + \frac{l_{AA}}{2}\right) + S_{up} \quad \text{Eq. 6-8}$$

$$S_{AB} = \frac{S_{down} - S_{up}}{l_Z + l_{AA} + l_{AB}} * \left(l_Z + l_{AA} + \frac{l_{AB}}{2}\right) + S_{up} \quad \text{Eq. 6-9}$$

where:

$$S_{down} = \frac{S_{1327} + S_{1326}}{2} \quad \text{Eq. 6-10}$$

$$S_{up} = \frac{S_{1323} + S_{1322} + S_{3923}}{3} \quad \text{Eq. 6-11}$$

and $S_{\#\#\#\#}$ is the speed at the given detector number.

With the length and estimated speed for each segment, average travel times were calculated. Similarly, using these average travel times and total volume, total segment travel times were calculated. These average and total travel times are the mainline component of system travel time. To complete the analysis, ramp delay must also be incorporated.

For the Before period, no ramp delay was accumulated since any vehicles wishing to access the freeway simply merged into traffic and experienced delay along the mainline. After ramp metering was imposed, variable-length queues developed at the ramps leading to some accumulation of delay for vehicles attempting to access the freeway. To estimate ramp delay, the queue and passage detectors at the ramp were used to build a cumulative queue using 30-second data.

However, using this in-out methodology resulted in significant queues building up over the course of metering which were never released. Using MnDOT cameras along the corridor, ramps along the corridor were observed manually for several morning peak periods. During these times, queues built up and tapered off within the peak period such that at the end of metering queues were short (only one or two vehicles remaining when the meters were deactivated). In contrast, the in-out methodology for calculating the queue resulted in significant standing queues at the end of metering, with some on the order of 40 or 50 vehicles.

To correct this imbalance, a correction methodology was applied to the ramp queue estimations. During each morning peak, the start and end of metering were located using data from the 'green' detector at each ramp. The green detector stores the target discharge rate of the ramp meter, so for any time at which the meters are operating, the green detector value is non-zero. Contiguous

active periods of metering were found and the number of 30-second increments were counted. Across this same period, the ramp queue was estimated and the ultimate remaining queue was calculated.

The total remaining queue was evenly subtracted across the entire metering period. In some cases, this resulted in a small negative queue being developed at some intermediate point during metering. As a final adjustment, the maximum negative queue was located and added to the entire metering period so the minimum queue for the period was set to zero. Figure 6-3 shows three curves generated for a sample metering period: the simple in-out curve (A), the curve adjusted based on the final queue (B), and the ultimate curve used for delay calculations which contains only positive queue values (C).

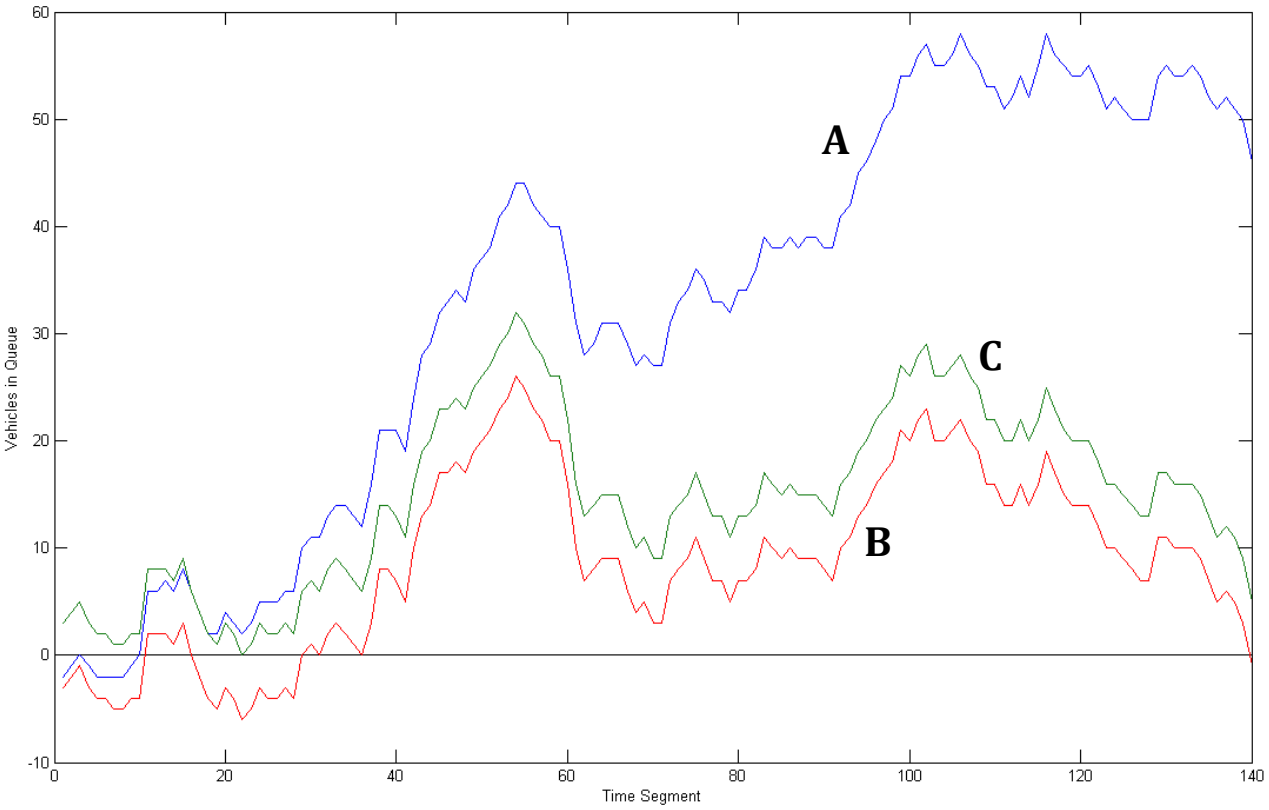

Figure 6-3. Ramp queue adjustment methodology illustrated as three curves.

These 30-second-based ramp queues were transformed into 5-minute delay values in order to align with the other data already generated for the corridor. The total delay for each 5-minute period was calculated as:

$$RampDelay_{r,t}^{5min} = 30sec * \sum_{i=0}^{9} RampQueue_{r,t-(i*30\text{sec})}^{30sec} \qquad \text{Eq. 6-12}$$

where $RampDelay_{r,t}$ is the 5-minute ramp delay for ramp *r* at time *t*. Thus, a total ramp delay time was estimated for every 5-minute period for each ramp. These values were stored into the same PostgreSQL database with the other travel time data.

6.2.1 Selection of Correlated Days

With travel time data for mainline segments and delay for each ramp meter, comparisons can be made between Before and After conditions. However, since the two sets of data span separate years, some method of selecting similar dates for comparison was required. This was accomplished by comparing the entrance boundary conditions across each day using the GEH goodness-of-fit measure.

The GEH Statistic is a formula used in traffic engineering, traffic forecasting, and traffic modelling to compare two sets of traffic volumes. The GEH formula was invented by Geoffrey E. Havers, a transport planner in London, England during the 1970s. Although similar to a chi-squared test, it is not strictly a statistical test but instead an empirical tool which has proven useful for transportation analysis. The formula for the "GEH Statistic" is:

$$GEH = \sqrt{\frac{2(B-A)^2}{B+A}} \qquad \text{Eq. 6-13}$$

where B and A are two hourly volumes to be compared. By using the GEH, a wide variety of flow ranges can be compared seamlessly. This is extremely important for transportation, and this project, where some detectors can experience flows on the order of 300 vph and others experience flows on the order of 1800 vph.

The GEH has been used as a tool to validate automated counts versus manual counts, compare traffic volumes obtained at a location across various years, or to analyze the traffic volumes produced by a travel demand forecasting model against real-world data for a region. The use of GEH as an acceptance criterion for travel demand forecasting models is recognized in the UK Highways Agency's Design Manual for Roads and Bridges (DMRB), Volume 12, Section 2, the Wisconsin microsimulation modeling guidelines, and has been integrated as a testing tool in simulation environments such as Aimsun.

For traffic modelling work, a GEH of less than 5 is considered a good match between, for example, modelled and observed hourly volumes (flows of longer or shorter durations should be converted to hourly equivalents to use these thresholds). GEHs in the range of 5 to 10 may be acceptable but require additional examination. GEH values greater than 10 are highly likely to represent a poor match between the two data sets and caution should be used in comparing the two data sets.

Within the context of this project, the GEH statistic was used in conjunction with 5-minute volumes for each entrance point along the region of interest. Ten entrance points were defined, including the mainline station S1388 at the upstream boundary of the corridor. For each entrance ramp, total volumes were found by summing queue and bypass detector counts. Queue detectors were selected to represent the ‘unfiltered’ demand at each ramp rather than the passage detector which is influenced by the ramp meter’s activity. At Valley View Road, the queue detector was defective during the study period, so the passage detector was substituted. Since that ramp meter was never active at that location, the passage detector was an acceptable replacement.

Thus a large comparison matrix was created with a GEH statistic value representing the fit between each date and all other dates in the study period. This included comparing all Before dates with each other and all After dates with each other, resulting in a triangular matrix. Ultimately, only the GEH values comparing Before versus After dates were used for further analysis.

Each date pair was assigned a GEH value given by:

$$GEH_{i,j} = \frac{\sum_{t=1}^{N_t}\sum_{s=1}^{N_s}\sqrt{\frac{2(V_{s,t,i}-V_{s,t,j})^2}{V_{s,t,i}+V_{s,t,j}}}}{N_t * N_s} \qquad \text{Eq. 6-14}$$

where $V_{s,t,i}$ is the hourly volume at location s at time t on Before date i, and N_t and N_s are the number of time segments and locations, respectively. $V_{s,t,j}$ is the value for the corresponding time and location on the After date j. Since 5-minute data was used for morning peak, N_t was 48. As already noted, boundary conditions were analyzed for each entrance ramp as well as the upstream mainline station, resulting in an N_s of 10.

A matrix containing the GEH statistic results between all Before and After dates was produced, each row summarizing the GEH statistics comparing a single Before date against all After dates and each column summarizing the GEH statistics comparing a single post-ramp metering date against all Before metering dates. In order to narrow these to the best grouping of dates, a methodology was created to winnow out poorly-matching dates and identify the most-closely matched clusters of dates. For each row and column, the average GEH was calculated to produce a meta-GEH score comparing a single day to all other days, as illustrated in Figure 6-4.

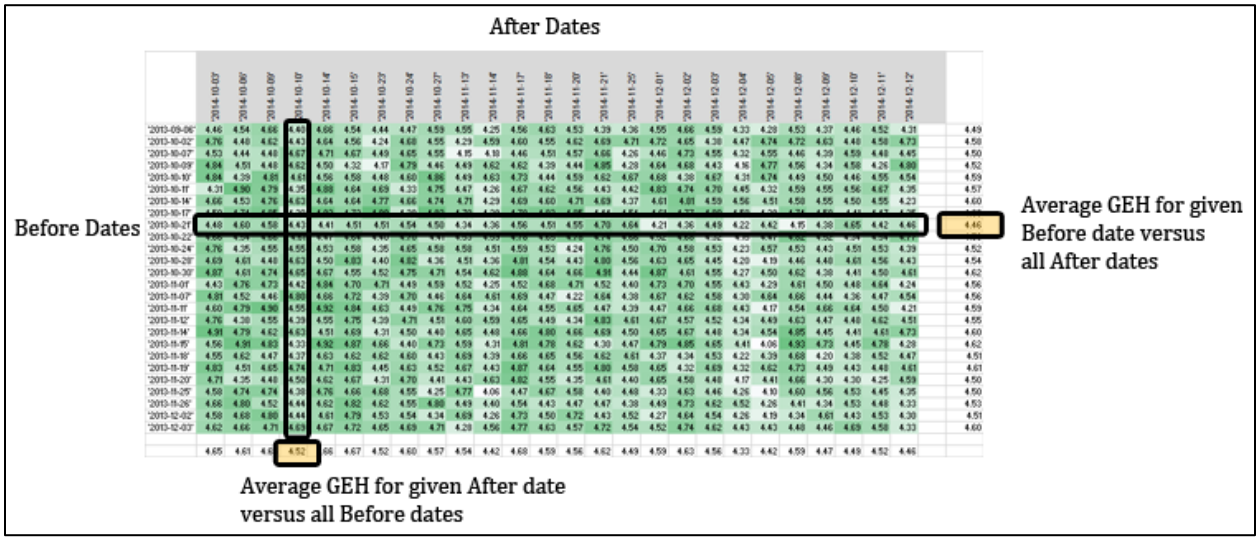

Figure 6-4. GEH statistic averaging to identify best-matching date clusters.

65 Before and 67 After dates were included in this analysis once dates with defective detectors were removed. To accurately compare the Before and After conditions, these were winnowed to the best matching cohort of dates by removing those with high meta-GEH scores. The two worst

After dates were first removed in order to equalize the number of dates within each group. Then, iteratively, the single worst Before and After dates were removed. Termination of this procedure was based on the worst remaining meta-GEH scores and the overall worst GEH score for any date pair remaining. These statistics were tracked at each iteration and can be seen in Figure 6-5.

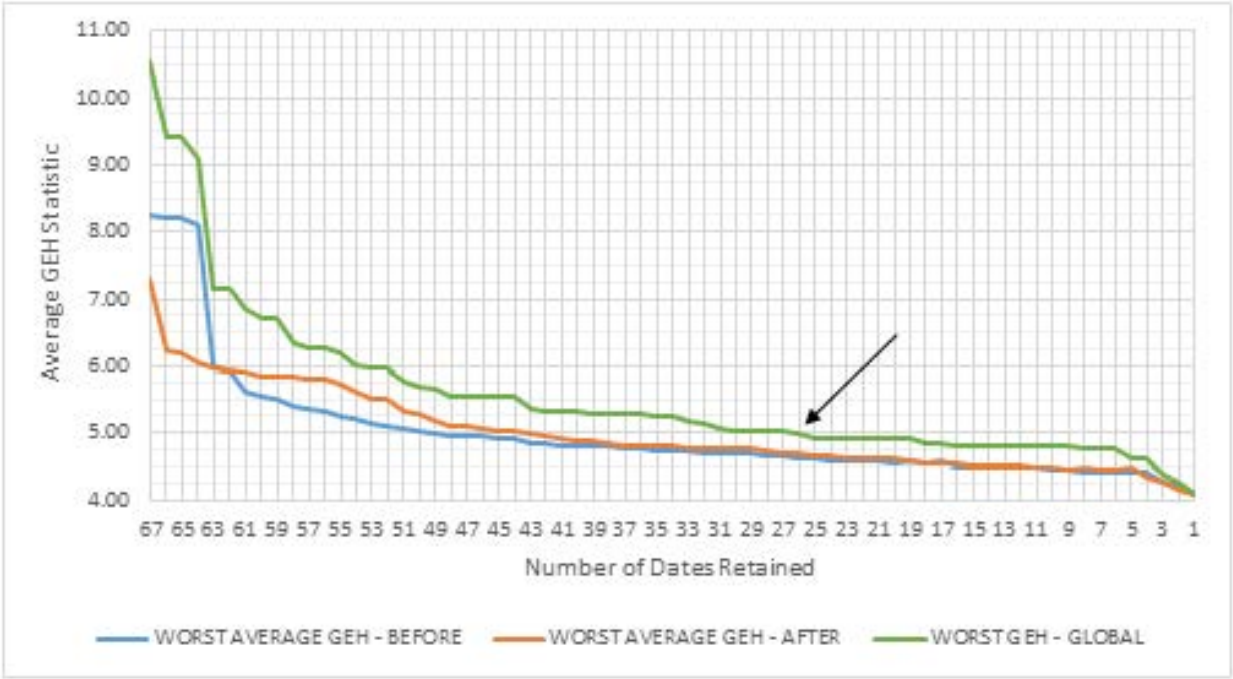

Figure 6-5. GEH meta-statistics through the date winnowing process.

As can be seen, the first dates to be eliminated by this methodology matched poorly with the remaining dates, causing significant improvements in overall GEH scores. This process slowed and GEH scores did not change dramatically for much of the process. Since the GEH statistic indicates 'good' matching when under a value of 5, that was selected as the cutoff for identifying well-matched date clusters. After winnowing to 26 dates Before and After ramp metering implementation (indicated in Figure 6-5), the worst GEH remaining fell to 4.99. Those 52 dates were then used to analyze the corridor, and are referred to as the "Correlated Days" group.

Through the analysis process, two other sets of Before/After date groups were used. Based on the GEH method above, the remaining dates were further narrowed by examining the total congestion (as depicted by speed contour plots). Dates which experienced little or no congestion were eliminated leaving those with 'normal' conditions. These dates are referred to as "Correlated Days with Normal Congestion".

Finally, several severe-weather days caused extremely high levels of congestion along the corridor. These were selected out for separate analysis, and are referred to as "Worst Congestion Days".

6.3 DELAY ANALYSIS

Vehicle delay was used as a second performance measure to further analyze the TH-212 corridor. Two methods were used to calculate delay for the corridor. For this analysis, only weekdays within October 2013 and 2014 were used. This practice corresponds to the dates which are used for the annual Congestion Report compiled by the RTMC.

However, in examining the results produced by the delay methodologies described below, one day (October 4, 2013) was found to include several malfunctioning detectors. The TICAS methodology described below included that date when generating average vehicle delay. When using the HART data, delay results were produced which both include and exclude that day.

6.3.1 Delay from TICAS

The Traffic Information and Condition Analysis System (TICAS) was developed for MnDOT as an analysis and evaluation tool for the Twin Cities. For this analysis, the offline version of the system was used with archived loop detector data to calculate delay along TH-212. TICAS breaks each corridor into 0.1-mile segments and estimates speed and flow rates during each time interval (30 second pieces, directly from the loop data gathered by MnDOT). For delay, TICAS uses speed to calculate a travel time and compares it against a free flow travel time. Flow is incorporated to produce vehicle-hours delay along the corridor. The exact free flow speed used within this delay methodology was not clarified within the TICAS documentation.

TICAS was used within a subarea of the corridor targeting the regions immediately impacted by the active ramp meters. Using the alphabetic segments indicated in Figure 6-1, this region includes segments E through U.

6.3.2 Delay from HART Data

A similar methodology was used based on the HART data described in a previous section. 5-minute volume and speed data were used at each segment along the entire corridor to produce delay. Since the exact free flow speed used by the TICAS methodology was not specified, three different possible free flow travel speeds were used to generate delay using the HART data: 45, 55, and 65 miles per hour. Each segment was examined for time periods with speeds below each of these thresholds. The difference between total vehicle travel time and free flow travel time (using the threshold speed) was saved as delay.

Using the same methodology as previously described, the ramp delay was also estimated for each of the entrances under UMD KAdaptive control. The total vehicle delay at the ramp was incorporated into a corridor total.

6.4 SAMPLE OUTPUT DATA AND FIGURES

From the data collected and generated by the previous methodologies, two types of figures were created: contour plots of speed for the corridor, and boxplots showing travel time by segment comparing Before and After states. The contour plots were generated using 30-second average speeds at each loop detector station. Figure 6-6 shows a sample day.

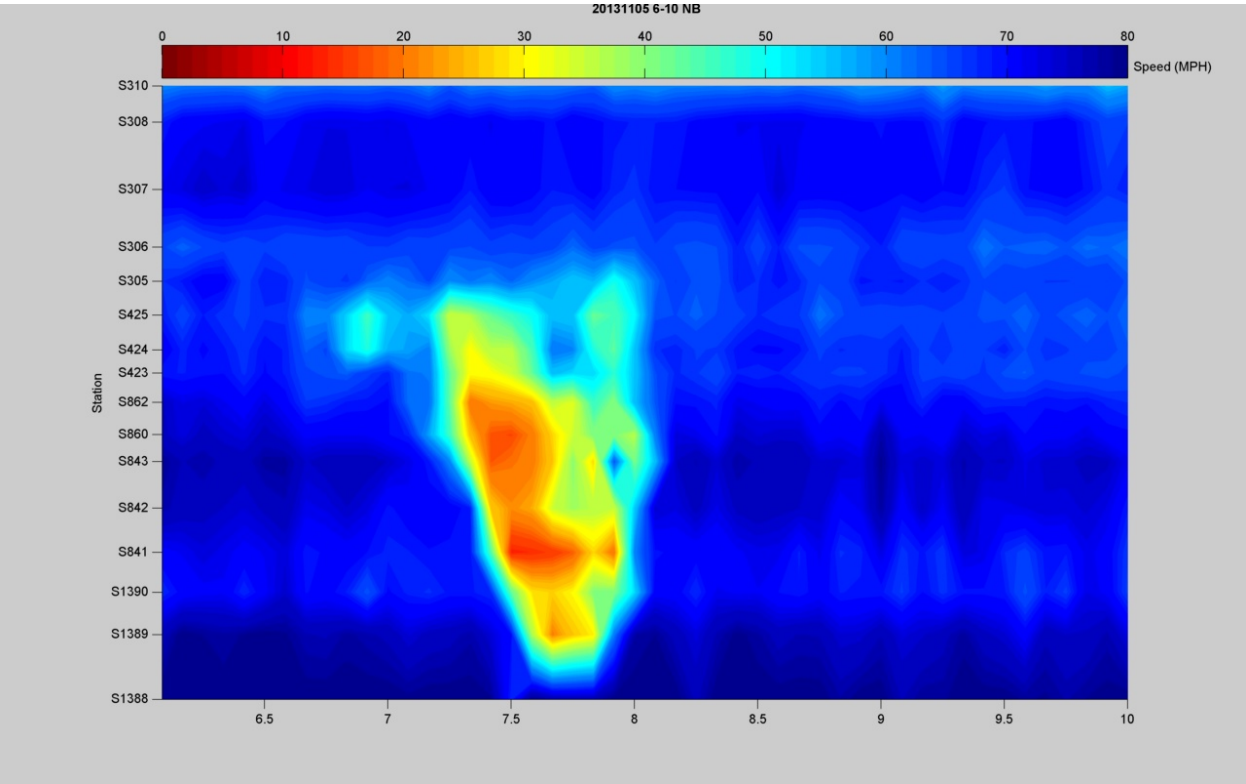

Figure 6-6. Sample contour plot figure for TH-212 corridor.

Figure 6-6 shows speed as a heat map with cool (blue) colors indicating high-speed, free-flowing conditions and warm (red) colors indicating low-speed, congested conditions. Along the horizontal axis, time is indicated in decimal hours between 6 and 10 AM. The vertical axis indicates distance through the corridor from upstream (bottom) to downstream (top) so that vehicles traverse the corridor from lower-left to upper-right and congestion propagates from upper-left to lower-right. Each station along the vertical axis is labeled and distance-adjusted to reflect the actual spacing between locations.

The other figure type generated from these data was boxplots showing travel time by roadway segment. Figure 6-7 is a sample based on the 33-segments described early in this chapter, while Figure 6-8 shows the same data as travel times between each loop detector station.

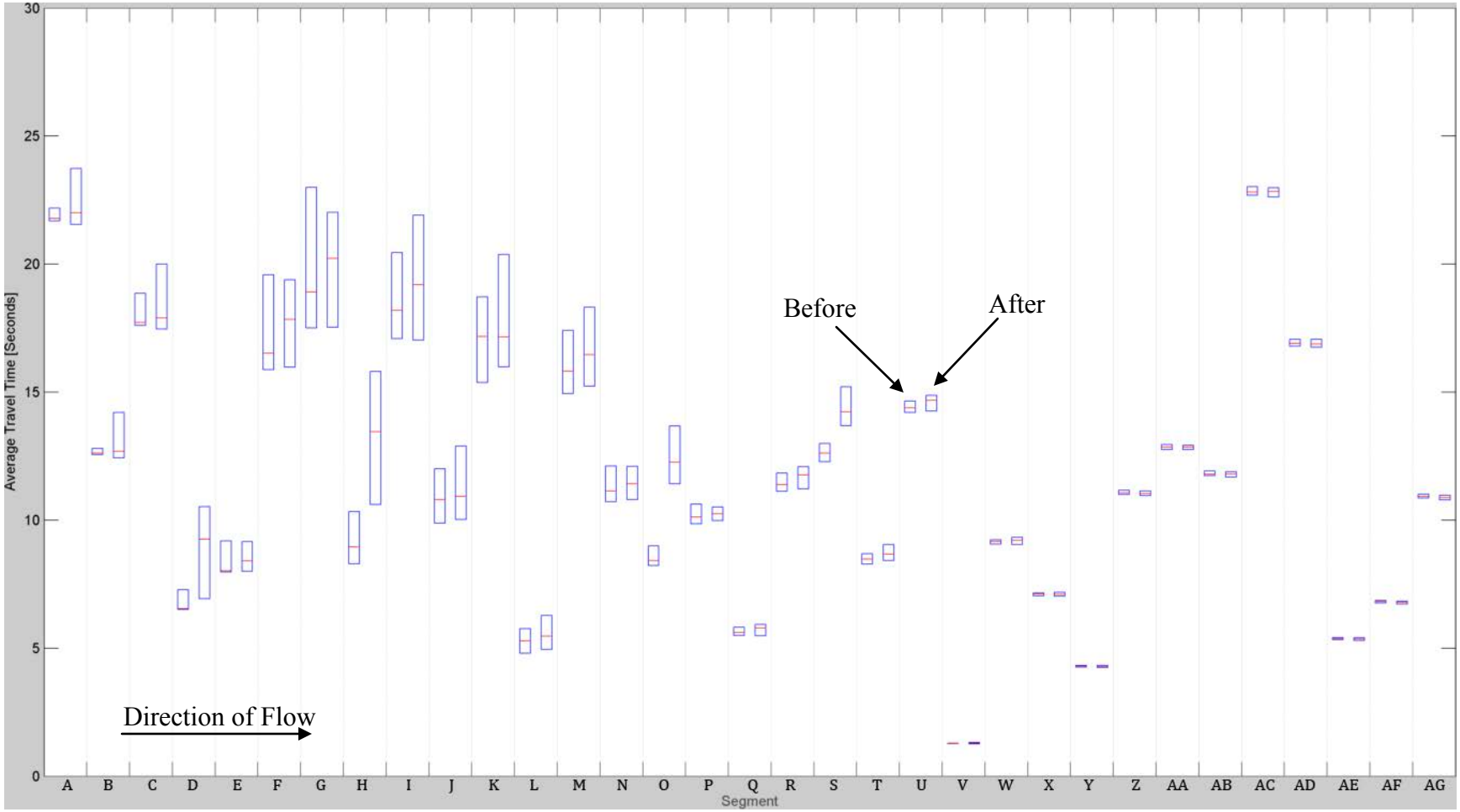

Figure 6-7. Average travel time by segment.

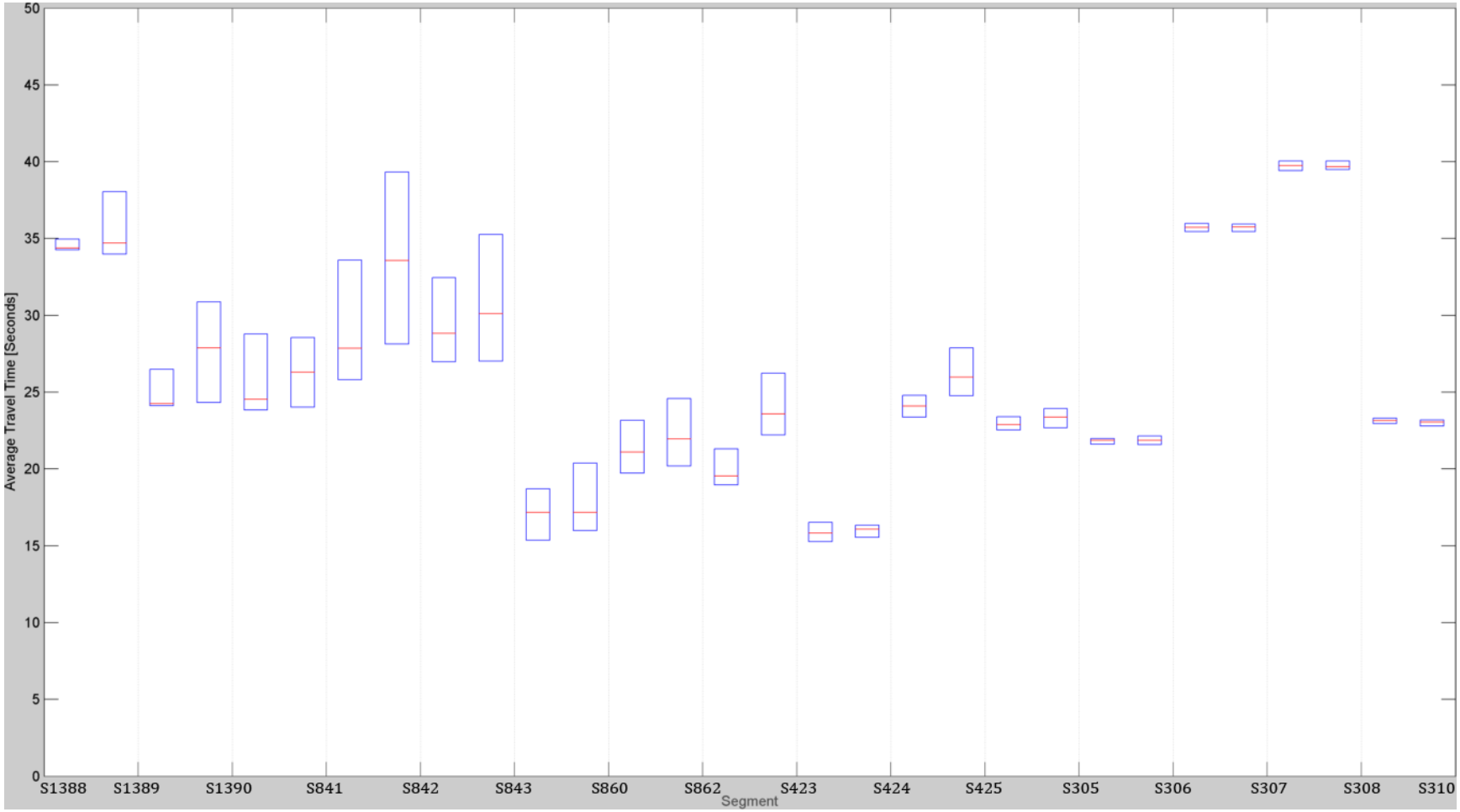

Figure 6-8. Average travel time between stations.

In each boxplot, the corridor is arranged across the horizontal axis with upstream at the left and downstream at the right. The vertical axis indicates average travel time values in seconds. Within each segment, whether one of the 33 or one of the 15 between stations, two boxes are shown. These show the Before and After travel times on the left and right, respectively. This is illustrated by the arrows in Figure 6-7. Each blue box indicates the top and bottom quartiles of travel time across the dates which make up each figure, and the median is indicated by the red line. Maximum extents and outliers were excluded from each diagram.

6.5 RESULTS

The two performance measures used to analyze the TH-212 corridor revealed a small positive impact from the implementation of the UMD KAdaptive algorithm. While overall total travel time held constant during normal congestion conditions, travel time was improved during particularly heavy congestion days. Delay within the smaller subarea showed a stronger positive impact, although the corridor as a whole showed more modest changes. The specific impacts captured by the two approaches are described below.

6.5.1 Total Travel Time Analysis Results

As outlined in the previous section, the comparison of the traffic conditions on TH-212 Before and After implementation of the UMD KAdaptive ramp metering algorithm was performed using several different groups of days. These different comparison groups were utilized in order to uncover the performance of the ramp metering on TH-212 under different traffic and environmental conditions.

6.5.1.1 All Correlated Days (Figure 6-10 and Figure 6-11)

This group contains all days from Before and After that showed strong correlation in demand on the corridor boundaries. The selection of days for this group did not include any criteria for the level or formation of congestion because the goal was to get an overall picture of the influence of the ramp metering strategy.

As noted in the previous section, each travel time plot presents the travel time on each road segment as a pair of box plots, Before on the left and After on the right of each pair. The pairs are separated by light dashed lines. As can be seen from the following figures, when focusing only on the mainline travel time (at the bottom in each figure) there doesn't seem to be any significant gain from the ramp metering implementation. When ramp delay is taken into account we see an increase on the travel time of the segments that include metered ramps (noted with braces); these are segments D, H, O, and S. In regard to days with no formation of congestion, both before and after subgroups had the same number of congestion free days. Also in this grouping of days there is no significant difference in the start and end of congestion. For completeness, the second set of figures involves road segments between stations which do not have the same number of lanes from start to finish.

6.5.1.2 Correlated Days with Normal Congestion (Figure 6-12 and Figure 6-13)

This group contains all days from Before and After that showed great correlation of the demand on the corridor boundaries excluding days that congestion was not formed. In both subgroups, the congestion varied in intensity but was always present.

As can be seen from the following figures, when focusing only on the mainline travel time there does not appear to be any significant gain from the ramp metering implementation. When ramp delay is taken into account we see an increase on the travel time of the segments that include metered ramps (noted with the braces). Like in the earlier group of days there is no significant difference in the start and end of congestion.

6.5.1.3 Worst Congestion days (Figure 6-14 and Figure 6-15)

In the previous two day groups, given that they were selected through the correlation methodology, there were no days with considerably different congestion patterns. Across all Before and After days collected for analysis there were a few days which, due to environmental factors (snow or icy rain), generated a notably different pattern which included stronger flow breakdown and heavier congestion. The contour plot presented in Figure 6-6 shows a day with typical congestion activity while Figure 6-9 shows the conditions in one of the snow days.

As can be seen in the travel time Figure 6-14 and Figure 6-15, in days with severe congestion the UMD KAdaptive algorithm has a significant positive impact on corridor travel times even when the ramp delay is taken into account. Given these results we can surmise that for the UMD KAdaptive algorithm to have an effect, sufficient demand must be present.

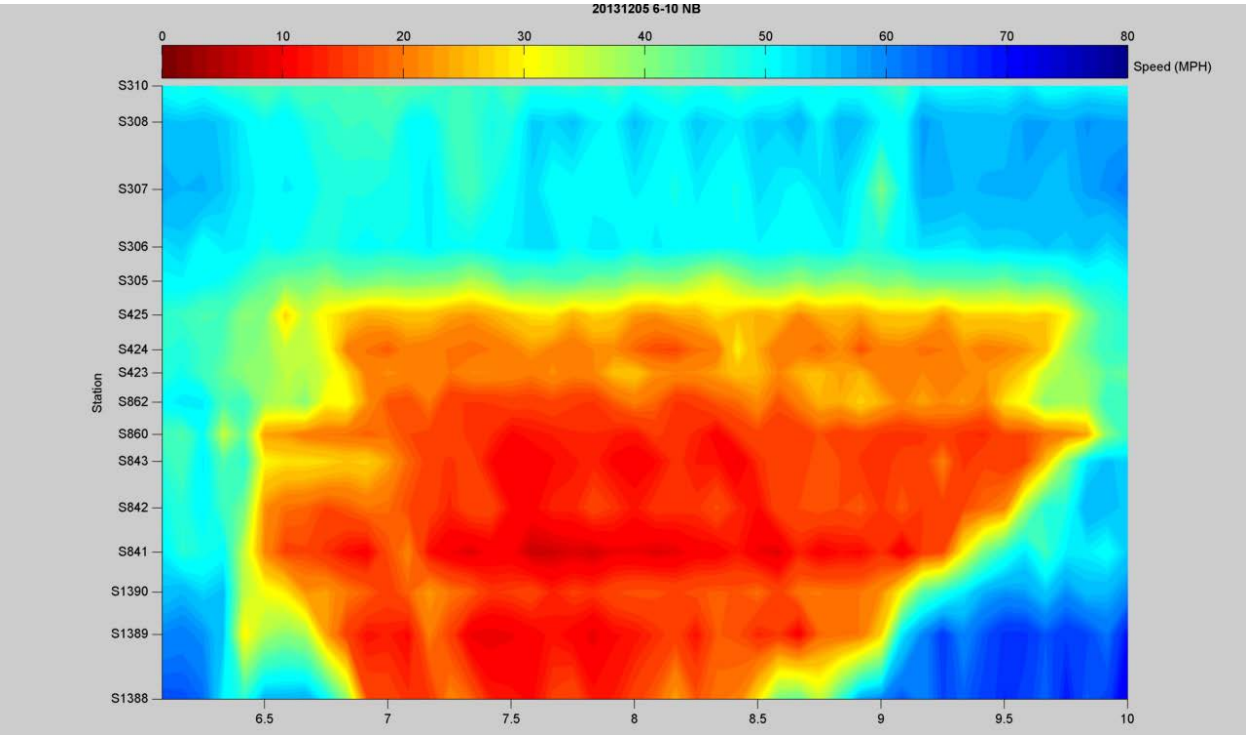

Figure 6-9. Example speed contour plot from a heavy-congestion day.

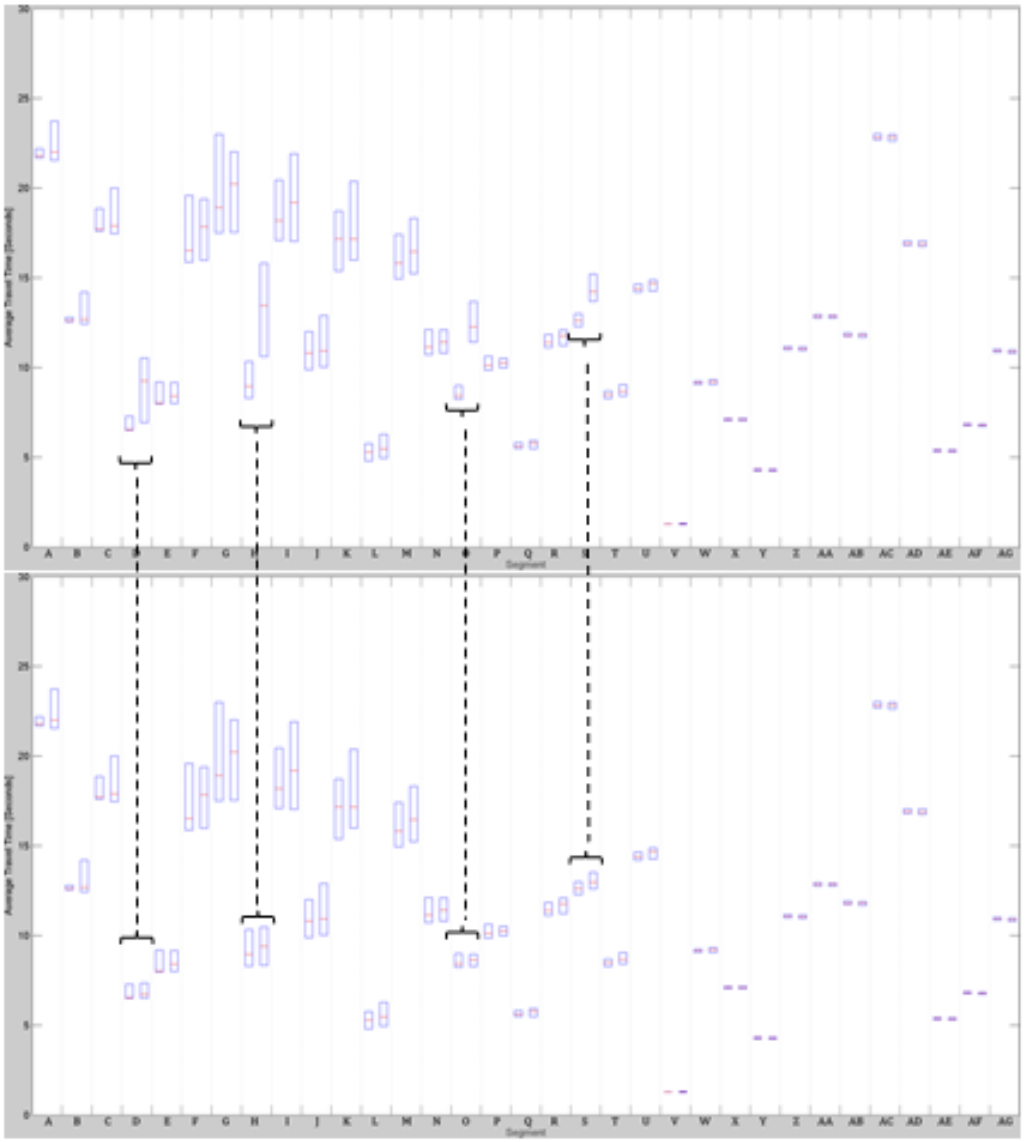

Figure 6-10. Average travel time in seconds for 'All Correlated Days' by segment.

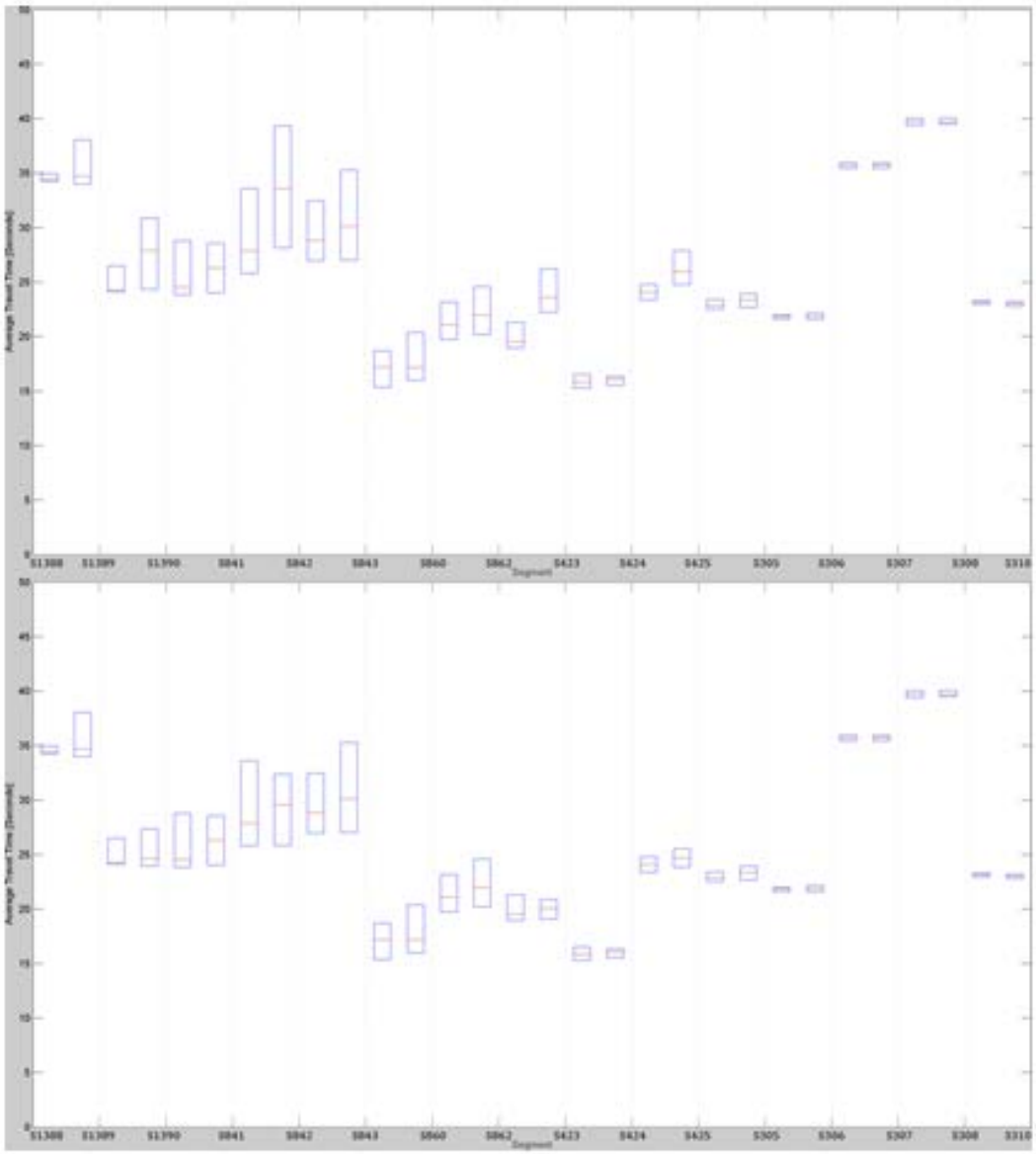

Mainline and Ramp Travel Times combined

Mainline Travel Times only

Figure 6-11. Average travel time in seconds for 'All Correlated Days' by station.

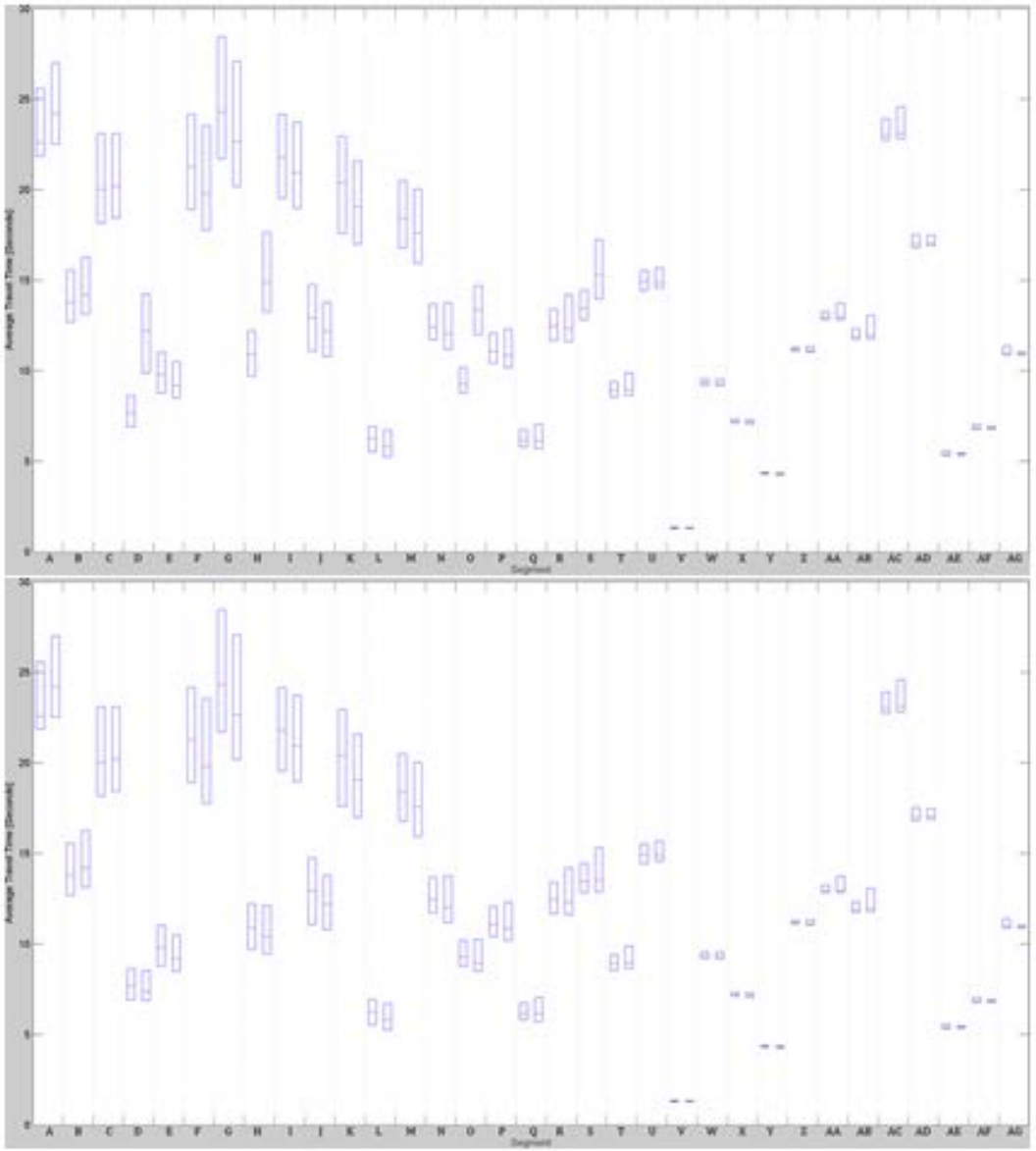

Figure 6-12. Average travel time in seconds for 'Correlated Days with Normal Congestion' by segment.

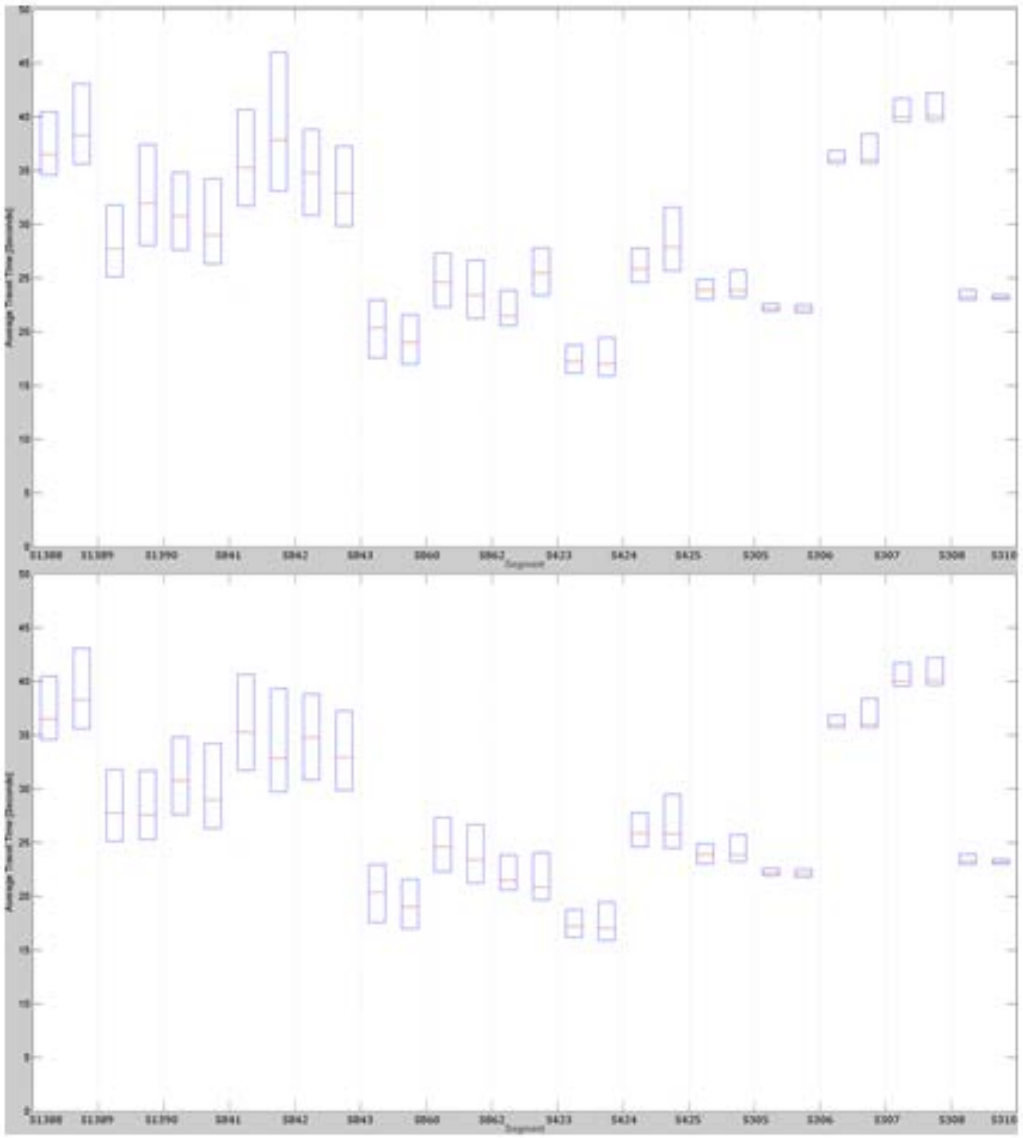

Mainline and Ramp Travel Times combined

Mainline Travel Times only

Figure 6-13. Average travel time in seconds for 'Correlated Days with Normal Congestion' by station.

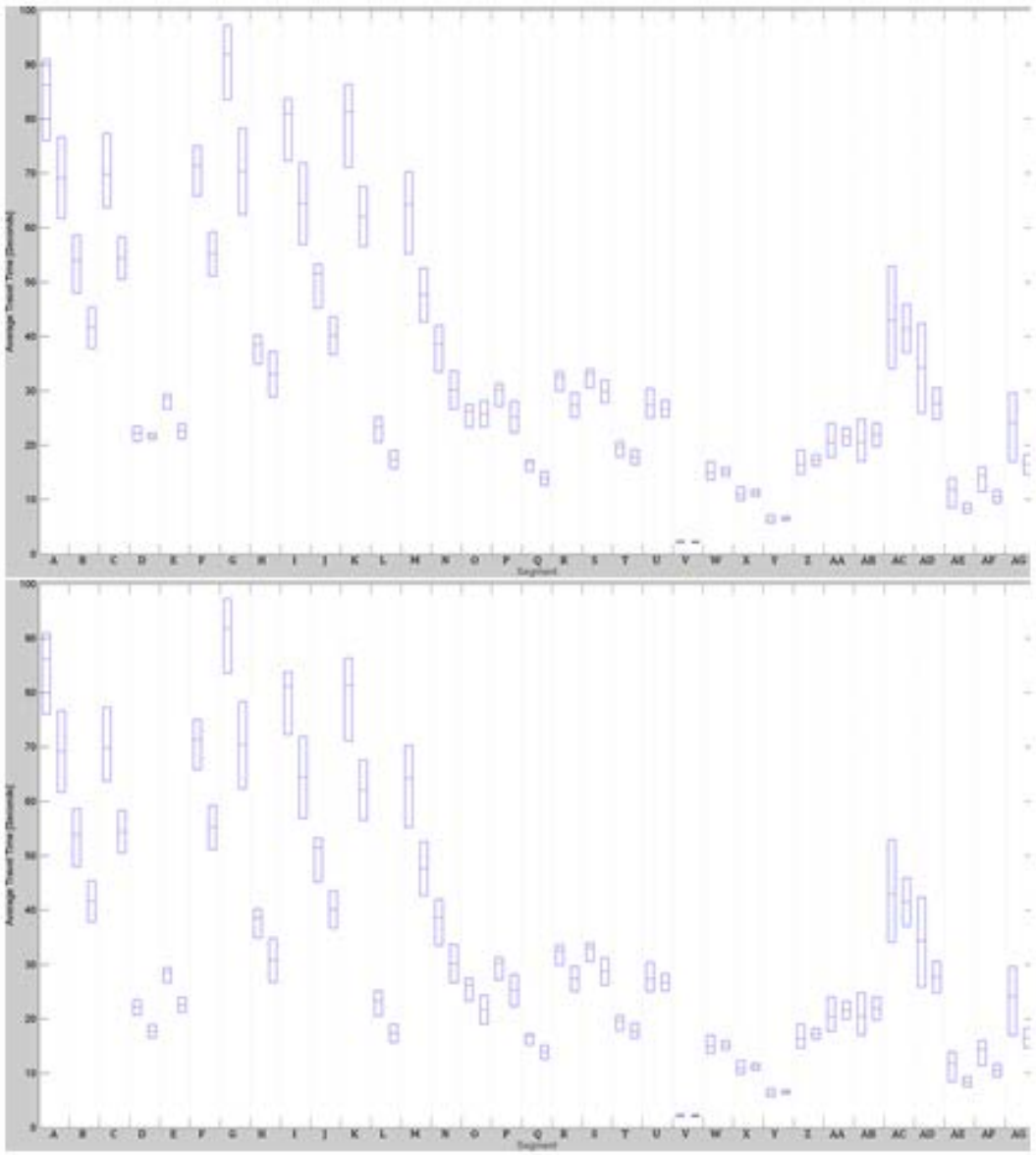

Figure 6-14. Average travel time in seconds for 'Worst Congestion Days' by segment.

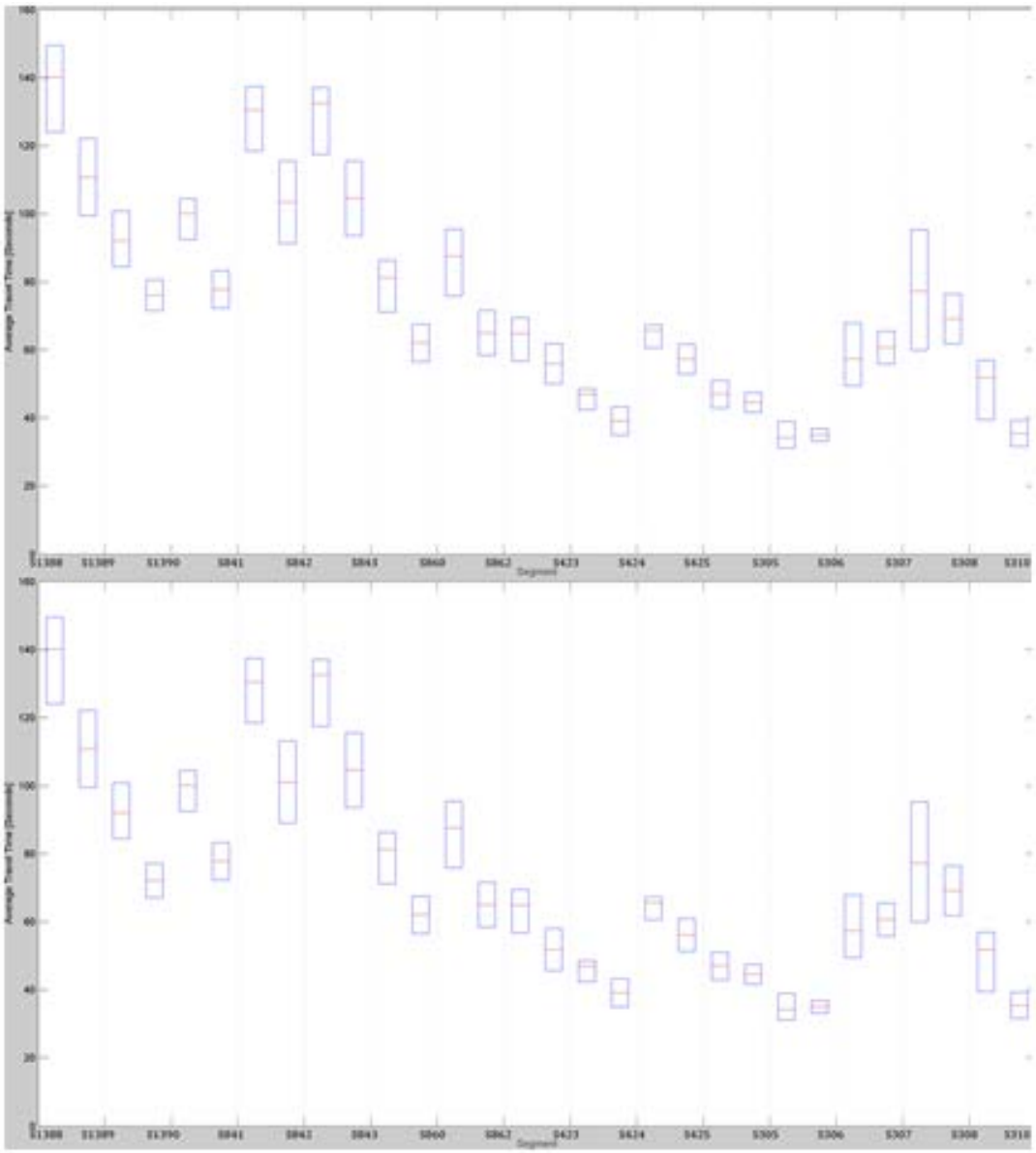

Mainline and Ramp Travel Times combined

Mainline Travel Times only

Figure 6-15. Average travel time in seconds for 'Worst Congestion Days' by station.

Table 6-1. Segment travel time statistics: A to L.

Data Set				A	B	C	D	E	F	G	H	I	J	K	L
All Correlated Days	Pre	No Ramp Meters	Upper Quartile	22.2	12.8	18.9	7.3	9.2	19.6	23.0	10.3	20.4	12.0	18.7	5.8
			Median	21.8	12.6	17.7	6.5	8.0	16.5	18.9	9.0	18.2	10.8	17.2	5.3
			Lower Quartile	21.7	12.6	17.6	6.5	8.0	15.9	17.5	8.3	17.1	9.9	15.4	4.8
	Post	Ramp Delay Included	Upper Quartile	23.7	14.2	20.0	10.5	9.2	19.4	22.0	15.8	21.9	12.9	20.4	6.3
			Median	22.0	12.7	17.9	9.3	8.4	17.8	20.2	13.4	19.2	10.9	17.2	5.5
			Lower Quartile	21.5	12.4	17.5	6.9	8.0	16.0	17.5	10.6	17.0	10.0	16.0	5.0
		Mainline Delay Only	Upper Quartile	23.7	14.2	20.0	7.4	9.2	19.4	22.0	10.5	21.9	12.9	20.4	6.3
			Median	22.0	12.7	17.9	6.7	8.4	17.8	20.2	9.4	19.2	10.9	17.2	5.5
			Lower Quartile	21.5	12.4	17.5	6.5	8.0	16.0	17.5	8.3	17.0	10.0	16.0	5.0
Correlated Days with Normal Congestion	Pre	No Ramp Meters	Upper Quartile	25.6	15.6	23.1	8.6	11.0	24.2	28.5	12.2	24.2	14.8	23.0	6.9
			Median	22.6	13.8	20.0	7.7	9.8	21.3	24.3	10.9	21.8	12.9	20.4	6.3
			Lower Quartile	21.8	12.7	18.2	6.9	8.8	18.9	21.7	9.7	19.5	11.1	17.6	5.5
	Post	Ramp Delay Included	Upper Quartile	27.0	16.3	23.1	14.2	10.5	23.5	27.1	17.6	23.7	13.8	21.6	6.7
			Median	24.2	14.2	20.2	12.2	9.2	19.8	22.6	14.9	20.9	12.2	19.0	5.8
			Lower Quartile	22.5	13.1	18.4	9.9	8.5	17.8	20.2	13.3	19.0	10.8	17.0	5.2
		Mainline Delay Only	Upper Quartile	27.0	16.3	23.1	8.5	10.5	23.5	27.1	12.1	23.7	13.8	21.6	6.7
			Median	24.2	14.2	20.2	7.4	9.2	19.8	22.6	10.4	20.9	12.2	19.0	5.8
			Lower Quartile	22.5	13.1	18.4	6.9	8.5	17.8	20.2	9.4	19.0	10.8	17.0	5.2
Worst Congestion Days	Pre	No Ramp Meters	Upper Quartile	90.9	58.6	77.3	23.5	29.4	75.0	97.2	40.2	83.8	53.3	86.4	25.2
			Median	86.2	53.9	69.9	22.2	28.6	71.4	91.9	38.5	81.0	51.5	81.3	23.3
			Lower Quartile	76.0	48.0	63.7	20.7	26.7	65.9	83.6	34.9	72.3	45.1	71.1	20.6
	Post	Ramp Delay Included	Upper Quartile	76.7	45.4	58.3	22.2	24.0	59.2	78.3	37.2	71.9	43.6	67.6	19.0
			Median	69.2	41.6	54.4	21.7	22.6	55.2	70.4	33.1	64.4	40.1	62.1	17.3
			Lower Quartile	61.7	37.8	50.5	21.1	21.1	51.2	62.4	28.9	56.9	36.7	56.5	15.7
		Mainline Delay Only	Upper Quartile	76.7	45.4	58.3	18.9	24.0	59.2	78.3	34.8	71.9	43.6	67.6	19.0
			Median	69.2	41.6	54.4	17.7	22.6	55.2	70.4	30.8	64.4	40.1	62.1	17.3
			Lower Quartile	61.7	37.8	50.5	16.6	21.1	51.2	62.4	26.7	56.9	36.7	56.5	15.7

Table 6-2. Segment travel time statistics: M to X.

Data Set				M	N	O	P	Q	R	S	T	U	V	W	X
All Correlated Days	Pre	No Ramp Meters	Upper Quartile	17.4	12.1	9.0	10.6	5.8	11.8	13.0	8.7	14.7	1.3	9.2	7.2
			Median	15.8	11.1	8.4	10.1	5.6	11.4	12.6	8.5	14.4	1.3	9.2	7.1
			Lower Quartile	14.9	10.7	8.2	9.9	5.5	11.1	12.3	8.3	14.2	1.3	9.1	7.0
	Post	Ramp Delay Included	Upper Quartile	18.3	12.1	13.7	10.5	5.9	12.1	15.2	9.1	14.9	1.3	9.3	7.2
			Median	16.5	11.4	12.3	10.3	5.8	11.8	14.2	8.7	14.7	1.3	9.2	7.1
			Lower Quartile	15.2	10.8	11.4	10.0	5.5	11.2	13.7	8.4	14.3	1.3	9.0	7.0
		Mainline Delay Only	Upper Quartile	18.3	12.1	8.9	10.5	5.9	12.1	13.5	9.1	14.9	1.3	9.3	7.2
			Median	16.5	11.4	8.6	10.3	5.8	11.8	13.0	8.7	14.7	1.3	9.2	7.1
			Lower Quartile	15.2	10.8	8.3	10.0	5.5	11.2	12.6	8.4	14.3	1.3	9.0	7.0
Correlated Days with Normal Congestion	Pre	No Ramp Meters	Upper Quartile	20.5	13.7	10.2	12.1	6.7	13.4	14.5	9.4	15.5	1.4	9.5	7.3
			Median	18.4	12.4	9.3	11.1	6.2	12.5	13.5	8.9	14.9	1.3	9.3	7.2
			Lower Quartile	16.8	11.7	8.8	10.4	5.8	11.7	12.8	8.6	14.4	1.3	9.2	7.1
	Post	Ramp Delay Included	Upper Quartile	20.0	13.8	14.7	12.3	7.0	14.2	17.2	9.9	15.7	1.3	9.5	7.3
			Median	17.6	12.0	13.4	10.9	6.1	12.3	15.3	9.0	14.9	1.3	9.3	7.2
			Lower Quartile	15.9	11.2	12.0	10.2	5.7	11.6	14.0	8.6	14.6	1.3	9.2	7.1
		Mainline Delay Only	Upper Quartile	20.0	13.8	10.2	12.3	7.0	14.2	15.3	9.9	15.7	1.3	9.5	7.3
			Median	17.6	12.0	9.0	10.9	6.1	12.3	13.5	9.0	14.9	1.3	9.3	7.2
			Lower Quartile	15.9	11.2	8.5	10.2	5.7	11.6	12.9	8.6	14.6	1.3	9.2	7.1
Worst Congestion Days	Pre	No Ramp Meters	Upper Quartile	70.3	42.0	27.5	31.3	17.3	33.6	33.9	20.6	30.4	2.5	17.0	12.3
			Median	64.3	38.6	26.2	30.2	16.8	32.6	33.1	19.7	27.4	2.2	14.9	10.8
			Lower Quartile	55.3	33.5	23.3	27.1	15.2	29.9	30.6	17.9	25.0	2.0	13.6	9.9
	Post	Ramp Delay Included	Upper Quartile	52.6	33.7	28.2	28.1	15.2	29.7	31.9	19.2	28.2	2.3	15.9	11.8
			Median	47.6	30.2	25.8	25.2	13.9	27.4	29.9	17.8	26.7	2.2	15.2	11.2
			Lower Quartile	42.7	26.7	23.4	22.3	12.6	25.1	27.8	16.5	25.2	2.1	14.4	10.6
		Mainline Delay Only	Upper Quartile	52.6	33.7	24.3	28.1	15.2	29.7	31.2	19.2	28.2	2.3	15.9	11.8
			Median	47.6	30.2	21.7	25.2	13.9	27.4	28.8	17.8	26.7	2.2	15.2	11.2
			Lower Quartile	42.7	26.7	19.1	22.3	12.6	25.1	26.3	16.5	25.2	2.1	14.4	10.6

Table 6-3. Segment travel time statistics: Y to AG.

Data Set				Y	Z	AA	AB	AC	AD	AE	AF	AG	Corridor Total
All Correlated Days	Pre	No Ramp Meters	Upper Quartile	4.3	11.2	12.9	11.9	23.0	17.1	5.4	6.9	11.0	405.5
			Median	4.3	11.1	12.9	11.8	22.8	16.9	5.4	6.8	10.9	383.1
			Lower Quartile	4.3	11.0	12.8	11.7	22.7	16.8	5.3	6.8	10.9	369.5
	Post	Ramp Delay Included	Upper Quartile	4.3	11.1	12.9	11.9	23.0	17.1	5.4	6.8	11.0	430.2
			Median	4.3	11.0	12.9	11.8	22.8	16.9	5.4	6.8	10.9	403.6
			Lower Quartile	4.2	11.0	12.8	11.7	22.6	16.8	5.3	6.7	10.8	376.1
		Mainline Delay Only	Upper Quartile	4.3	11.1	12.9	11.9	23.0	17.1	5.4	6.8	11.0	408.8
			Median	4.3	11.0	12.9	11.8	22.8	16.9	5.4	6.8	10.9	391.2
			Lower Quartile	4.2	11.0	12.8	11.7	22.6	16.8	5.3	6.7	10.8	369.6
Correlated Days with Normal Congestion	Pre	No Ramp Meters	Upper Quartile	4.4	11.3	13.3	12.3	23.9	17.5	5.6	7.0	11.4	458.3
			Median	4.3	11.2	13.0	11.9	23.0	17.0	5.4	6.8	11.0	418.1
			Lower Quartile	4.3	11.1	12.8	11.8	22.7	16.8	5.3	6.8	10.9	397.6
	Post	Ramp Delay Included	Upper Quartile	4.4	11.3	13.7	13.1	24.6	17.5	5.5	6.9	11.0	480.7
			Median	4.3	11.1	13.0	12.0	23.1	17.0	5.4	6.8	10.9	431.8
			Lower Quartile	4.3	11.0	12.8	11.8	22.8	16.9	5.4	6.8	10.9	403.7
		Mainline Delay Only	Upper Quartile	4.4	11.3	13.7	13.1	24.6	17.5	5.5	6.9	11.0	467.7
			Median	4.3	11.1	13.0	12.0	23.1	17.0	5.4	6.8	10.9	413.1
			Lower Quartile	4.3	11.0	12.8	11.8	22.8	16.9	5.4	6.8	10.9	390.0
Worst Congestion Days	Pre	No Ramp Meters	Upper Quartile	7.2	19.1	24.0	24.8	52.9	42.4	13.9	16.0	29.6	####
			Median	6.3	16.4	20.4	20.5	43.0	34.3	11.8	14.4	24.2	####
			Lower Quartile	5.7	14.7	17.7	17.0	34.1	25.9	8.5	11.4	17.0	####
	Post	Ramp Delay Included	Upper Quartile	6.9	18.3	23.2	24.0	45.9	30.5	9.3	11.7	18.3	####
			Median	6.5	17.2	21.6	21.9	41.5	27.6	8.4	10.5	16.5	996.8
			Lower Quartile	6.2	16.2	19.9	19.7	37.1	24.7	7.5	9.4	14.7	905.2
		Mainline Delay Only	Upper Quartile	6.9	18.3	23.2	24.0	45.9	30.5	9.3	11.7	18.3	####
			Median	6.5	17.2	21.6	21.9	41.5	27.6	8.4	10.5	16.5	985.4
			Lower Quartile	6.2	16.2	19.9	19.7	37.1	24.7	7.5	9.4	14.7	892.6

Table 6-4. Station to station travel time statistics.

Data Set				S1388 to S1389	S1389 to S1390	S1390 to S841	S841 to S842	S842 to S843	S843 to S860	S860 to S862	S862 to S423	S423 to S424	S424 to S425	S425 to S305	S305 to S306	S306 to S307	S307 to S308	S308 to S310	Corridor Total
All Correlated Days	Pre	No Ramp Meters	Upper Quartile	35.0	26.5	28.8	33.6	32.4	18.7	23.2	21.3	16.5	24.8	23.4	22.0	36.0	40.1	23.3	405.5
			Median	34.4	24.2	24.5	27.9	28.8	17.2	21.1	19.5	15.8	24.1	22.9	21.9	35.7	39.8	23.1	383.1
			Lower Quartile	34.3	24.1	23.8	25.8	27.0	15.4	19.7	19.0	15.3	23.4	22.5	21.6	35.5	39.4	23.0	369.5
	Post	Ramp Delay Included	Upper Quartile	38.0	30.9	28.6	39.3	35.3	20.4	24.6	26.2	16.3	27.9	23.9	22.1	35.9	40.0	23.2	430.2
			Median	34.7	27.9	26.3	33.6	30.1	17.2	22.0	23.6	16.1	26.0	23.4	21.9	35.8	39.7	23.1	403.6
			Lower Quartile	34.0	24.3	24.0	28.1	27.0	16.0	20.2	22.2	15.5	24.8	22.7	21.6	35.5	39.5	22.8	376.1
		Mainline Delay Only	Upper Quartile	38.0	27.4	28.6	32.4	35.3	20.4	24.6	20.8	16.3	25.5	23.9	22.1	35.9	40.0	23.2	408.8
			Median	34.7	24.6	26.3	29.6	30.1	17.2	22.0	20.1	16.1	24.7	23.4	21.9	35.8	39.7	23.1	391.2
			Lower Quartile	34.0	24.0	24.0	25.8	27.0	16.0	20.2	19.1	15.5	23.8	22.7	21.6	35.5	39.5	22.8	369.6
Correlated Days with Normal Congestion	Pre	No Ramp Meters	Upper Quartile	40.5	31.8	34.8	40.7	38.8	23.0	27.3	23.8	18.7	27.8	24.9	22.6	36.9	41.7	23.9	458.3
			Median	36.5	27.7	30.8	35.3	34.8	20.4	24.6	21.5	17.2	25.9	23.9	22.2	36.0	40.0	23.2	418.1
			Lower Quartile	34.6	25.1	27.6	31.7	30.8	17.6	22.3	20.6	16.2	24.6	23.0	21.9	35.7	39.5	23.0	397.6
	Post	Ramp Delay Included	Upper Quartile	43.1	37.4	34.3	46.0	37.3	21.6	26.7	27.8	19.4	31.6	25.7	22.5	38.4	42.2	23.4	480.7
			Median	38.3	32.0	29.0	37.9	32.9	19.0	23.4	25.5	17.0	27.9	23.9	22.1	36.0	40.1	23.2	431.8
			Lower Quartile	35.6	28.0	26.3	33.1	29.9	17.0	21.2	23.4	15.9	25.7	23.2	21.8	35.7	39.7	23.0	403.7
		Mainline Delay Only	Upper Quartile	43.1	31.7	34.3	39.3	37.3	21.6	26.7	24.1	19.4	29.5	25.7	22.5	38.4	42.2	23.4	467.7
			Median	38.3	27.6	29.0	32.9	32.9	19.0	23.4	20.8	17.0	25.8	23.9	22.1	36.0	40.1	23.2	413.1
			Lower Quartile	35.6	25.3	26.3	29.7	29.9	17.0	21.2	19.7	15.9	24.5	23.2	21.8	35.7	39.7	23.0	390.0
Worst Congestion Days	Pre	No Ramp Meters	Upper Quartile	149.5	100.8	104.5	137.5	137.0	86.4	95.5	69.5	48.6	67.3	51.0	39.0	67.9	95.3	57.0	1271.3
			Median	140.1	92.1	100.1	130.4	132.5	81.3	87.6	64.8	47.0	65.7	47.1	34.2	57.4	77.2	51.9	1250.0
			Lower Quartile	124.0	84.4	92.5	118.5	117.5	71.1	75.8	56.7	42.3	60.6	42.9	31.2	49.4	59.9	39.4	1101.7
	Post	Ramp Delay Included	Upper Quartile	122.1	80.6	83.2	115.5	115.5	67.6	71.6	61.8	43.3	61.6	47.5	36.9	65.5	76.5	39.3	1088.5
			Median	110.8	76.1	77.8	103.4	104.6	62.1	65.0	55.9	39.1	57.2	44.5	35.0	60.7	69.1	35.4	996.8
			Lower Quartile	99.5	71.6	72.3	91.3	93.6	56.5	58.4	50.0	34.9	52.9	41.6	33.2	55.9	61.8	31.6	905.2
		Mainline Delay Only	Upper Quartile	122.1	77.2	83.2	113.2	115.5	67.6	71.6	58.0	43.3	60.9	47.5	36.9	65.5	76.5	39.3	1078.2
			Median	110.8	72.1	77.8	101.1	104.6	62.1	65.0	51.8	39.1	56.1	44.5	35.0	60.7	69.1	35.4	985.4
			Lower Quartile	99.5	67.1	72.3	89.1	93.6	56.5	58.4	45.7	34.9	51.3	41.6	33.2	55.9	61.8	31.6	892.6

6.5.2 Delay Analysis Results

Although overall the ramp metering strategy seemed to have minimal impact on total corridor travel time, looking at delay gives a more nuanced picture. TICAS produced total vehicle delays for October 2013 and 2014 as well as total vehicle miles traveled (VMT). As seen in Table 6-5, 2013 produced just under 2200 vehicle-hours of delay versus just over 1900 for the same period in 2014, a decrease of more than 12 percent. Simultaneously the total VMT of the selected corridor (only covering the ramp meters) increased by 3 percent. As noted above, this includes the October 2013 day which had malfunctioning detectors. In order to remove that day, the average delay and VMT were calculated instead. Using those measures, TICAS found a decrease in daily average vehicle delay at 11.5% from 2013 to 2014 corresponding with an increase in daily VMT of 2%.

Table 6-5. TICAS delay results.

	Total Delay	Total VMT
Before (October 2013)	2189	1189350
After (October 2014)	1923	1225201
Change	-266	35851
% Change	-12.1%	3.0%

	Average Delay	Average VMT
Before (Excluding 10/4/2013)	94.5	52208
After	83.6	53270
Change	-10.9	1061
% Change	-11.5%	2.0%

These data clearly show the ramp metering system improved mainline operation within their area of influence. The TICAS method, however, only examined this exact area of influence. To more completely understand the impact of the ramp meters, a larger area must be included in order to catch edge effects or situations where improvement in one area causes issues elsewhere.

The delay calculations made with the HART data show exactly this. Three pairs of figures are shown below which describe vehicle-delay by segment, similar to the total travel time figures in previous sections. The first figure in each pair shows the lower quartile, median, and upper quartile for each segment, while the second only includes the median. The first pair, Figure 6-16 and Figure 6-17, show delay accumulated for vehicles traveling under 65 MPH; the second pair, Figure 6-18 and Figure 6-19, show delay accumulated for vehicles traveling under 55 MPH; the final pair, Figure 6-20 and Figure 6-21, show delay accumulated for vehicles traveling under 45 MPH. These values only consider mainline accumulation of delay; ramp delay will be considered shortly.

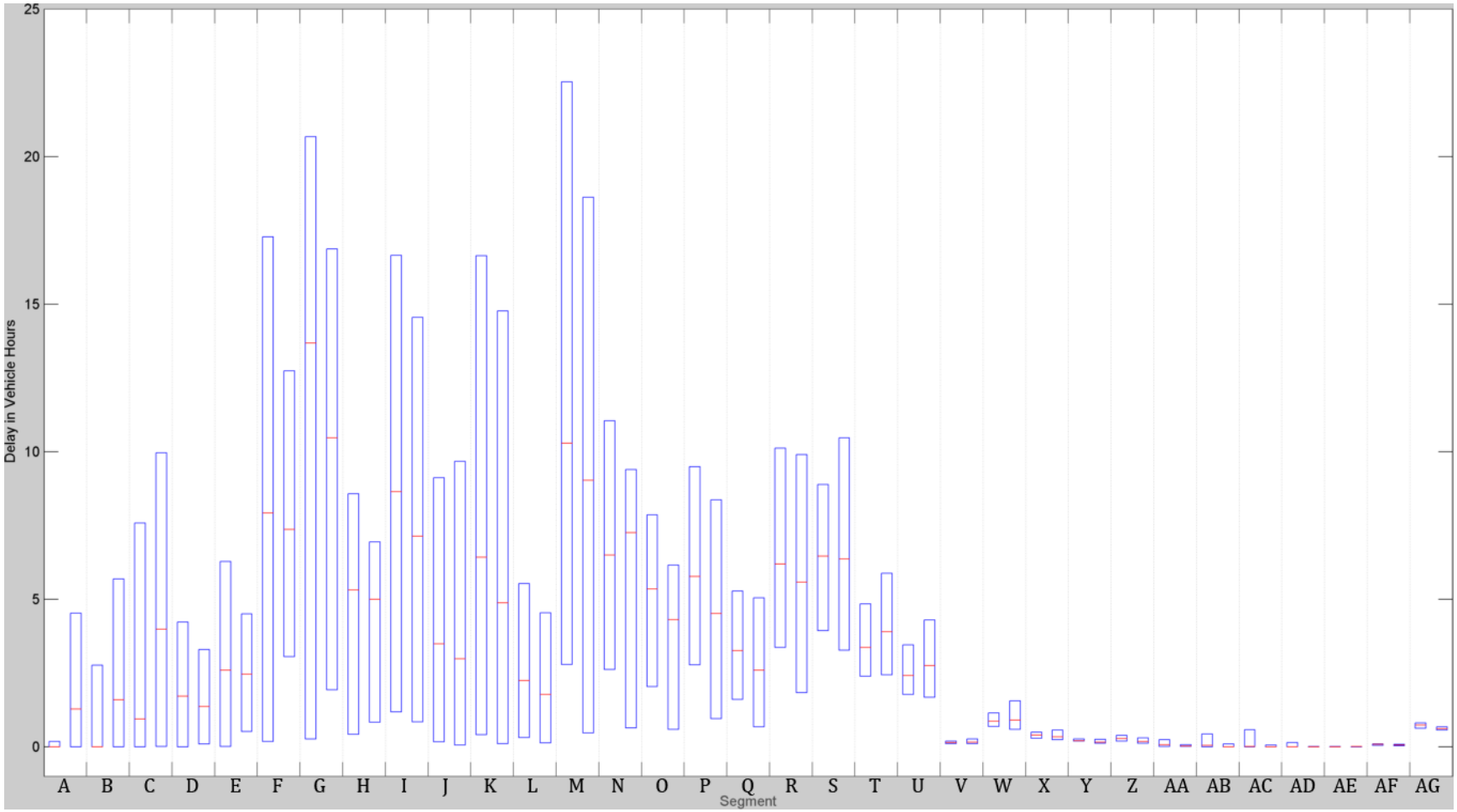

Figure 6-16. Boxplot of delay from vehicles under 65 MPH in vehicle-hours by segment.

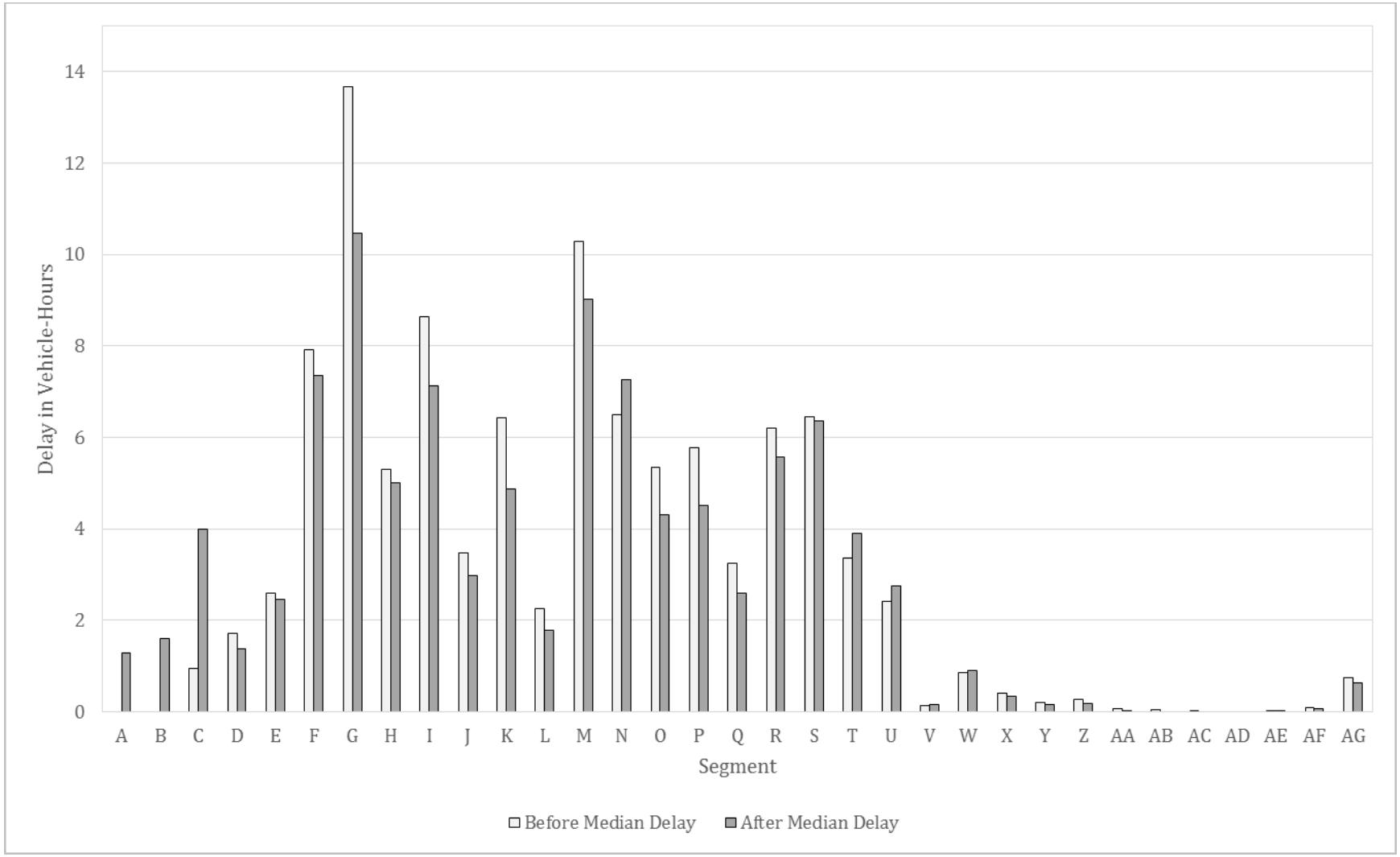

Figure 6-17. Medians of delay from vehicles under 65 MPH in vehicle-hours by segment.

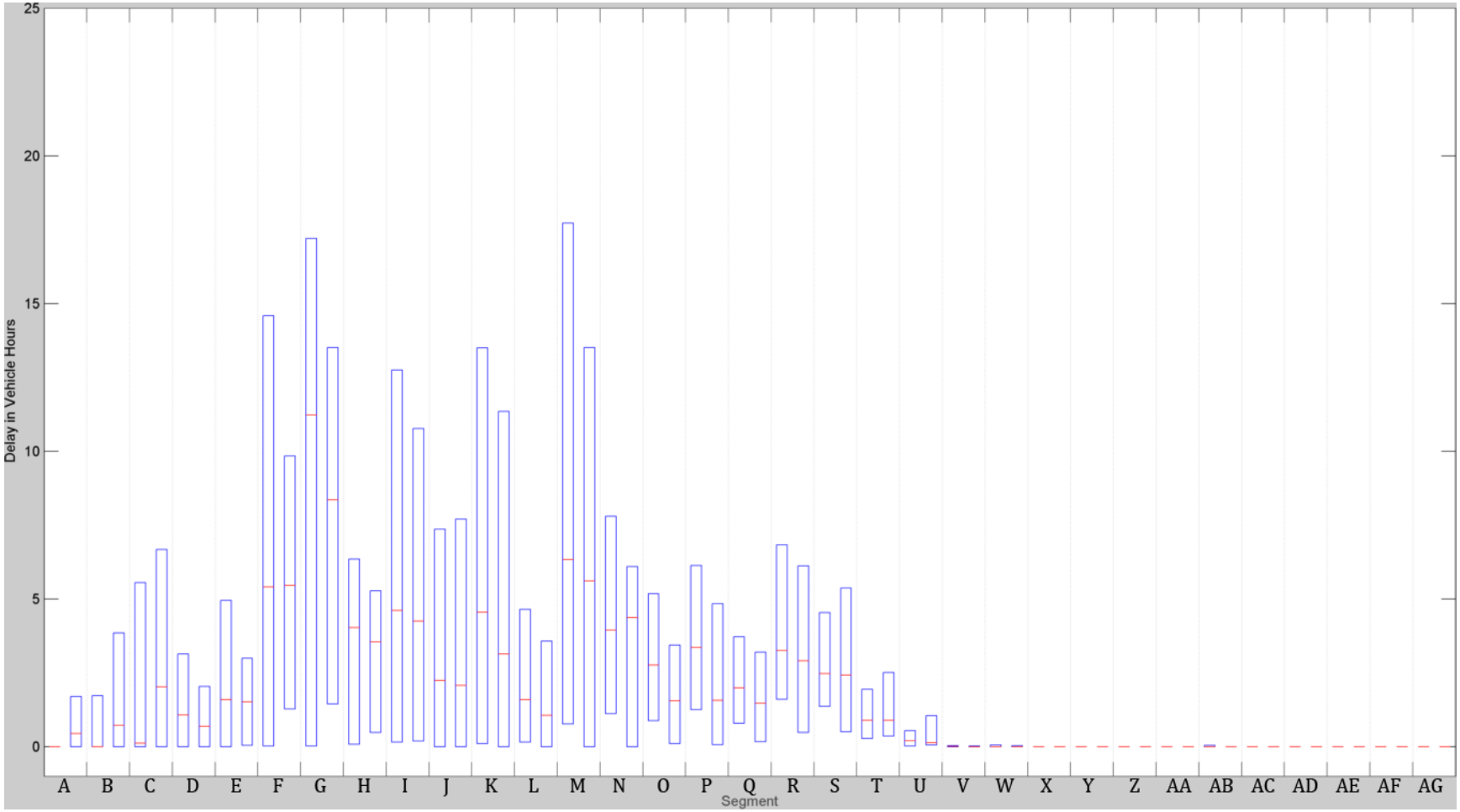

Figure 6-18. Boxplot of delay from vehicles under 55 MPH in vehicle-hours by segment.

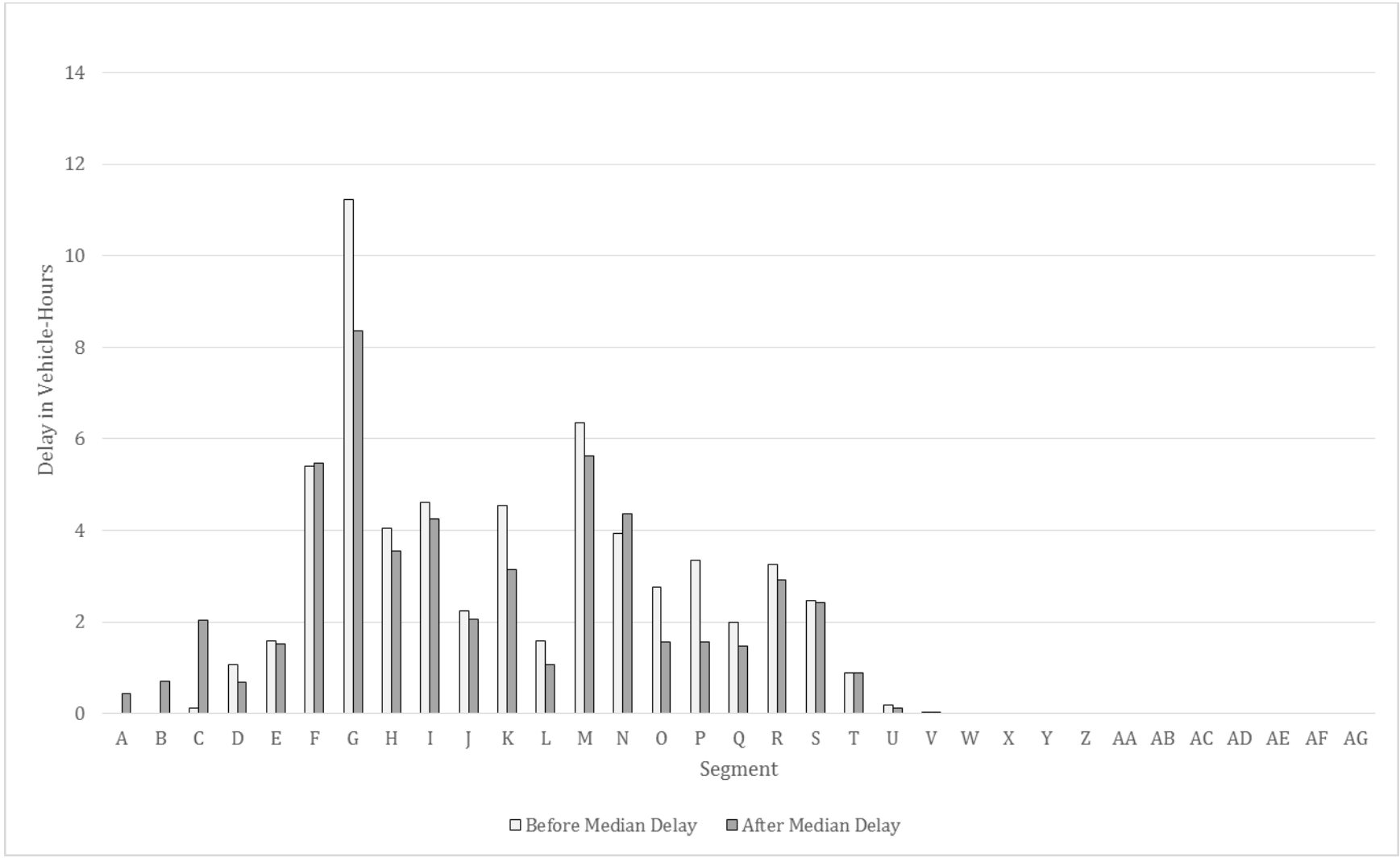

Figure 6-19. Medians of delay from vehicles under 55 MPH in vehicle-hours by segment.

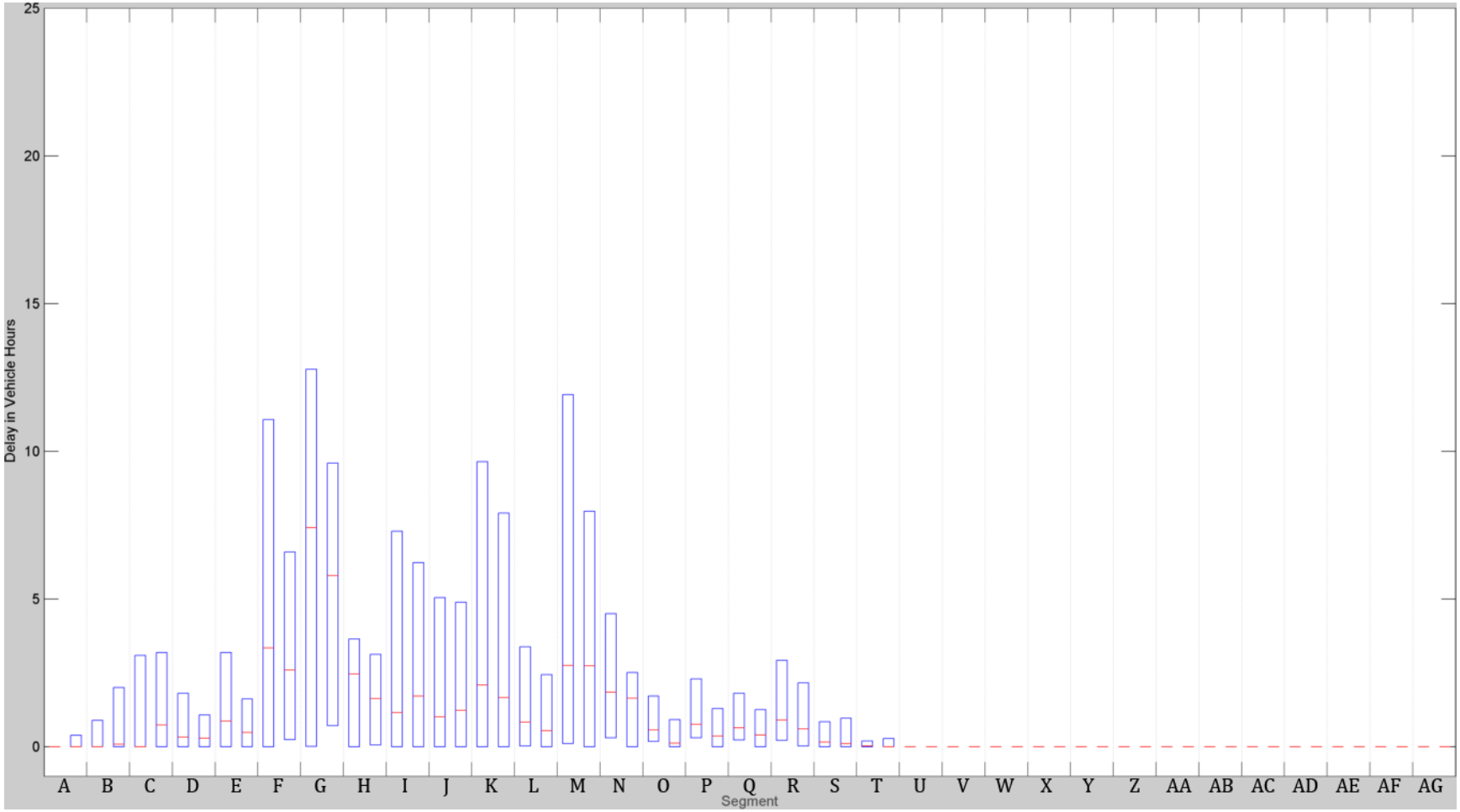

Figure 6-20. Boxplot of delay from vehicles under 45 MPH in vehicle-hours by segment.

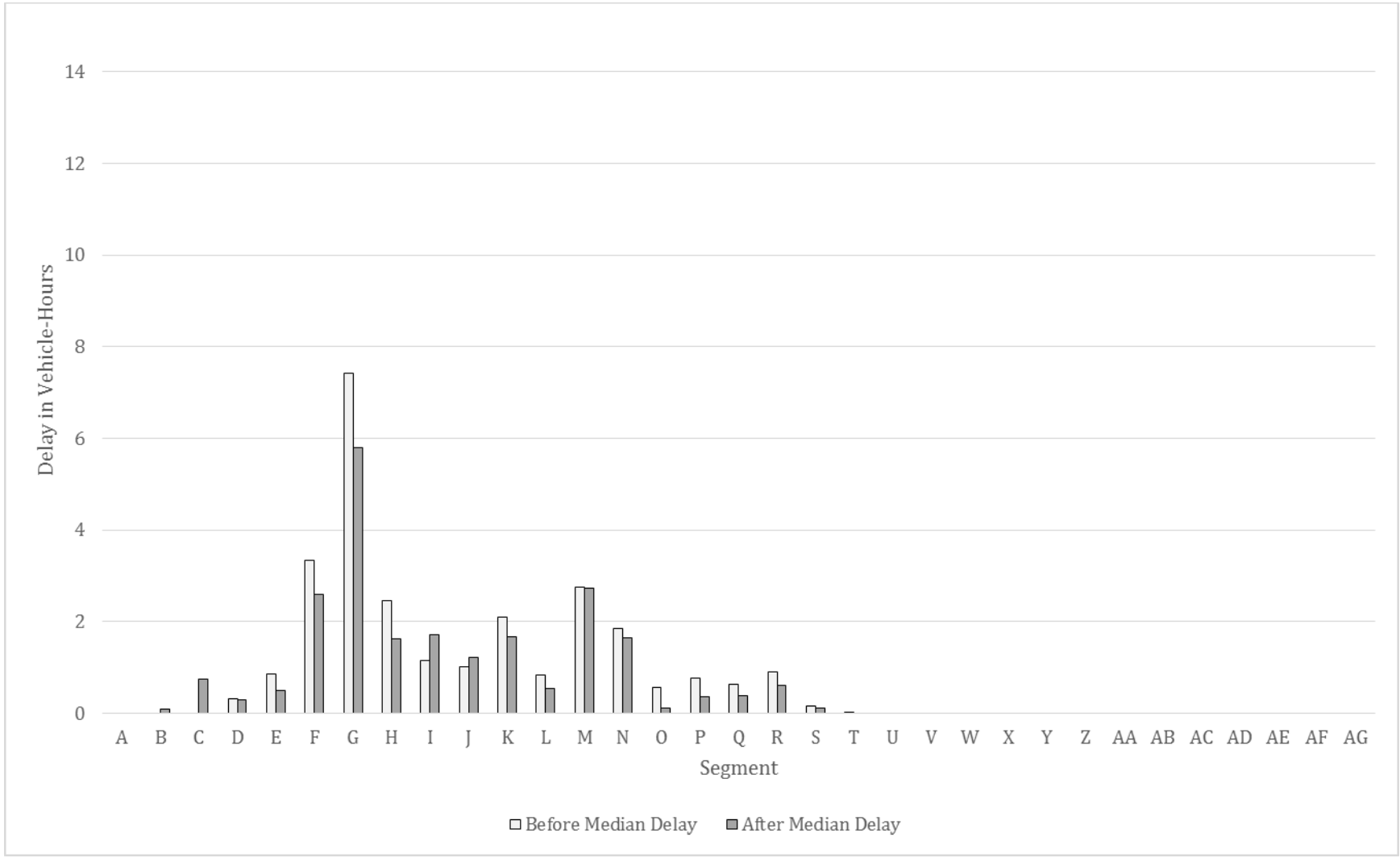

Figure 6-21. Medians of delay from vehicles under 45 MPH in vehicle-hours by segment.

In each pair of figures, several notable patterns emerge. As indicated previously, the region analyzed by TICAS does show a notable decrease in delay along the mainline. Of the 17 segments between E and U, only three show slight increases in accumulated delay year-on-year from vehicles traveling 65 MPH or slower (Figure 6-17). Some segments show significant decreases in delay, notably G, I, and K. This is mirrored when considering vehicles under 55 MPH, with three segments showing no change or a slight rise in delay and all others showing decreasing accumulated delay (Figure 6-19). Finally, for vehicles under 45 MPH, only two segment shows a rise in delay year-on-year (Figure 6-21).

A second feature to note in these figures is the decrease of variability in accumulated delay between Before and After. Especially within the E-to-U segment range, post-ramp metering delay varies within a narrower band, experiencing less extreme highs and lows compared to the median. This is easily seen in Segment F in Figure 6-16, in which the median drops only slightly but the two quartiles narrow dramatically. This indicates a smoothing effect from the ramp meters which results in a more reliable accumulation of delay and thus a more reliable travel experience within the corridor.

The third notable feature captured by these figures is that non-trivial delay was generated from segments outside of the corridor considered by TICAS. The downstream portion of the corridor, Segments V to AG which correspond to the region between I-494 and TH-62, show essentially no delay from any speed group. However, upstream of the ramp meters, notable delay is incurred. Segments A through C show a pattern inverse to the region within the ramp meter controlled area. Median delay rose in the After conditions and delay variability increased. Segment D, immediately upstream of the first ramp meter entrance, acts with the metered corridor and shows a positive impact from the system.

From these data we can see that the ramp metering system is smoothing operations along the mainline but is serving to extend the area affected by daily congestion (a finding which was not obvious from inspecting the speed contour figures described above). Vehicles upstream of the controlled region travel with decreased speed. However, as can be inferred by comparing Figure 6-17 (delay under 65 MPH) and Figure 6-21 (delay under 45 MPH), speeds are generally falling only to between 45 and 65 MPH as vehicles approach the rear of the congestion queue, with relatively few vehicles encountering actual congestion. This indicates that the current controlled region may need to be expanded to fully encapsulate the possible congested area along the corridor as demand increases.

Finally, as noted, the region between I-494 and TH-62 accumulates only minor delay and only when considering vehicles under 65 MPH. Thus the current operational strategy to leave the two entrance ramps in that region unmetered is acceptable as the meters would never need to activate to deal with congestion.

As was noted above, neither TICAS nor the HART-based analyses described thus far include delay incurred at the ramps themselves due to vehicle queues. TICAS specifically targets mainline only since mainline operation is the primary focus of ramp metering strategies in

general, with ramp delays and arterial performance as a secondary constraint. However, these secondary delays are still important to fully quantify the usefulness of ramp metering.

Table 6-6 below shows the average delay in vehicle-hours accumulated for the ramp-controlled region (Segments E through U) and the entire corridor for Before versus After conditions. These data include only delay from vehicles traveling under 45MPH, corresponding to those that would count toward congestion according to MnDOT practice. Note that October 4, 2013, the date with malfunctioning detectors, was removed from the before set. For each region considered, mainline-only and total system delays are given.

Table 6-6. Delay within the ramp-controlled region and entire corridor with and without ramp delay.

	Ramp-Controlled Region		Entire Corridor	
	Average Delay (Mainline Only)	Average Delay (Including Ramps)	Average Delay (Mainline Only)	Average Delay (Including Ramps)
Before (Excluding 10/4/2013)	50.4	50.4	56.7	56.7
After	45.3	95.5	57.4	103.4
Change	-5.1	45.1	0.7	46.7
% Change	-10.1%	89.5%	1.2%	82.4%

As can be seen, the mainline within the meter-controlled area shows a dramatic improvement in line with that found by TICAS. The entire corridor shows little change which corresponds with the total travel time calculations described by previous methodologies. With the incorporation of ramp delay, both the ramp-controlled area and corridor as a whole show an increase in delay. The improvements along the mainline are not sufficient to offset the delays incurred at the meters.

One reason this may be occurring is that ramp delay is accumulating on only four ramps. Given the control algorithm only has these four ramps as control tools for the entire corridor, it is logical that increased delays can be observed. If the control strategy were enforced along the entire corridor, these delays would spread over a larger number of ramps and collectively impact the system less.

7 CONCLUSIONS

The project presented in this report was performed by the Minnesota Traffic Observatory (MTO), which was called to assist in the deployment of two density-based ramp control strategies and to design and execute a field test involving all three ramp metering strategies: Stratified Zone Metering, serving as base conditions, and the two new density-based algorithms. A section of TH-100 northbound between 50th Street and I-394 was selected as the first study site. During the course of this project, multiple problems, operational issues, and unfortunate timing altered the original project goals and priorities. Although the UMN algorithm was integrated with the IRIS traffic operations system and was deployed in the field, an analysis of its performance based on the collected data was not completed because it was later discovered that the geometry of TH-100 did not allow for proper operation of the control algorithm. Although all three algorithms were affected by the peculiar geometry and detector layout of this section of TH-100, the UMN algorithm was the one most affected. Unfortunately, when this issue was discovered it was too late to switch test sites, and it was decided that the TH-100 evaluation would only include the UMD algorithm.

Later, during 2013 and 2014, the UMD algorithm underwent adjustments and was implemented on most of the ramp metering system. One specific location involves a recently reconstructed section of TH-212 in the southwest corner of the metro area. TH-212 was not controlled in the past and started being controlled by the UMD KAdaptive algorithm in the summer of 2014. MnDOT modified the scope of this project to include a before–after evaluation of the ramp metering system on TH-212.

Two types of analysis were performed for the evaluation of the new density ramp metering on TH-100: an analysis based on travel time data and an analysis based on loop detector data. Both methodologies compared traffic measurements between pairs of days with similar traffic and environmental conditions. The manually collected travel times show that during the PM period under the SZM control a shorter congested period developed in terms of time as compared to the PM period under the UMD. Regardless, the congestion under the SZM seems to be stable with no evidence of recovery while the congestion under the UMD algorithm shows evidence of recovery, supporting the assumption that the control managed to recover from the heavy congestion, albeit briefly. Focusing on more detail, it can be noted that the congestion under the UMD algorithm seems to be more stable while the congestion under the SZM has great fluctuations for the entire length of the site, indicating the presence of shockwaves. This can indicated that the UMD algorithm, although handling more demand, was able to meter steadily while the SZM was closer to the tipping point and got trapped in a series of restrict and dump cycles. Both algorithms show greater instability closer to the bottleneck, with the UMD algorithm keeping conditions in the mainline more fluid upstream as compared to the SZM. The UMD algorithm seems to handle the large demand ramp of TH-7 better, and conditions immediately upstream of it are less congested. One other observation is that the UMD algorithm shows some sharp spikes of very large travel time, which could represent short-lived heavy congestion conditions from which the control is able to recover.

The loop detector data analysis on TH-100 show that the UMD KAdaptive metering strategy performs better than the SZM when conditions on TH-100 are not extremely congested. The UMD KAdaptive algorithm allows, on average, more vehicles to flow into the mainline and keeps the on-ramp occupancy relatively low. In the mainline, the flows are also bigger with the UMD KAdaptive algorithm and in 3 out of 5 day-pairs the speeds are also higher. In general, for the same occupancy, the flows are less when the SZM algorithm is applied. The main reason is that the UMD KAdaptive algorithm is more protective in the morning and queue detector occupancies are lower. Thus, the queue violation is not activated as often and the ramp metering is active (and successful) for longer time periods.

In the before–after analysis of the UMD KAdaptive algorithm on TH-212, we see that there are small gains from ramp metering in terms of total travel time. Focusing on the delays, which represent the gains to the traveling public from avoiding congestion, we see that an approximate 12% reduction in delay and a 3% increase in VMT is observed when considering only the metered part of TH-212. These gains are reduced when the entire corridor is considered because the metering seems to spread lower speeds farther upstream but no severe congestion. When the ramp delays are included, we see an overall increase in delay with ramp metering, indicating that the present strategy (only four meters active), the gains on the mainline are not big enough to offset the delays accumulated in the ramps.

8 REFERENCES

1. Ahn, S., Bertini,R. L., Auffray,B., Ross,J. H. , and Eshel.O. Evaluating Benefits of Systemwide Adaptive Ramp-Metering Strategy in Portland, Oregon. Transportation Research Record: 2007, pp. 47–56. DOI: 10.3141/2012-06

2. Banks, J.H. Effect of Response Limitations on Traffic-Responsive Ramp Metering. Transportation Research Record 1394, 1993, pp. 17-25.

3. Barceló, J., Ferrer, J. L. and Grau,R (1994). AIMSUN2 and the GETRAM simulation environment. Internal report, Departamento de Estadística e Investigación Operativa. Facultad de Informática. Universitat Politècnica de Catalunya.

4. Bielefeldt,C., Condie,H., Elia, B.S., Rotem, A., Haj-Salem, H., Ramananjaona, C., Middelham, F., and Ernhofer, O. European Ramp Metering Project (EURAMP) Evaluation Results, Contract No. 507645, 2007.

5. Bogenberger, K., and May, A. D. (1999). "Advanced Coordinated Traffic Responsive Ramp Metering Strategies." California PATH Paper UCB-ITS-PWP-99-19.

6. Bogenberger,K., and May, A.D. Advanced coordinated traffic responsive ramp metering strategies, California PATH Working Paper UCB-ITS-PWP-99-1, Institute of Transportation Studies, University of California, Berkeley, 1999.

7. Box G. E. P. and Hunter,J. S. (1961). "The 2k-p fractional factorial designs." Technometrics 3: 311-351,449-458.

8. Box, G. E. P. and Wilson, K. B. (1951). "On the experimental attainment of optimum conditions." Journal of Royal Statistical Society, Series B 13 (1): 1-38.

9. Box, G.E.P. and Behnken, D.W. (1960). "Some new three-level designs for the study of qualitative variables." Technometrics 2, 455-475.

10. Cambridge Systematics (2001). "Twin Cities ramp Meter Evaluation." Final Report, Minnesota Department of Transportation, 2001.

11. Cambridge Systematics, Inc. Twin Cities Ramp Meter Evaluation. Prepared for Minnesota Department of Transportation pursuant to Laws 2000: Chapter 479, HF2891. Oakland, California, 2001.

12. Chang, T.H. and Li, Z.Y. (2002). "Optimization of mainline traffic via an adaptive coordinated ramp-metering control model with dynamic OD estimation." Transportation Research 10C: 99-120.

13. Chu, L. and Yang, X. (2003). "Optimization of the ALINEA Ramp-metering Control Using Genetic Algorithm with Micro-simulation." 82nd Transportation Research Board Annual Meeting, Washington D.C., 2004.

14. Chu, L., Recker, W., and Yu, G. 2009. Integrated ramp metering design and evaluation platform with Paramics. Technical Rep. PATH No. UCB-ITS-PRR-2009-10, Institute of Transportation Studies, University of California at Berkeley, Berkeley, California

15. Ciarallo, F.W., and Mirchandani, P.B. RHODES – ITMS – MILOS: Ramp Metering System Test. Final Report FHWA-AZ02-481, The University of Arizona, 2002.

16. Cook, R. D., and Weisberg, S. (1999). "Applied Regressional Analysis Computing and Graphics." New York: Wiley

17. Craney, Trevor, A. and Surles, James,G. (2002). "Model-dependent variance inflation factor cutoff values." Source: Quality Engineering, v 14, n 3, 2002, p 391-403

18. Critchfield, G. C., and Willard, K.E. (1986). Probabilistic Analysis of Decision Trees Using Mote Carlo Simulation, Medical Decision Making, 6(1):85-92.

19. Elefteriadou, L. (1997). "Freeway Merging Operations: A Probabilistic Approach." Proceedings of the 8th International Federation of Automatic Control Symposium on Transportation Systems, Chania, Greece, pp. 1351-1356.

20. Elefteriadou, L., Kondyli, A., Washburn, S., Brilon, W., Lohoff, J., Jacobson, L., Hall, F., and Persaud, B. Proactive ramp management under the threat of freeway-flow breakdown. Procedia-Social and Behavioral Sciences, 16, 2011, pp. 4-14.

21. Federal Highway Administration. (1990). Highway Statistics, Washington, DC.

22. Franklin, M.F. (1984). "Constructing tables of minimum aberration pn-m designs." Technometrics 26:225–232. 33. Suen C., Chen H., Wu C.F.J. (1997). "Some identities on qn-m designs with application to minimum aberration designs." Ann Statist 25:1176–1188.

23 .Fries, A. and Hunter,W.G. (1980). "Minimum aberration 2k-p designs." Technometrics 22: 601-608

24. Geldermann, J., and Rentz, O. (2001). Integrated Technique Assessment with Imprecise Information as a Support for the Identification of Best Available Techniques (BAT), OR Spektrum, 23(1):137-157.

25. Gipps, P.G. (1986). "A model for the structure of lane-changing decisions." Transportation Research B 20B(5) 403-414.

26. Goldberg, D.E. (1989). Genetic Algorithm in Search. Optimization and Machine Learning. Addison-Wesley Pub. Co., Inc.

27. Hasan, M., Jha, M. and Ben-Akiva, M.E. (2002). "Evaluation of ramp control algorithms using microscopic traffic simulation." Transportation Research 10C: 229- 256.

28. Highway Capacity Manual (2000). Transportation Research Board, National Research Council, Washington, D.C.

29. Highways Agency, Ramp Metering Summary Report, Publication 5053147_04_02_141, 2007.

30. Hourdakis, J. and Michalopoulos, P.G. (2002). "Evaluation of ramp control effectiveness in two Twin Cities freeways." 81st Transportation Research Board Annual Meeting, Washington D.C., 2002.

31. ITS America. (1995). National ITS Program Plan, Washington, DC.

32. ITSA Fact Sheets, Development of advanced traffic management systems in the US by state agencies, March 1, 1995.

33. Jacobson, L., Henry, K., and Mahyar, O. Real-time metering algorithm for centralized control, Transportation Research Record 1232, 1989, pp. 17-26.

34. Kang, S., Gillen, D., Assessing the benefits and costs of intelligent transportation systems: Ramp meters. Working paper UCB-ITS-PRR- 99-19, California PATH Program, Institute of Transportation Studies, University of California, Berkeley, CA, 1999.

35. Kimley-Horn and Associates, Inc. I-580 Ramp Metering – Phase 2 Final Report. Prepared for City of Pleasonton, City of Livermore, California Department of Transportation (Caltrans), and Metropolitan Transportation Commission (MTC). California, 2008.

36. Kleijnen, J.P.C (1993). "Experimental design for sensitivity analysis, optimization, and validation of simulation models." In J. Banks, editor, Handbook of Simulation. Wiley, New York.

37. Kwon, E., and Park, C. (2012). "Development of Freeway Operational Strategies with IRIS-in-Loop simulation. Available http://www.its.umn.edu/Publications/ResearchReports/reportdetail.html?id=2092.

38. Lau, D. (2001). "Minnesota Department of Transportation: Stratified Metering Algorithm." Internal Report.

39. Lipp, L., Corcoran, L., and Hickman, G. Benefits of central computer control for the Denver ramp metering system, Transportation Research Record 1320, 1991, pp. 3-6.

40. McCamley, F., and Rudel, R.K. (1995). "Graphical Sensitivity Analysis for Generalized Stochastic Dominance." Journal of Agricultural and Resource Economics, 20(2):403-403.

41. Meldrum, D., and Taylor, C. Freeway traffic data prediction using artificial neural networks and development of a fuzzy logic ramp metering algorithm, Final Technical Report, Washington State Department of Transportation Report No. WA-RD 365.1, Washington, 1995.

42. Metropolitan Transportation Commission (MTC). Freeway Performance Initiative: Regional System Efficiency and Integration in the Works, Oakland, California, 2011. Available http://apps.mtc.ca.gov/meeting_packet_documents/agenda_1666/05d_1_FPI_Fact_Sheet_Final_5.2.11.pdf

43. Michalopoulos, P., Hourdos, J., and Xin, W. Evaluation and Improvement of the Stratified Ramp Metering Algorithm Through Microscopic Simulation - Phase II. Mn/DOT Final Report MN/RC – 2005-48, 2005.

44. Monsere, C.M., Bertini, R.L., Ahn, S., and Eshel, O. Using Archived ITS Data to Measure Operational Benefits of a System-Wide Adaptive Ramp Metering (SWARM) System (No. FHWA-OR-RD-09-10), 2008.

45. Montgomery, D.C (1997). Design and Analysis of Experiments. Wiley and Sons Ltd.: New York.

46. Myers R.H. and Montgomery D.C. (1995). Response Surface Methodology, Process and Product Optimization Using Designed Experiments. Wiley Series.

47. National Bureau of Standards (1959). "Fractional Factorial experiment designs for factors at two and three levels." Applied Mathematics Series 54. US Government Printing Office, Washington.

48. Nearctis Deliverable 7, 2010. Online: http://www.nearctis.org/home/resources-desk/deliverables/

49. Nearctis Deliverable 8, 2010. Online: http://www.nearctis.org/home/resources-desk/deliverables/

50. Nelder, J.A., Mead, R (1965). "A Simplex Method for Function Minimization." Computer Journal 7: 308-323.

51. Operation TimeSaver. (1996). "Intelligent Transportation Infrastructure Benefits: and Experienced." FHWA, US Department of Transportation.

52. Paesani, G., Kerr, J., Perovich, P., and Khosravi, E. System wide adaptive ramp metering in Southern California, In: CD-ROM. ITS America 7th Annual Meeting, 1997.

53. Papageorgiou, M. (1983). "Application of Automatic Control Concepts to Traffic Flow Modeling and Control." Springer, New York.

54. Papageorgiou, M., and Kotsialos, A. Freeway ramp metering: An overview, IEEE Transactions Intelligent Transportation Systems, vol. 3, no. 4, 2002, pp. 271–281.

55. Papageorgiou, M., Blosseville, J.M., and Hadj-Salem, H. Modeling and real-time control of traffic flow on the southern part of Boulevard Peripherique in Parris, Part II: Coordinated on-ramp metering, Transportation Research, Vol. 24A, 1990, pp. 361-370.

56. Papageorgiou, M., Hadj-Saem, H. and Midddelham, F. (1997). "ALINEA local ramp metering: summary of field test results." Transportation Research Board, 6th Annual Meeting, Washington, DC.

57. Papageorgiou, M., Hadj-Salem, H., and Blosseville, J.-M. ALINEA: a local feedback control law for on-ramp metering, Transportation Research Record 1320, 1991, pp. 58–64.

58. Papamichail, I. and Papageorgiou, M. Traffic-responsive linked ramp-metering control. IEEE Transactions on Intelligent Transportation Systems, 9, 2008, pp. 111–121.

59. Park, K and Carter, B. (1995). "On the effectiveness of genetic search in combinatorial optimization." Proceeding of the 1995 ACN symposium on Applied Computing.

60. Pearce, V. (2000). What have we learned about ITS? Chapter 2: What have we learned about Freeway Incident and Emergency Management and Electronic Toll Collection? Technical Reports & Papers, US Department of Transportation.

61. Polus, A. and Pollatschek, M. (2002). "Stochastic Nature of Freeway Capacity and its Estimation." Canadian Journal of Civil Engineering, Vol 29: pp. 842-852, 2002.

62. Stat-Ease, (2003). Design-Expert® 6 User's Guide, Stat-Ease, Inc. 2003.

63. Stephanedes, Y. and Chang, K.K. (1993). "Optimal control of freeway corridors." ASCE Journal of Transportation Engineering 119, 504-514.

64. Suen, C., Chen, H., Wu, C.F.J. (1997). "Some identities on qn-m designs with application to minimum aberration designs." Ann Statist 25:1176–1188

65. Wattleworth, J.A. (1967). "Peak-period analysis and control of a freeway system." Highway Research Record 157.

66. Xin, W., Michalopoulos, P. G., Hourdakis, J., and Lau, D. Minnesota's new ramp control strategy: design overview and preliminary assessment. Transportation Research Record 1867(1), 2004, pp. 69-79.

67. Zhang, M., Kim,T., Nie X., Jin,W., Chu,L., and Recker,W. (2001). „Evaluation of On-ramp Control Algorithms." California PATH Research Report UCB-ITS-PRR- 2001-36.

68. Zhange, H., Ritchie, S., and Recker, W. (1996). "Some general results on the optimal ramp metering control problem." Transportation Research C 4, 51-69.

Appendix A -
FIGURES FOR TH-100 ANALYSIS

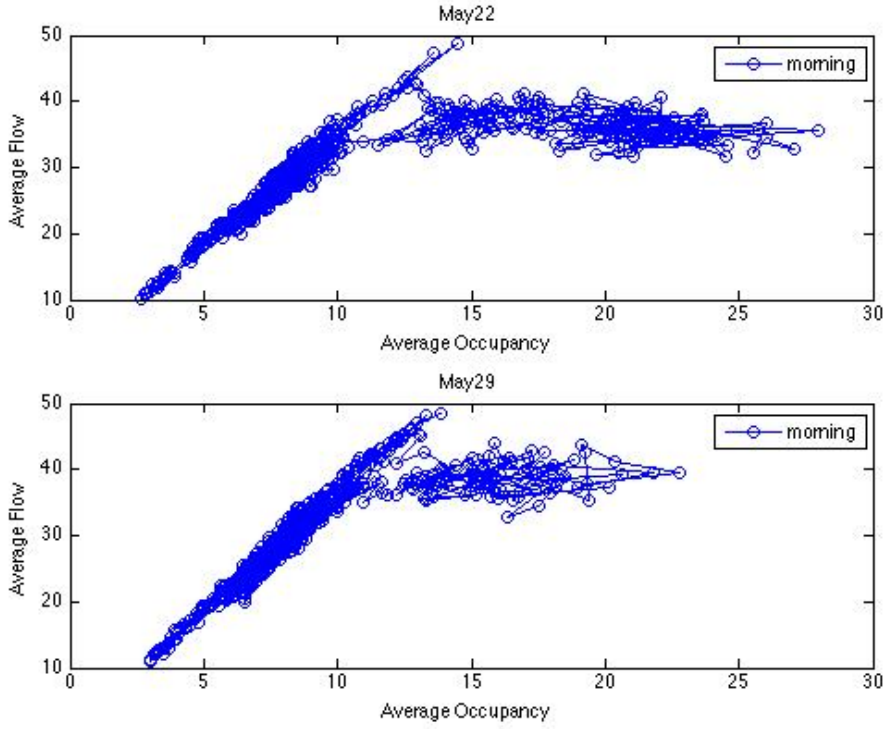

Figure A-1. Macroscopic Fundamental Diagram (MFD) – mornings, May 22 and May 29.

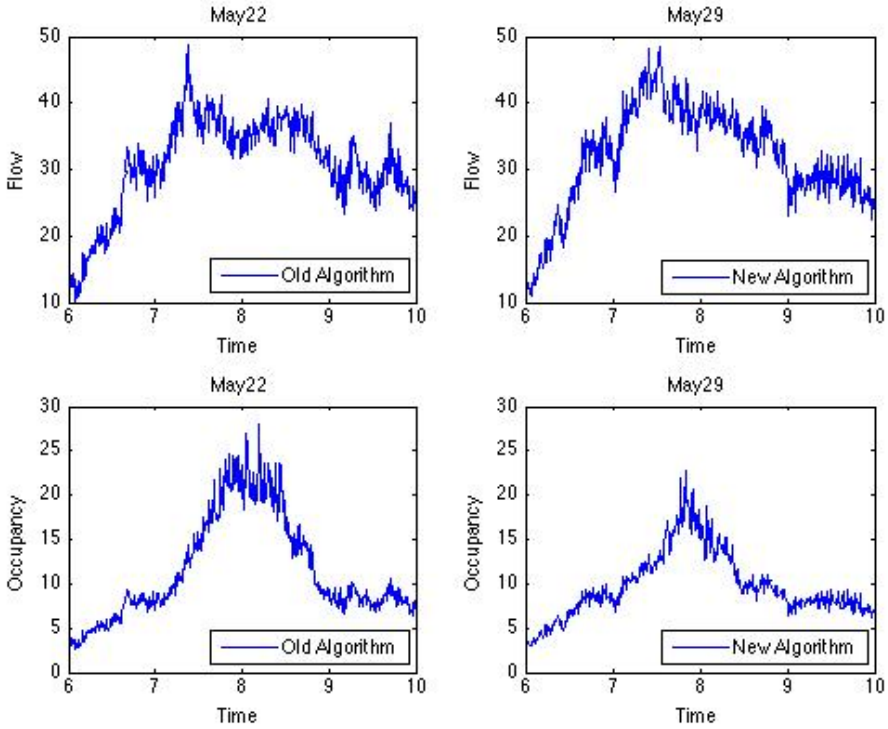

Figure A-2. Average corridor flow and occupancy – mornings, May 22 and May 29.

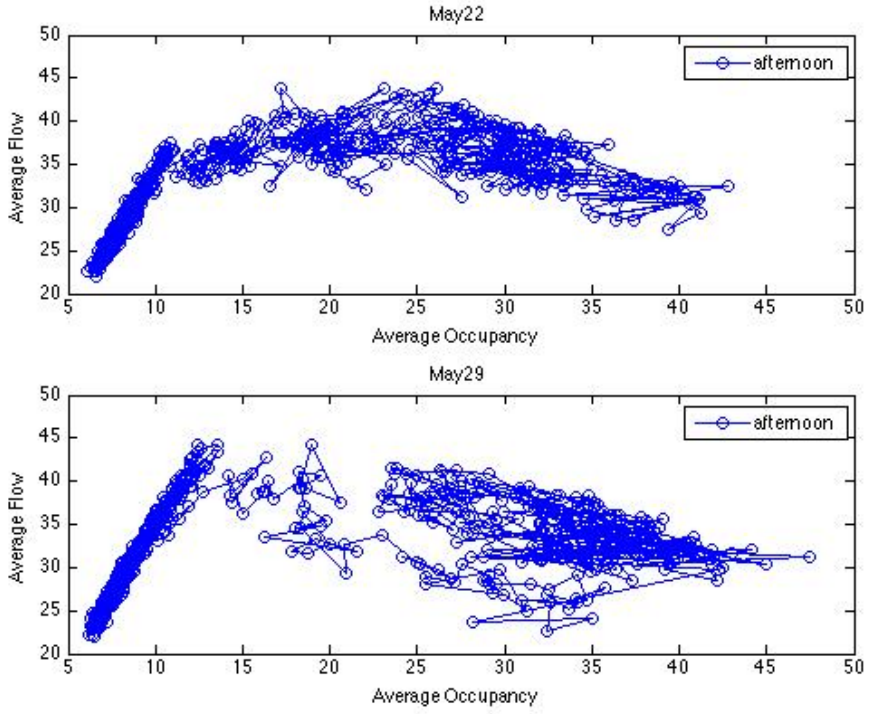

Figure A-3. Macroscopic Fundamental Diagram (MFD) – afternoons, May 22 and May 29.

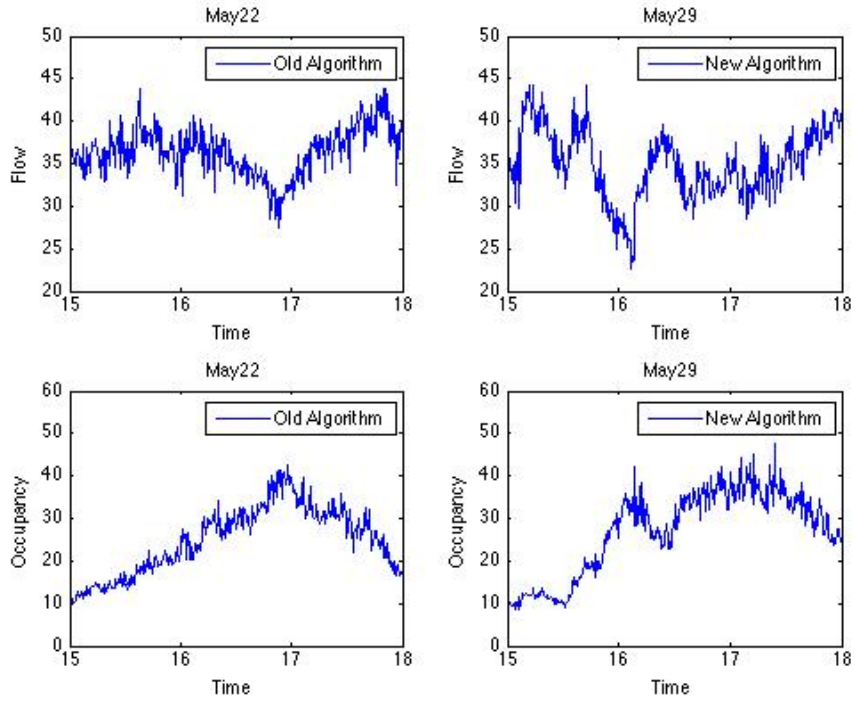

Figure A-4. Average corridor flow and occupancy – afternoons, May 22 and May 29.

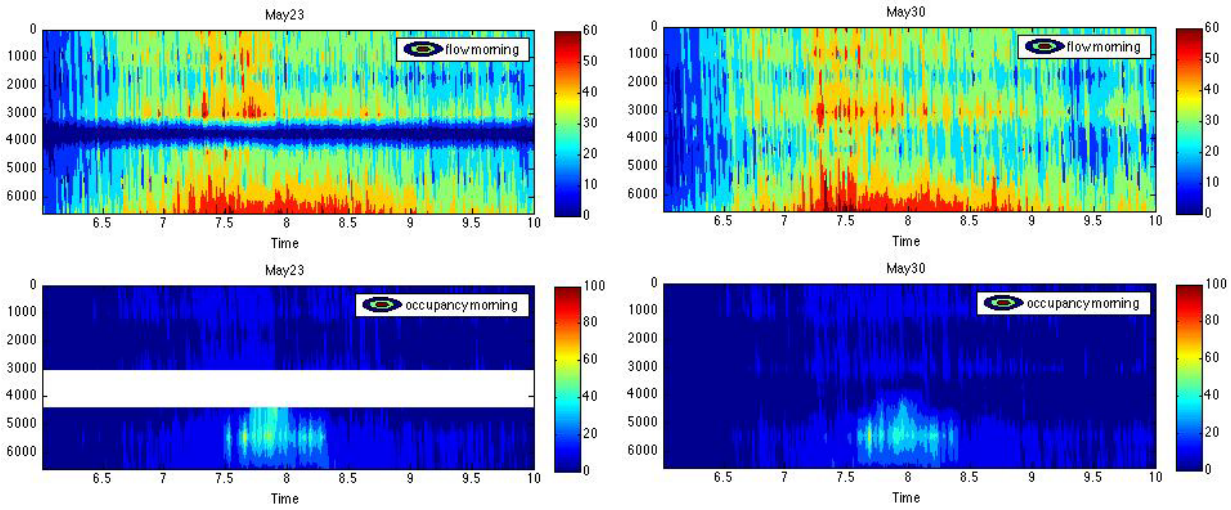

Figure A-5. Flow and occupancy contour plots – mornings, May 23 and May 30.

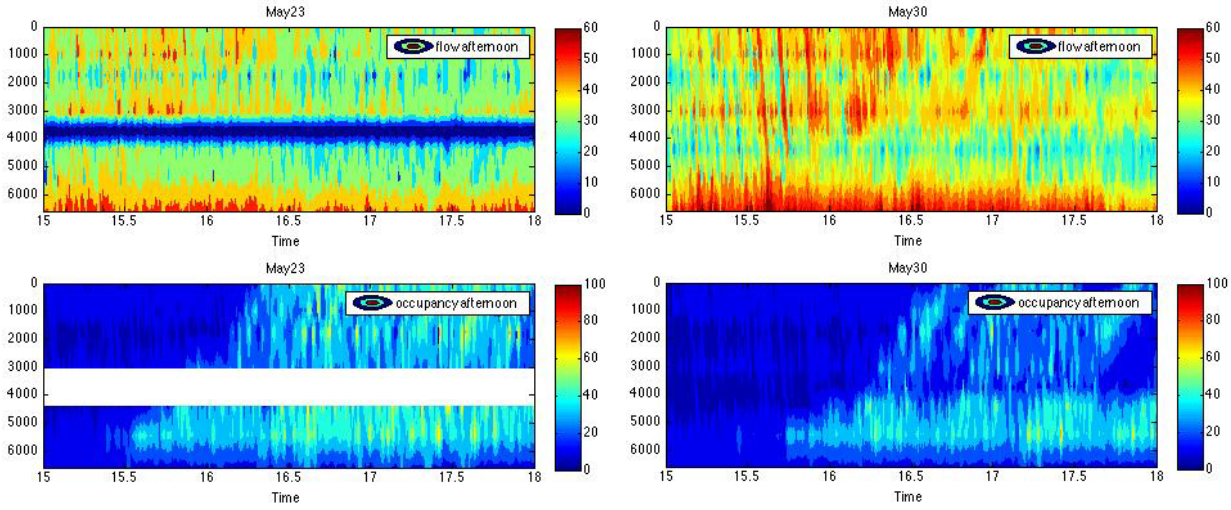

Figure A-6. Flow and occupancy contour plots – afternoons, May 23 and May 30.

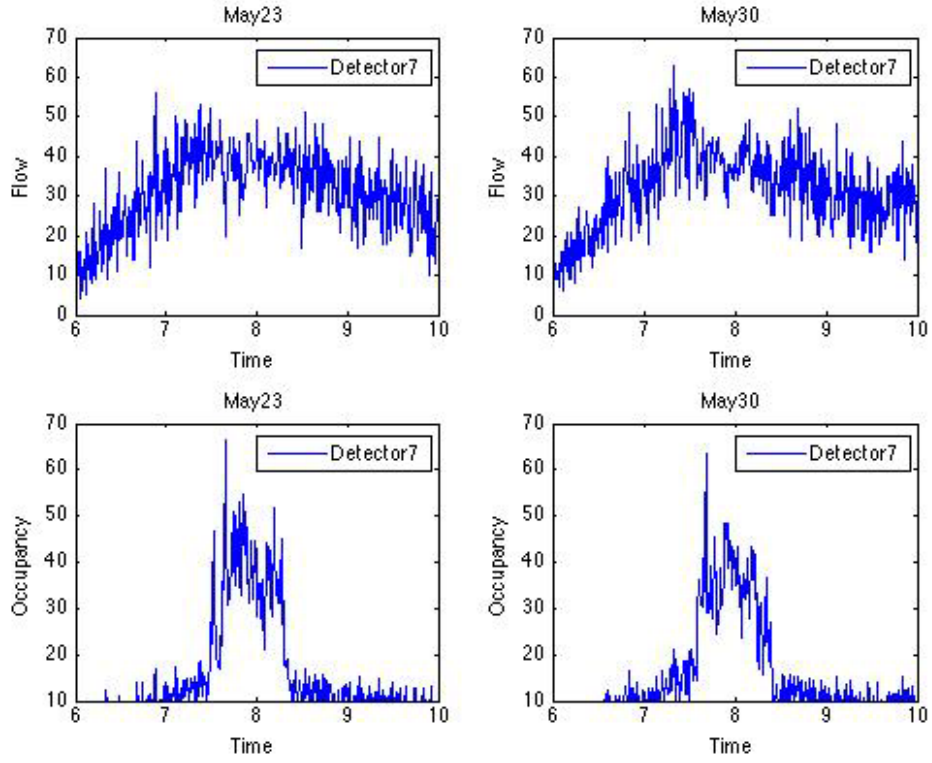

Figure A-7. Mainline flow and occupancy at the active bottleneck – mornings, May 23 and May 30.

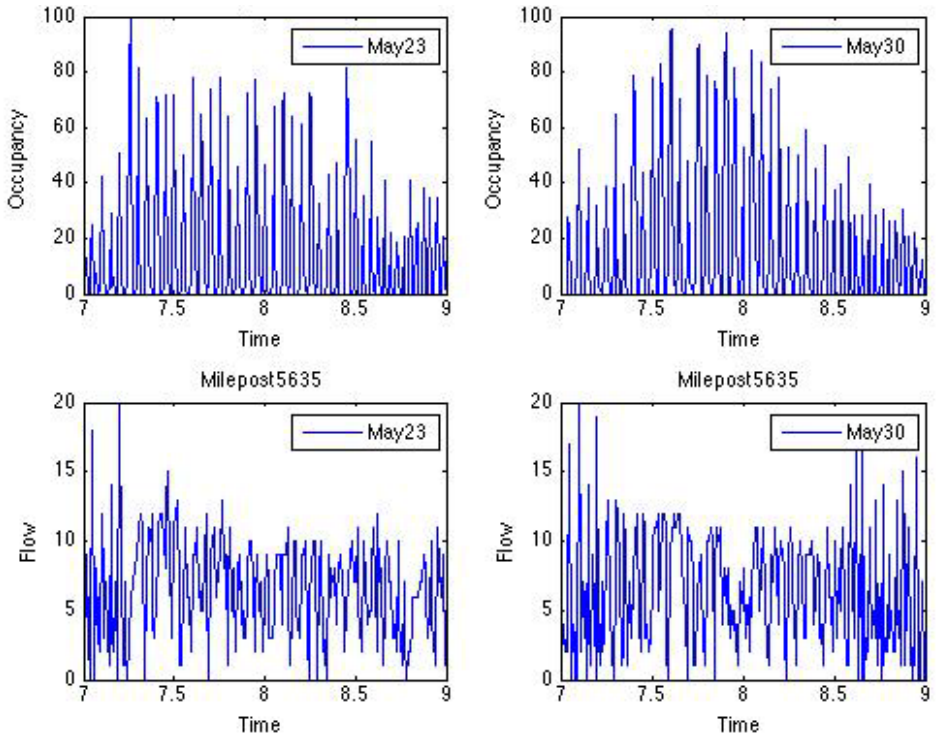

Figure A-8. Flow (passage detector 2022) and occupancy (queue detector 3652) downstream of the active bottleneck – mornings, May 23 and May 30.

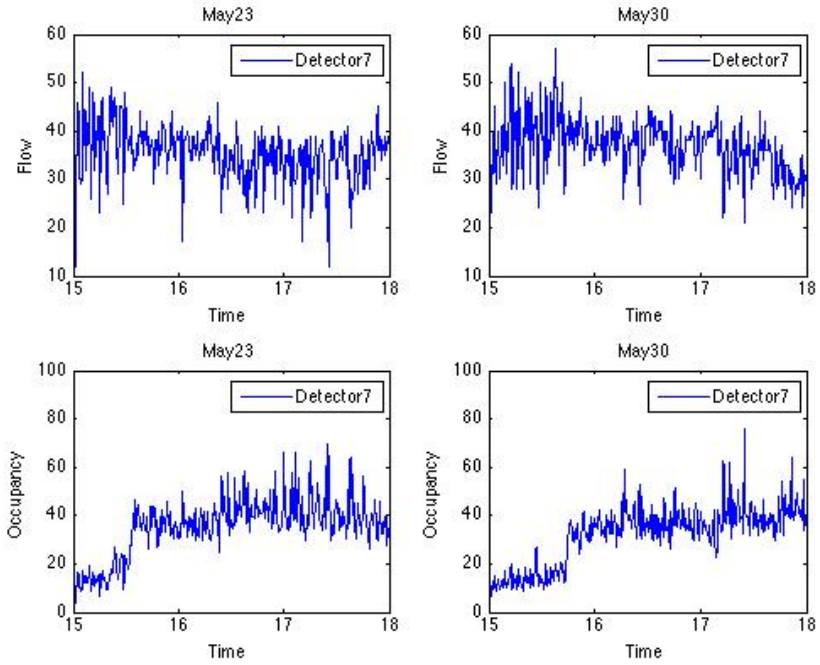

Figure A-9. Mainline flow and occupancy at the active bottleneck – afternoons, May 23 and May 30.

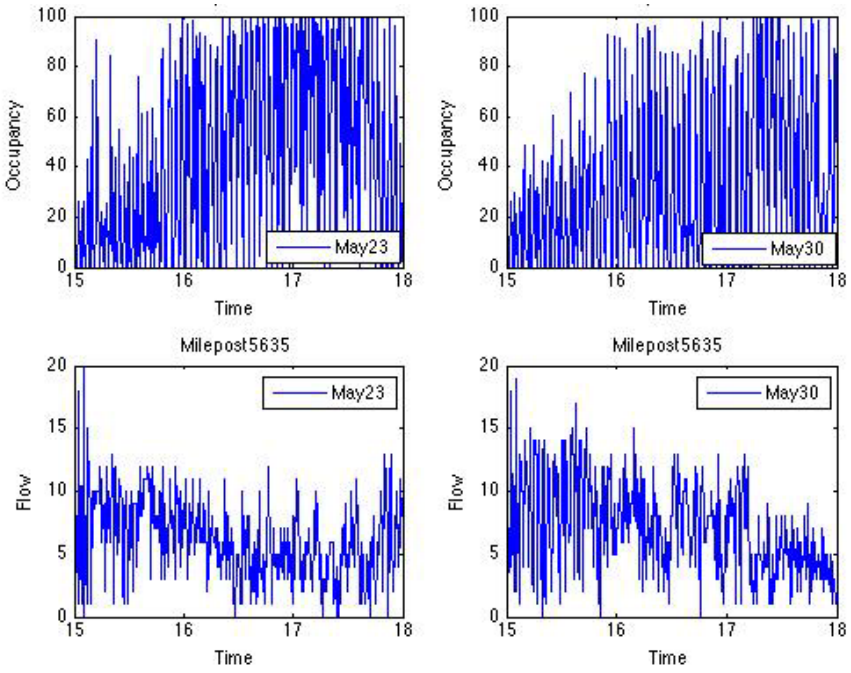

Figure A-10. Flow (passage detector 2022) and occupancy (queue detector 3652) downstream of the active bottleneck – afternoons, May 23 and May 30.

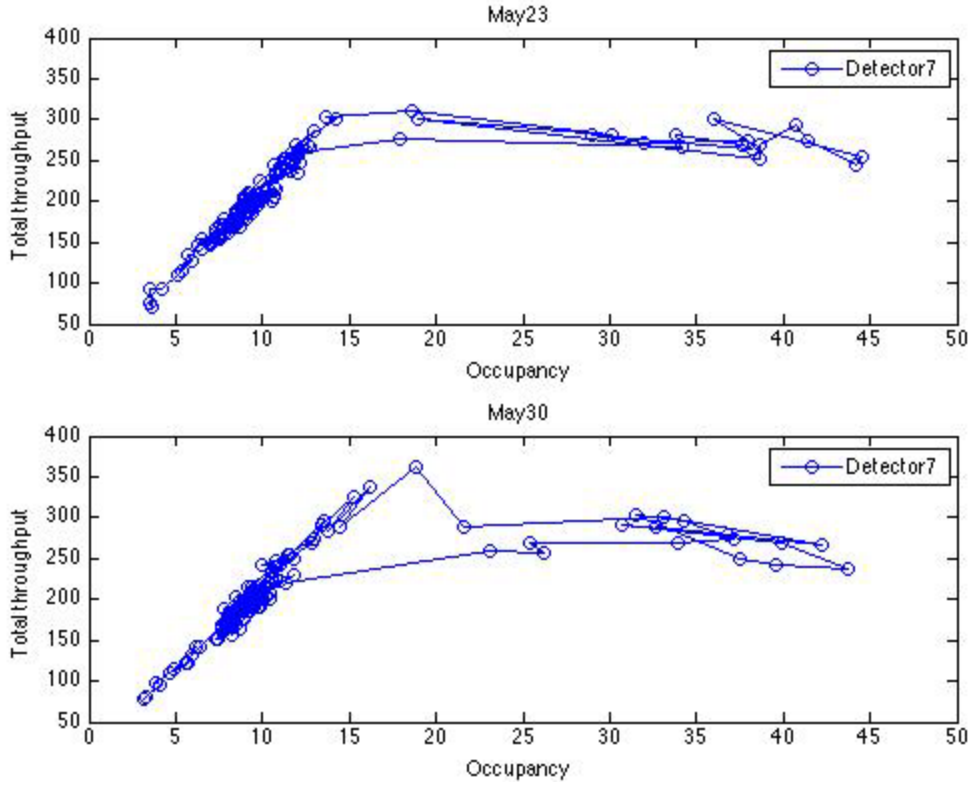

Figure A-11. Total throughput (mainline upstream and ramp) versus occupancy (only mainline upstream) – mornings, May 23 and May 30.

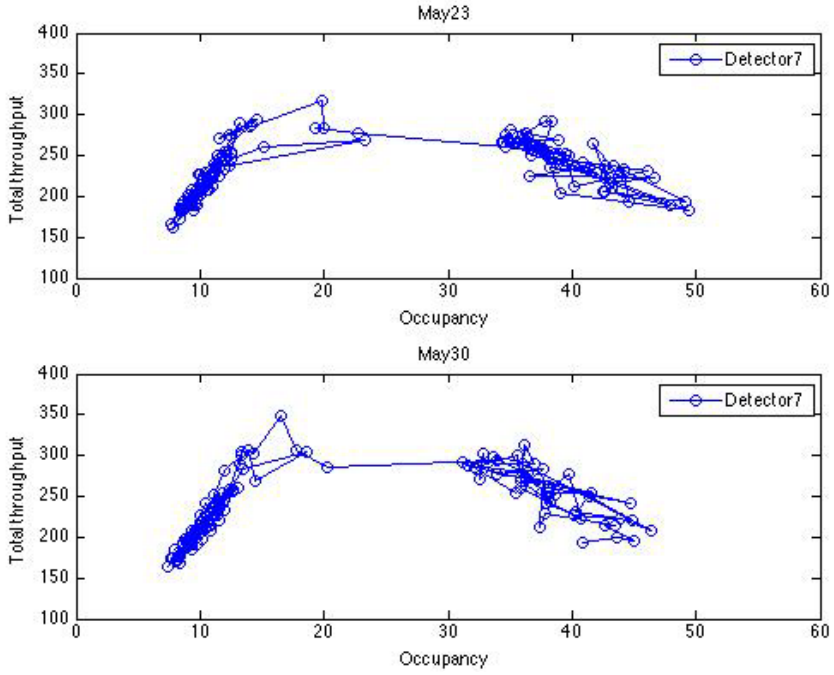

Figure A-12. Total throughput (mainline upstream and ramp) versus occupancy (only mainline upstream) – afternoons, May 23 and May 30.

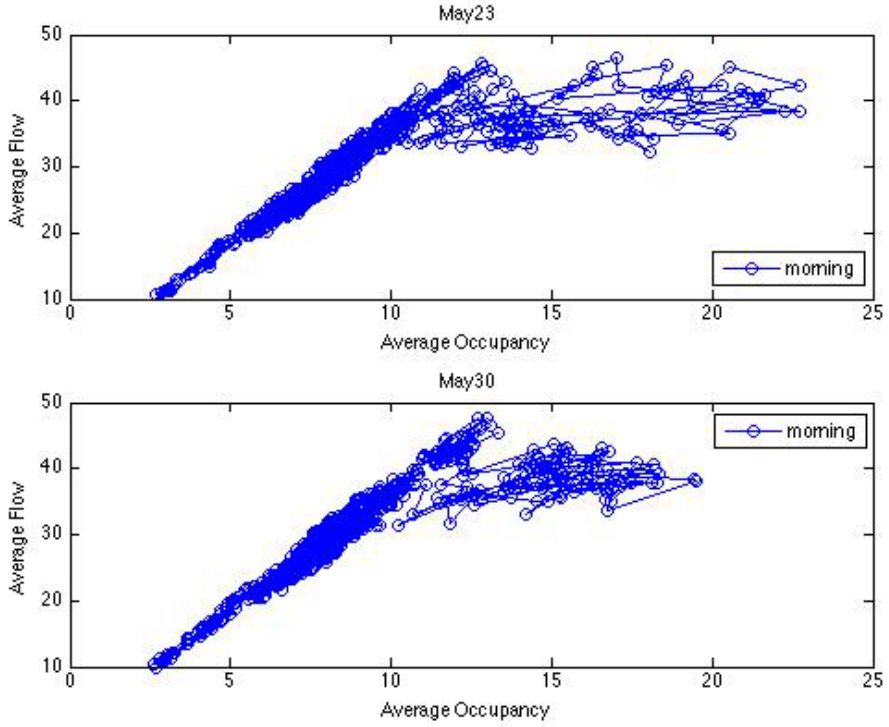

Figure A-13. Macroscopic Fundamental Diagram (MFD) – mornings, May 23 and May 30.

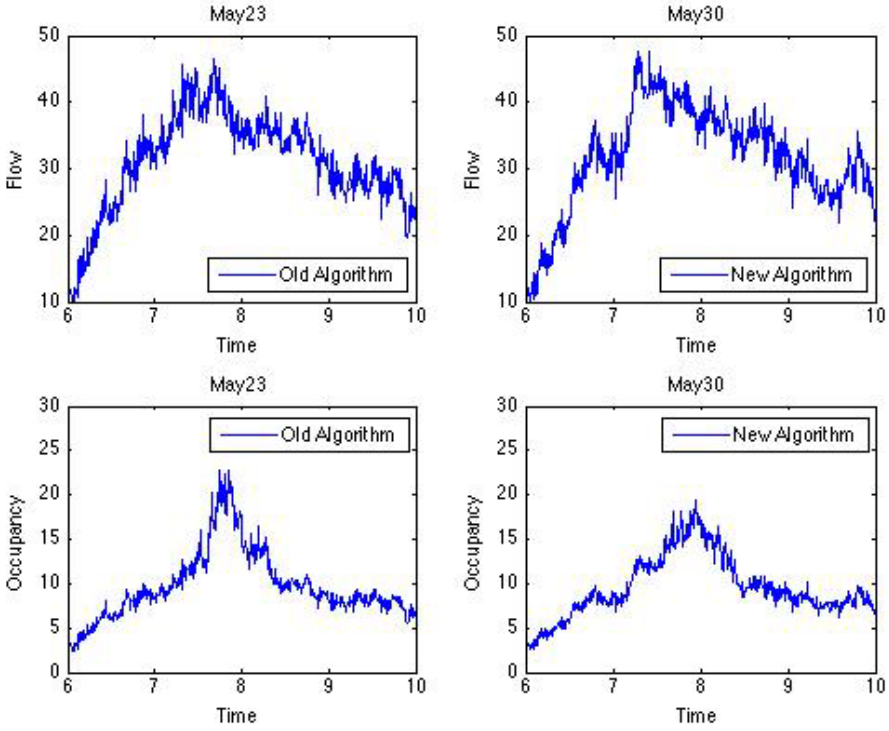

Figure A-14. Average corridor flow and occupancy – mornings, May 23 and May 30.

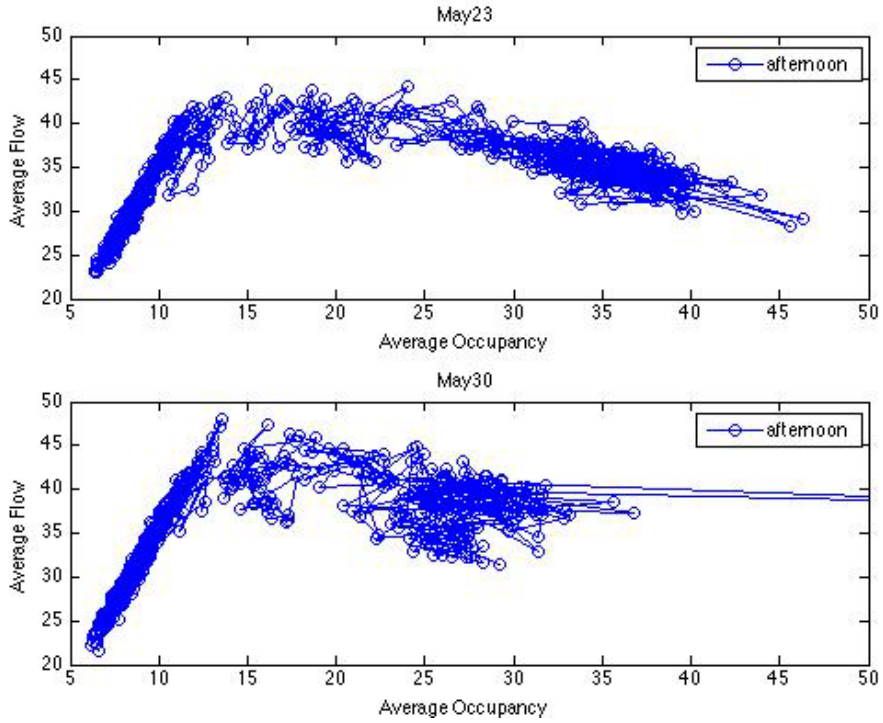

Figure A-15. Macroscopic Fundamental Diagram (MFD) – afternoons, May 23 and May 30.

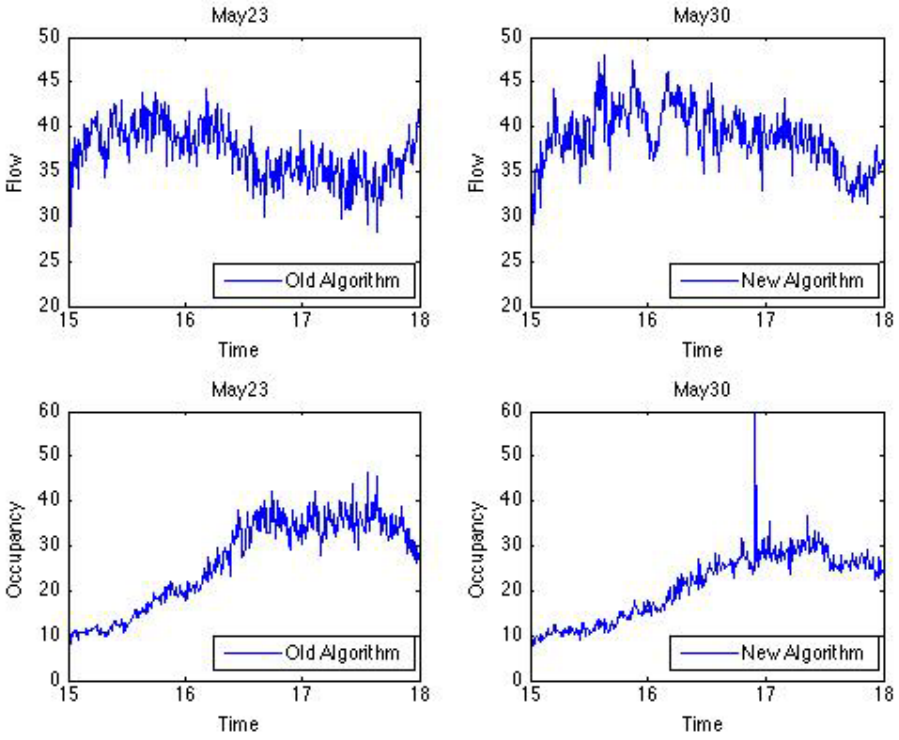

Figure A-16. Average corridor flow and occupancy – afternoons, May 23 and May 30.

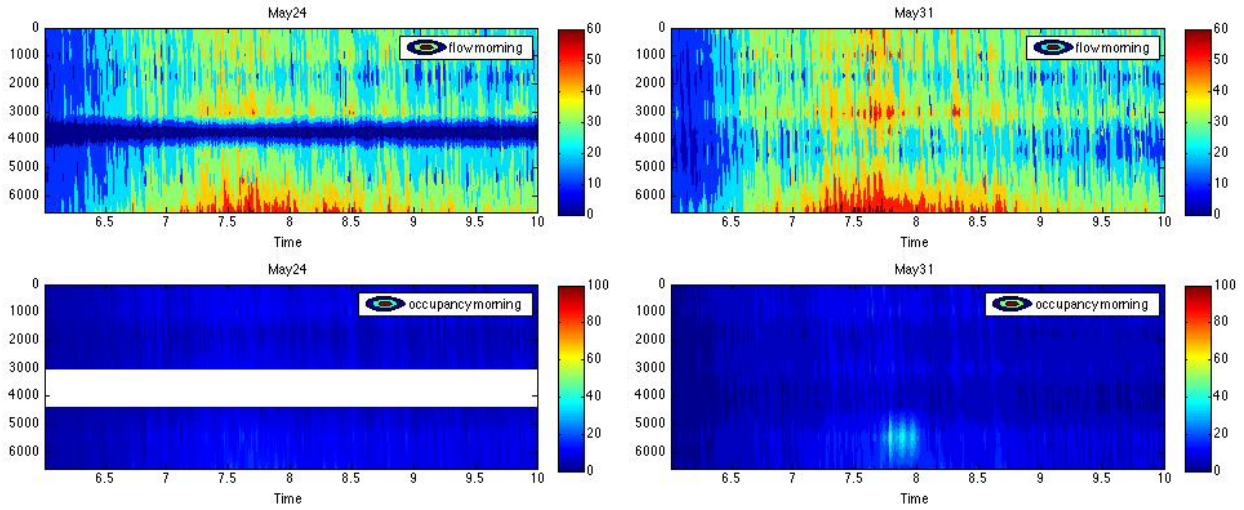

Figure A-17. Flow and occupancy contour plots – mornings, May 24 and May 31.

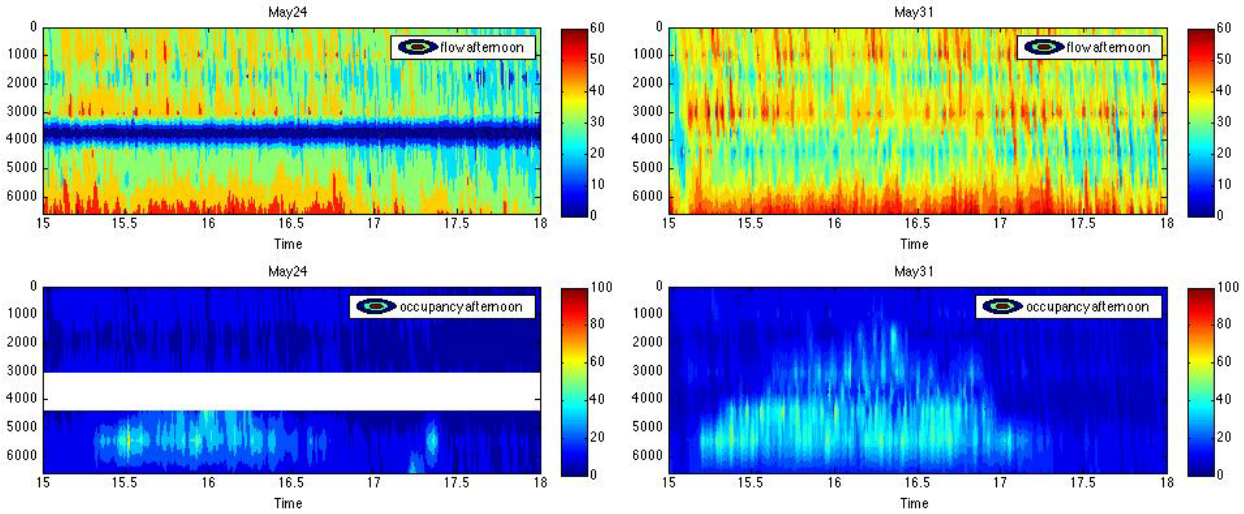

Figure A-18. Flow and occupancy contour plots – afternoons, May 24 and May 31.

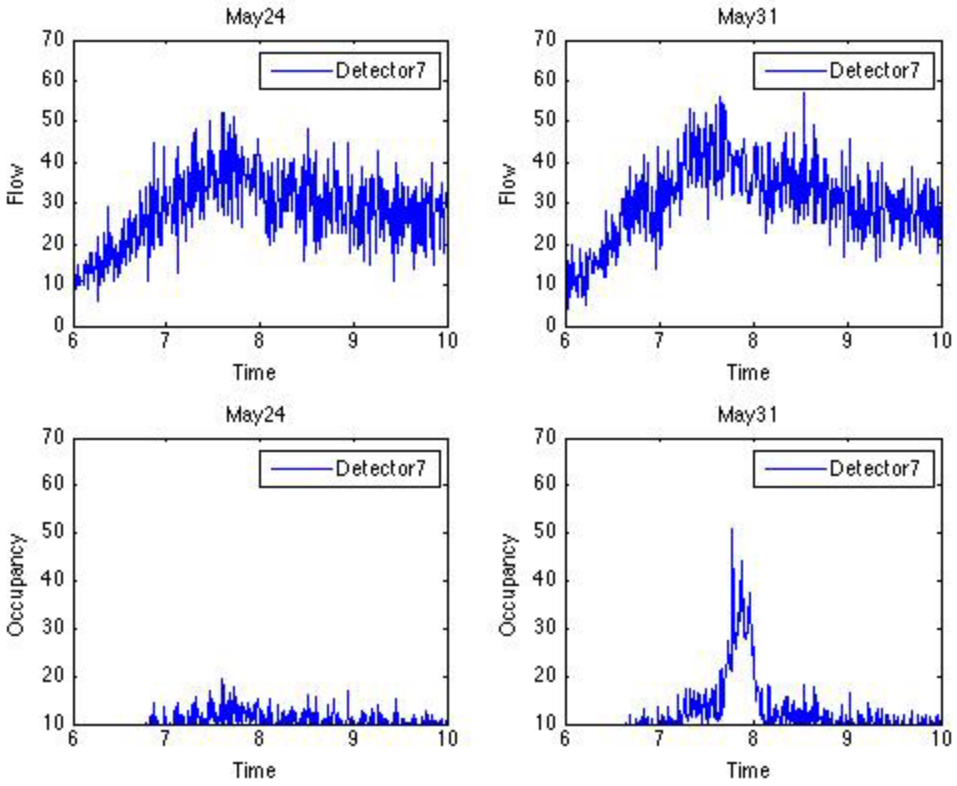

Figure A-19. Mainline flow and occupancy at the active bottleneck – mornings, May 24 and May 31.

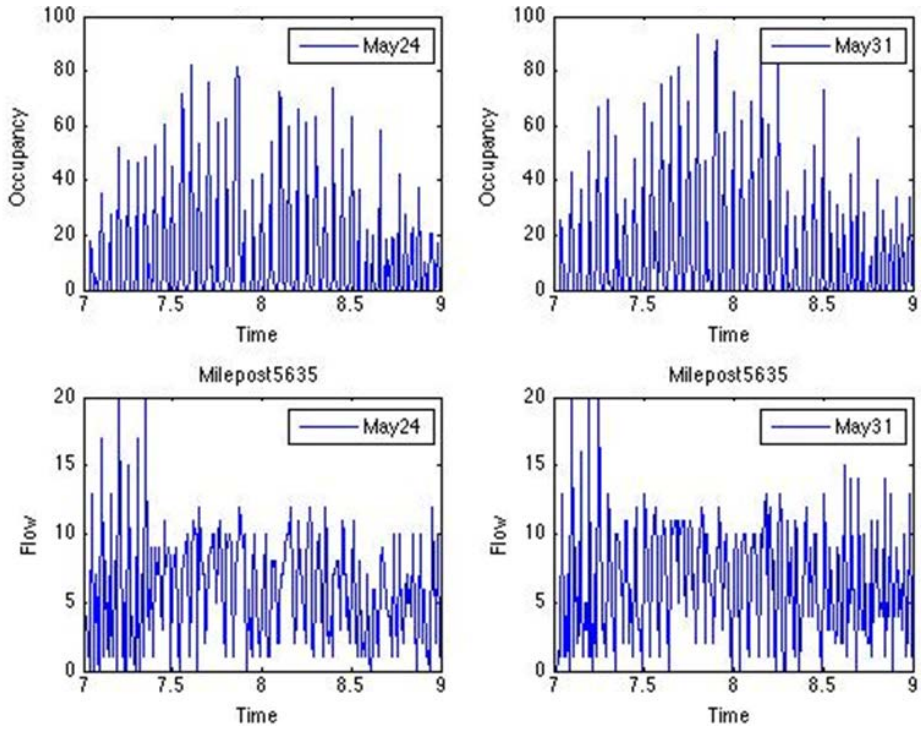

Figure A-20. Flow (passage detector 2022) and occupancy (queue detector 3652) downstream of the active bottleneck – mornings, May 24 and May 31.

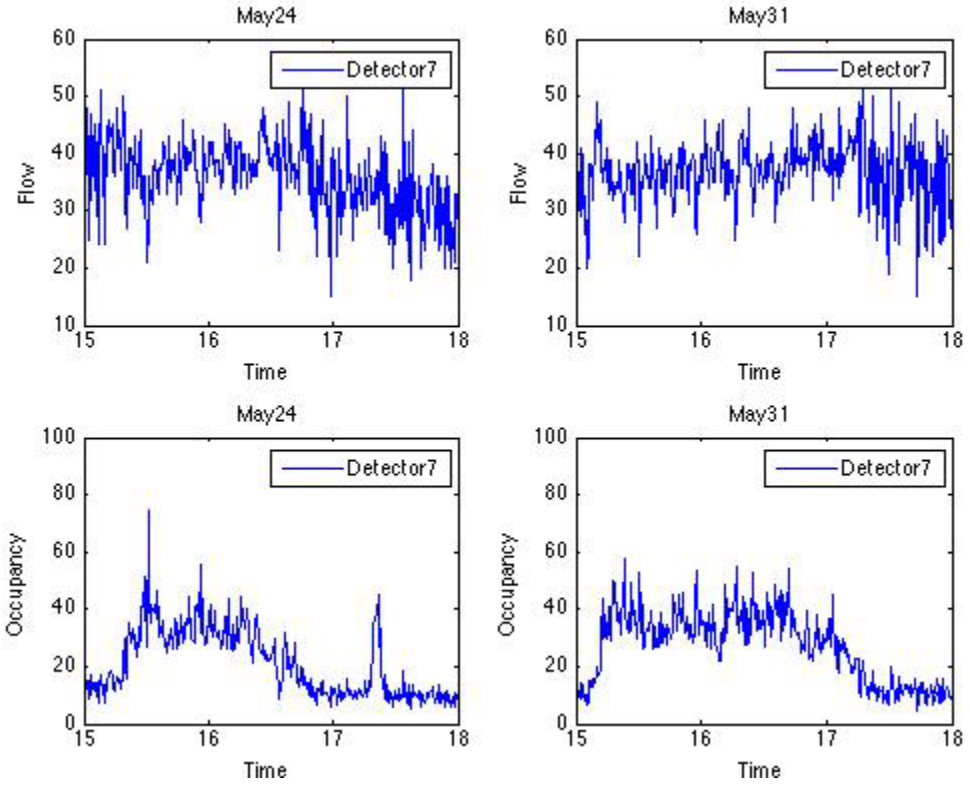

Figure A-21. Mainline flow and occupancy at the active bottleneck – afternoons, May 24 and May 31.

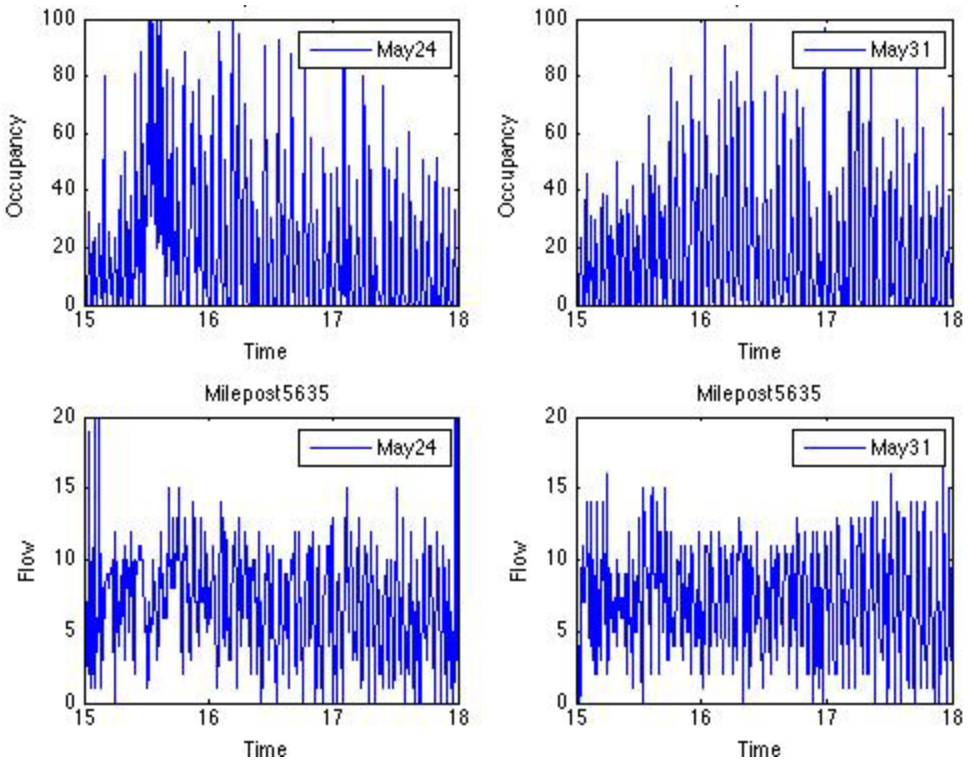

Figure A-22. Flow (passage detector 2022) and occupancy (queue detector 3652) downstream of the active bottleneck – afternoons, May 24 and May 31.

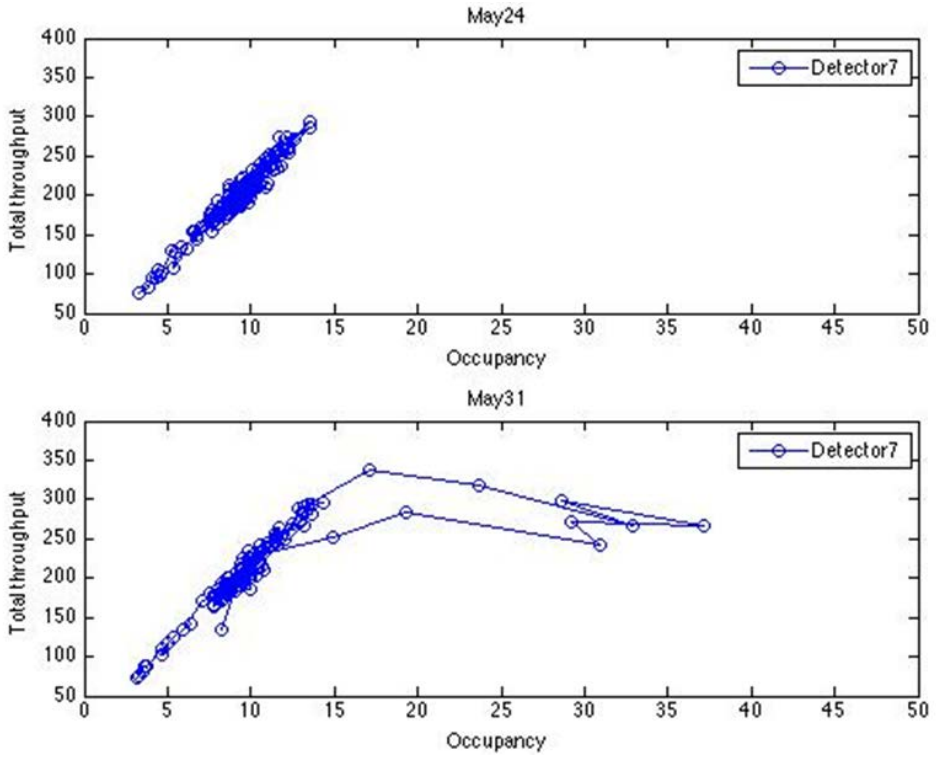

Figure A-23. Total throughput (mainline upstream and ramp) versus occupancy (only mainline upstream) – mornings, May 24 and May 31.

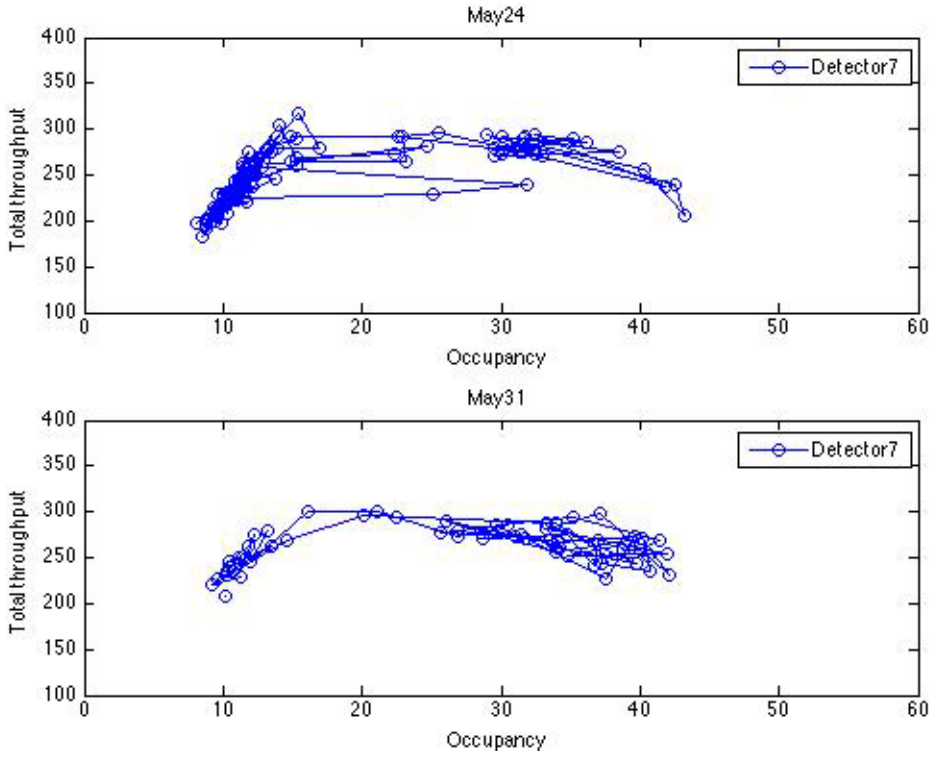

Figure A-24. Total throughput (mainline upstream and ramp) versus occupancy (only mainline upstream) – afternoons, May 24 and May 31.

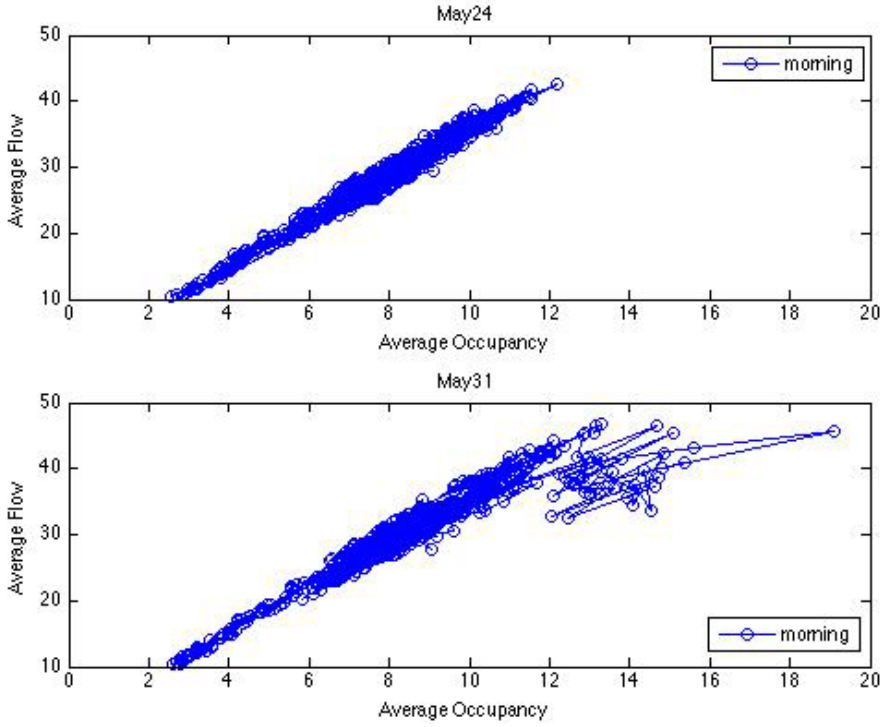

Figure A-25. Macroscopic Fundamental Diagram (MFD) – mornings, May 24 and May 31.

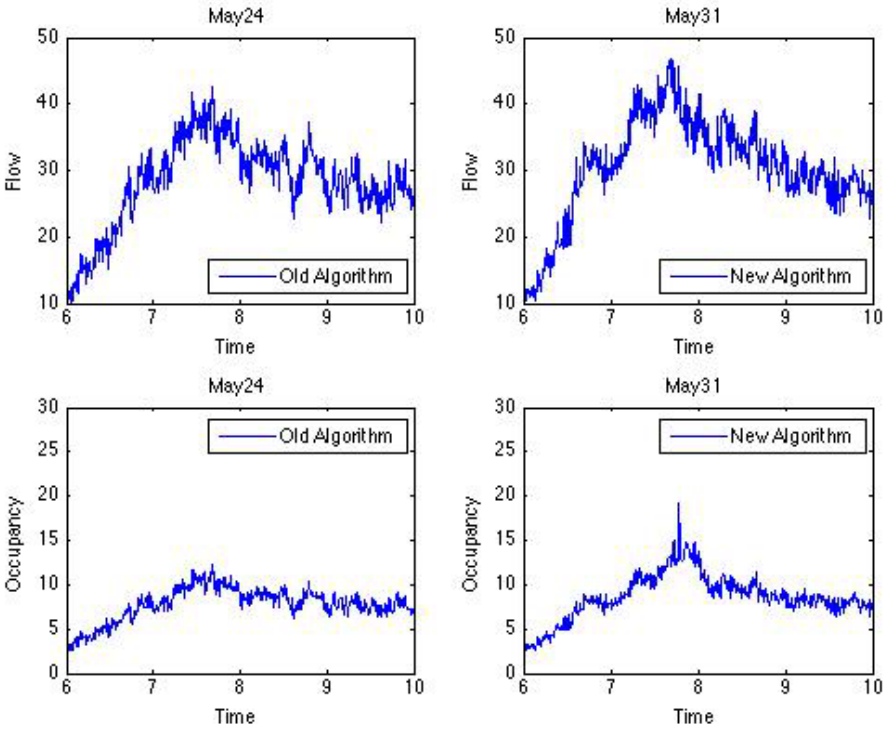

Figure A-26. Average corridor flow and occupancy – mornings, May 24 and May 31.

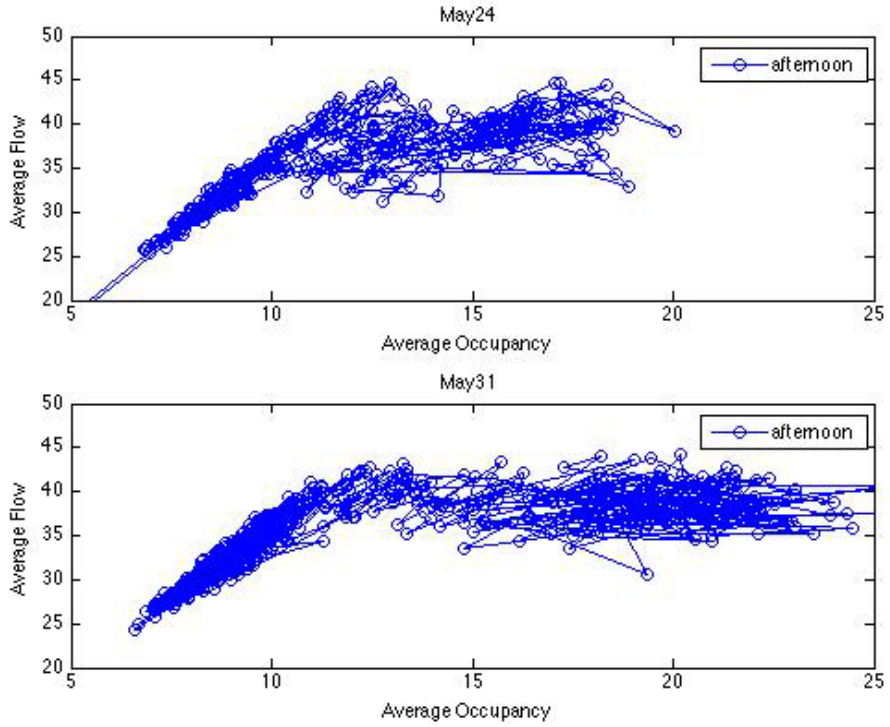

Figure A-27. Macroscopic Fundamental Diagram (MFD) – afternoons, May 24 and May 31.

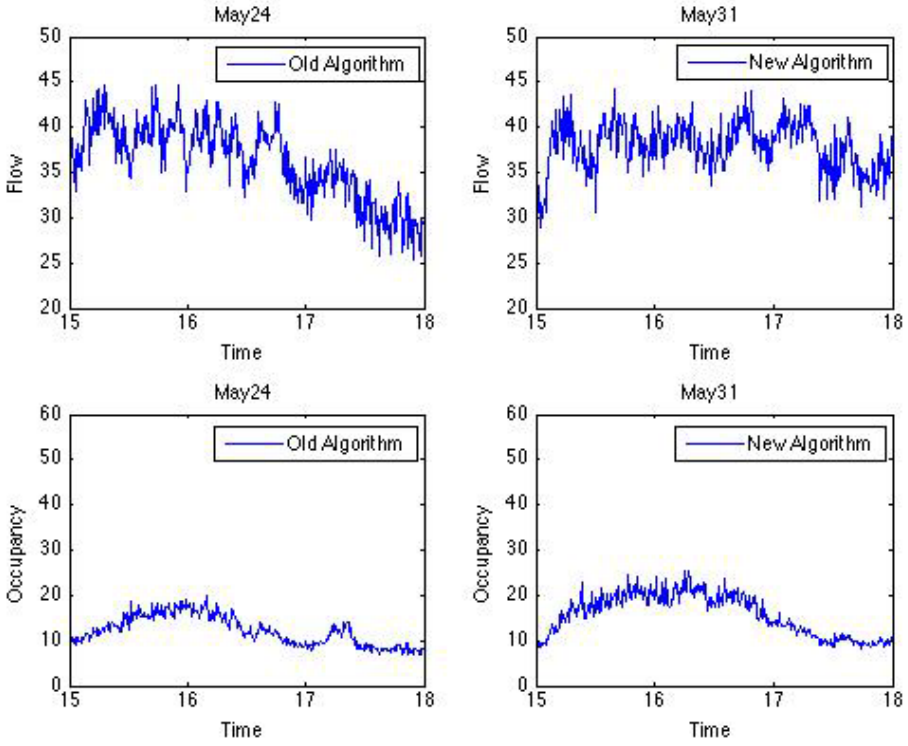

Figure A-28. Average corridor flow and occupancy – afternoons, May 24 and May 31.

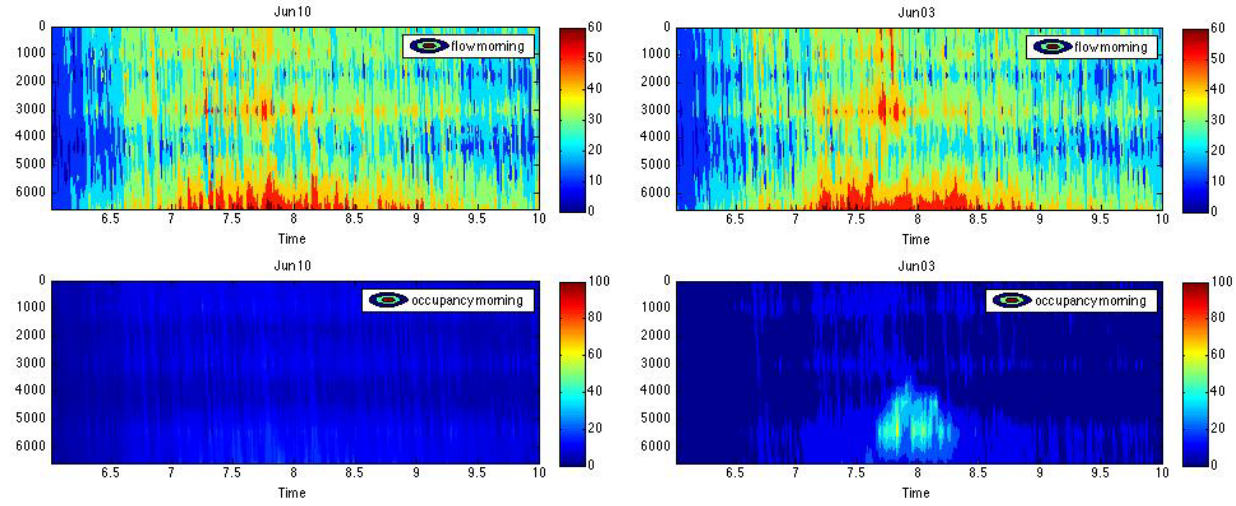

Figure A-29. Flow and occupancy contour plots – mornings, June 3 and June 10.

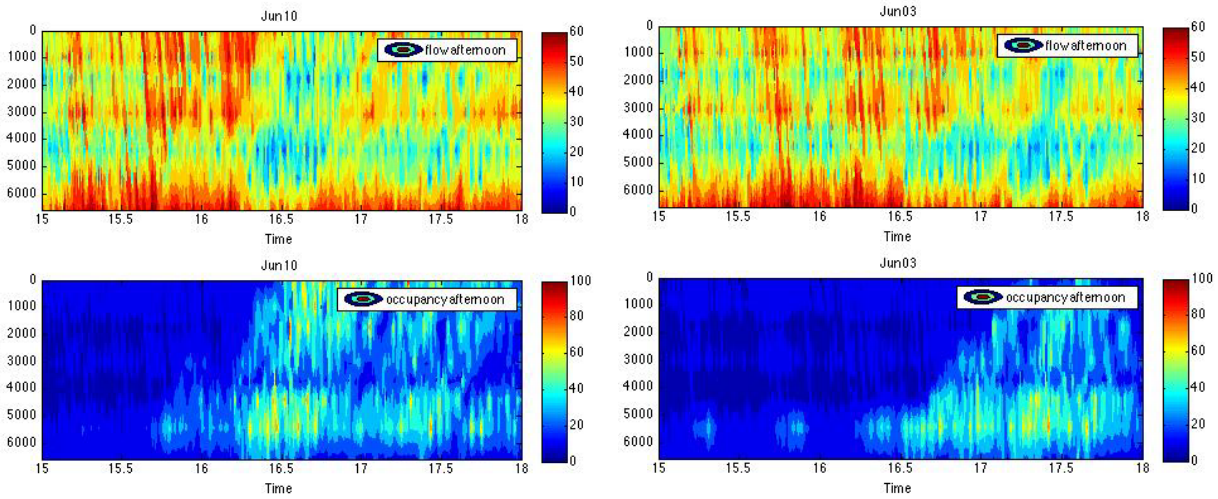

Figure A-30. Flow and occupancy contour plots – afternoons, June 3 and June 10.

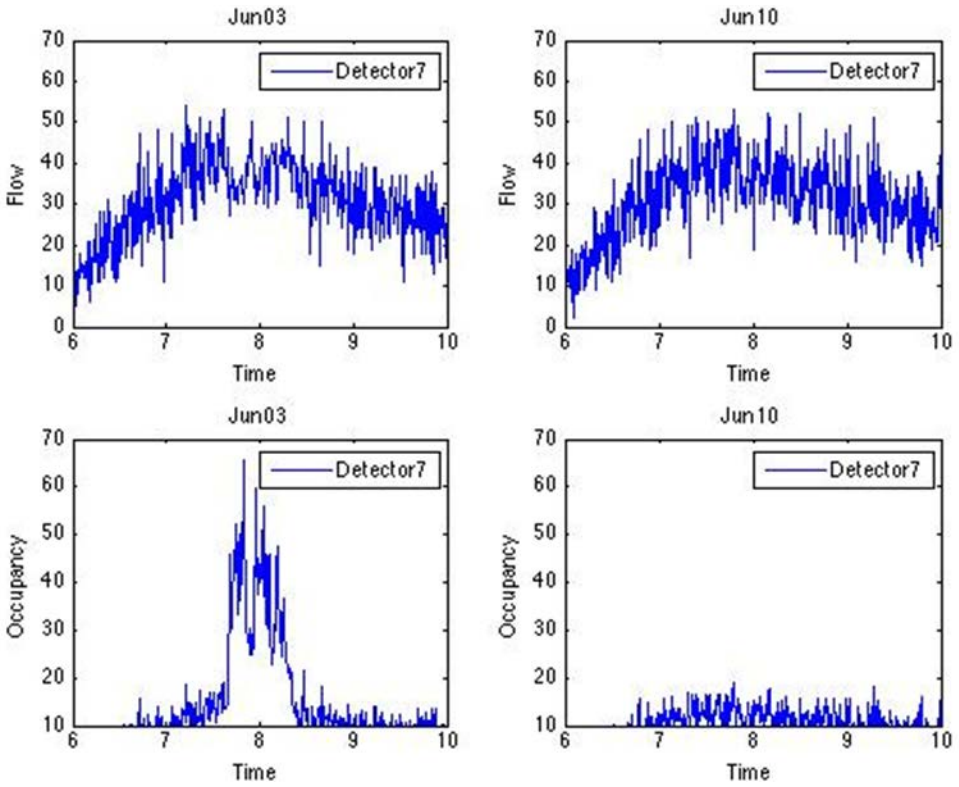

Figure A-31. Mainline flow and occupancy at the active bottleneck – mornings, June 3 and June 10.

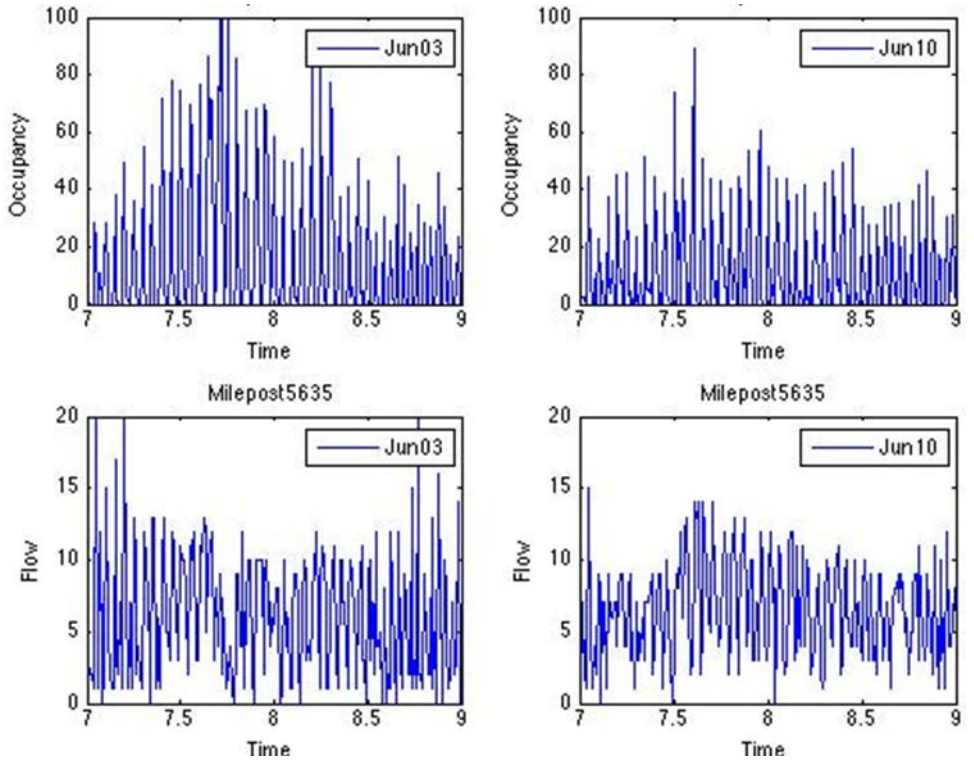

Figure A-32. Flow (passage detector 2022) and occupancy (queue detector 3652) downstream of the active bottleneck – mornings, June 3 and June 10.

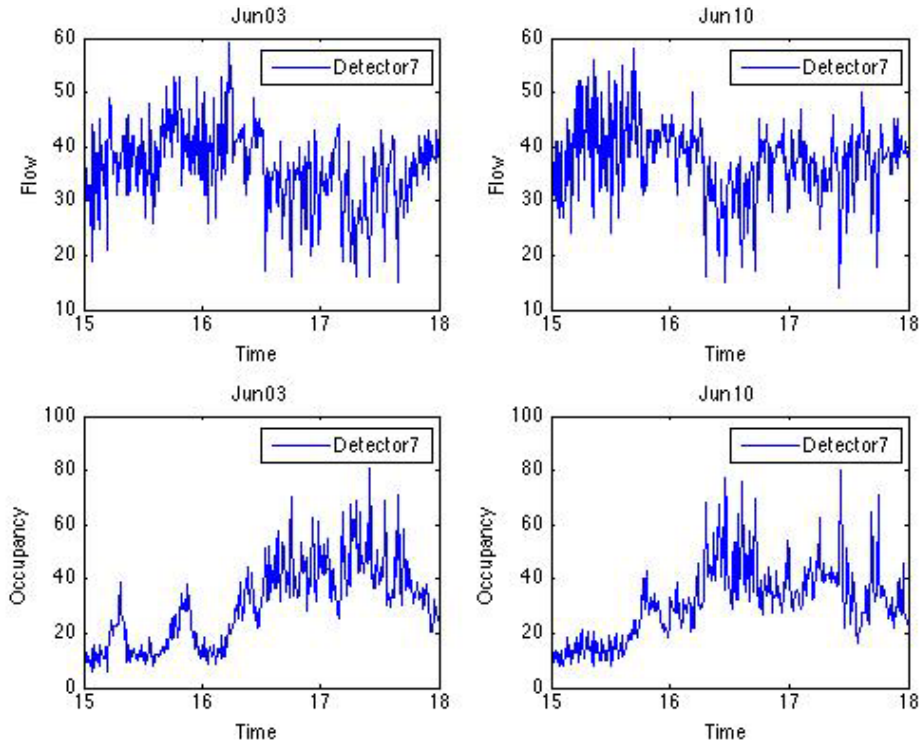

Figure A-33. Mainline flow and occupancy at the active bottleneck – afternoons, June 3 and June 10.

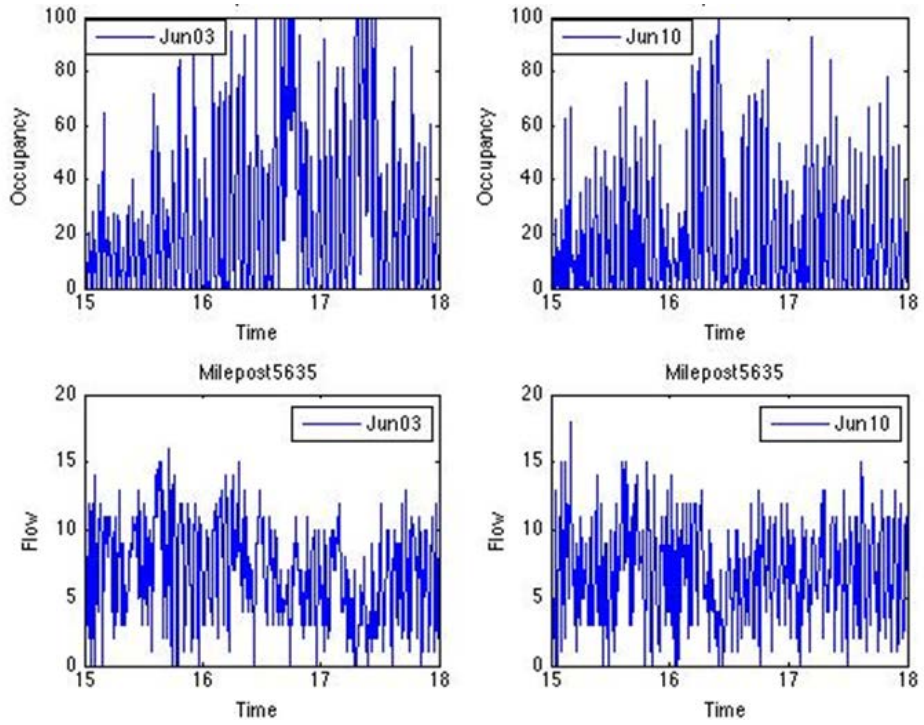

Figure A-34. Flow (passage detector 2022) and occupancy (queue detector 3652) downstream of the active bottleneck – afternoons, June 3 and June 10.

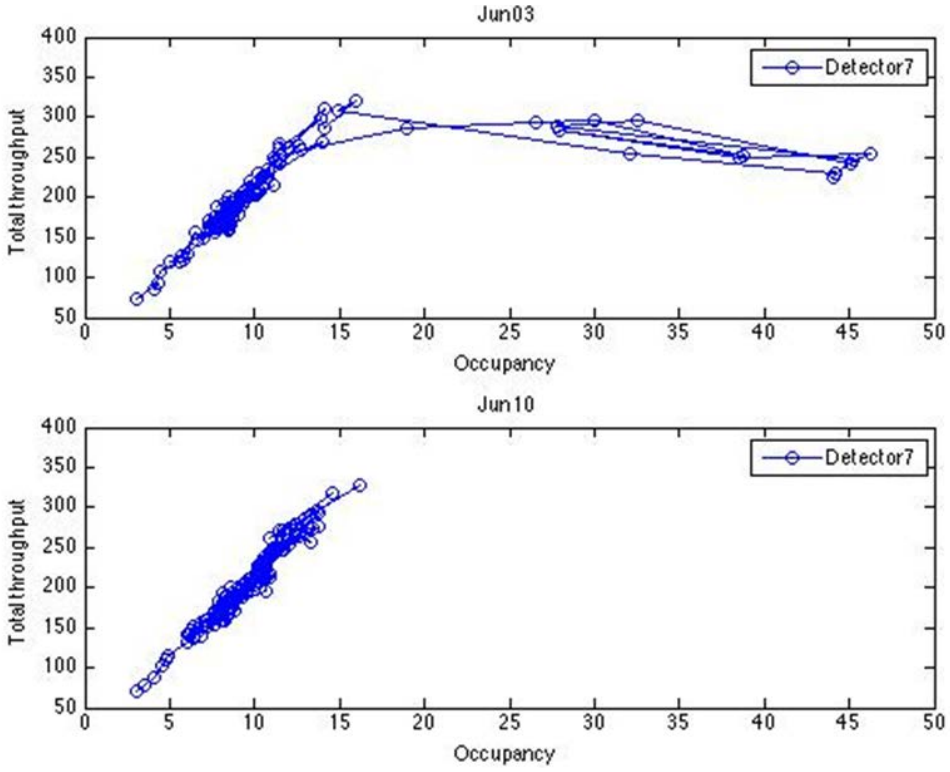

Figure A-35. Total throughput (mainline upstream and ramp) versus occupancy (only mainline upstream) – mornings, June 3 and June 10.

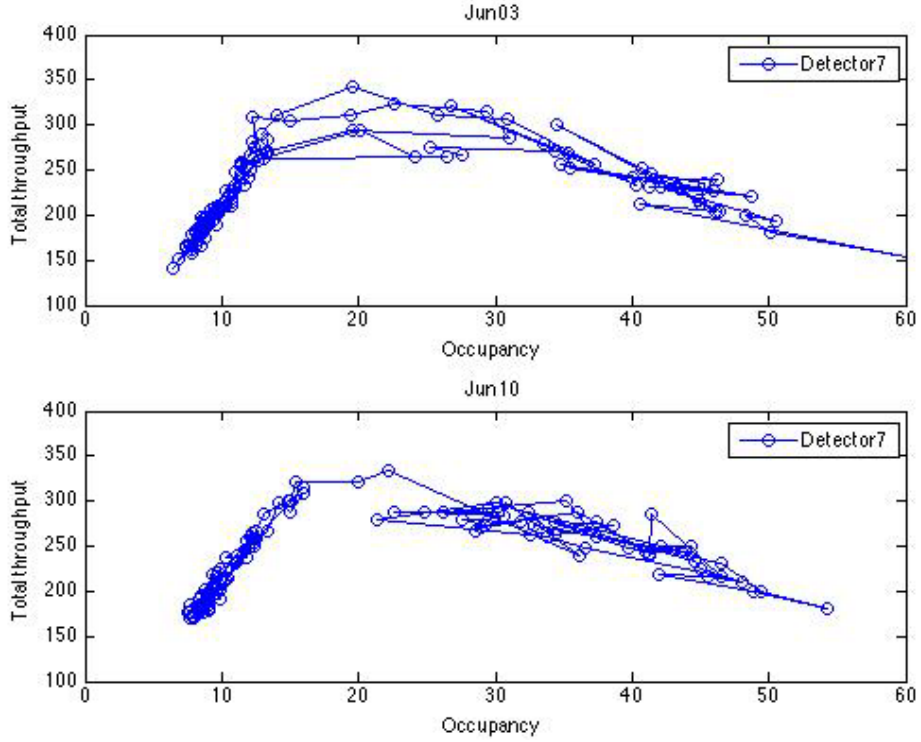

Figure A-36. Total throughput (mainline upstream and ramp) versus occupancy (only mainline upstream) – afternoons, June 3 and June 10.

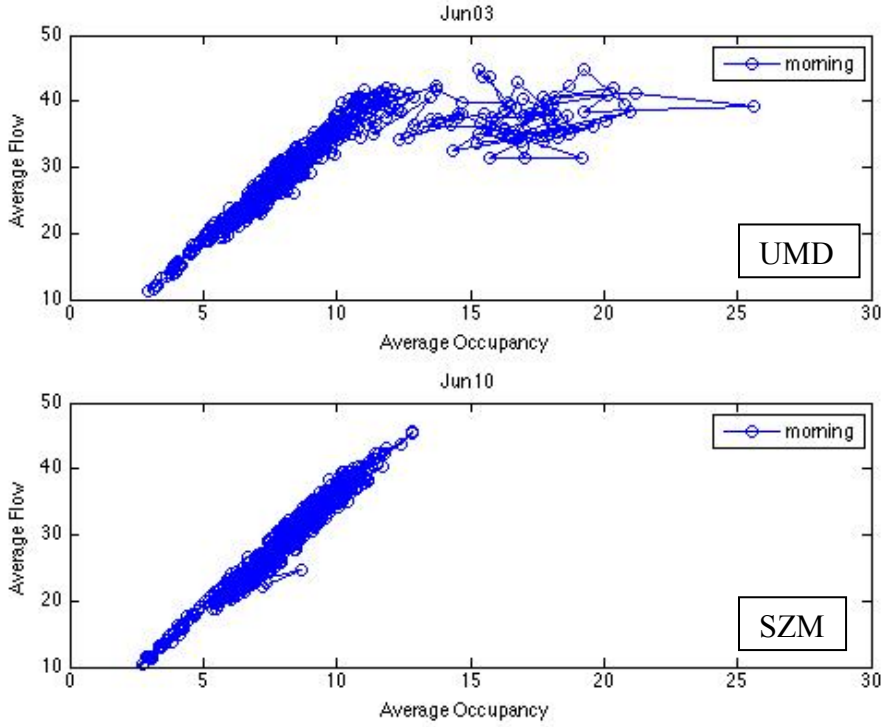

Figure A-37. Macroscopic Fundamental Diagram (MFD) – mornings, June 3 and June 10.

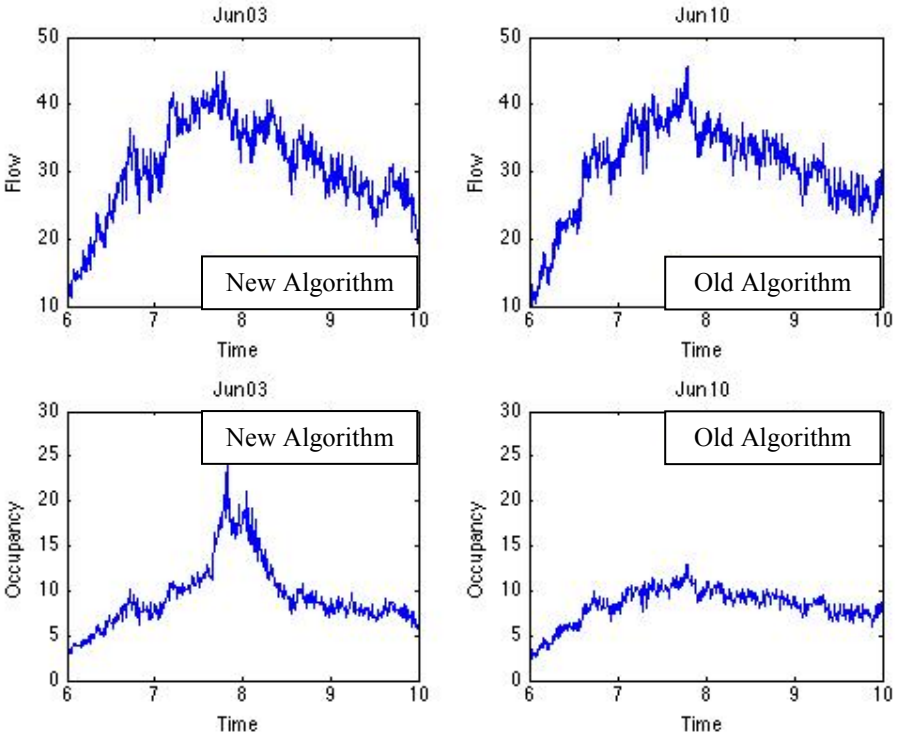

Figure A-38. Average corridor flow and occupancy – mornings, June 3 and June 10.

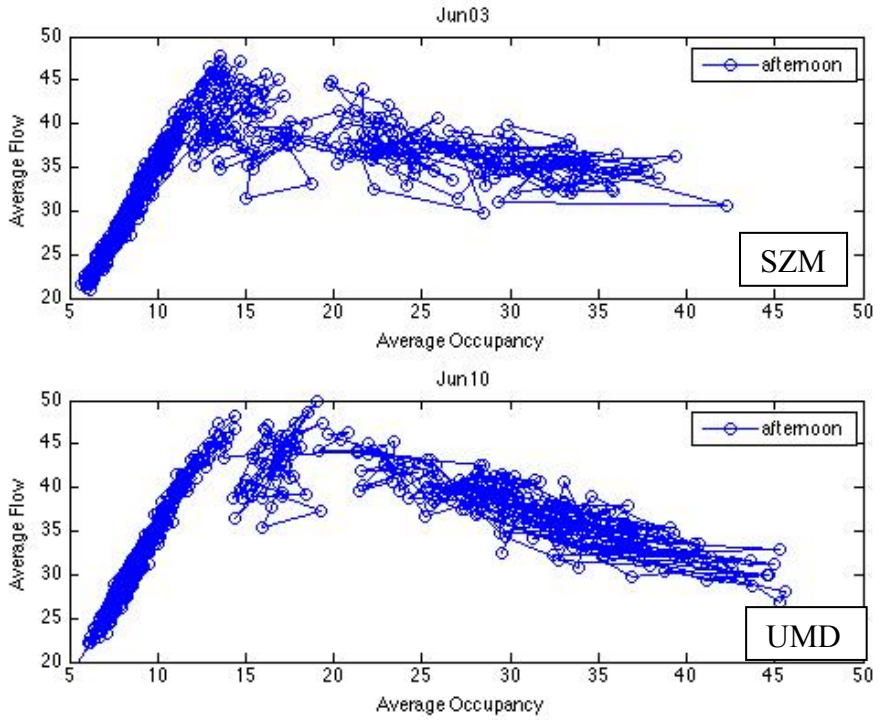

Figure A-39. Macroscopic Fundamental *Diagram* (MFD) – afternoons, June 3 and June 10.

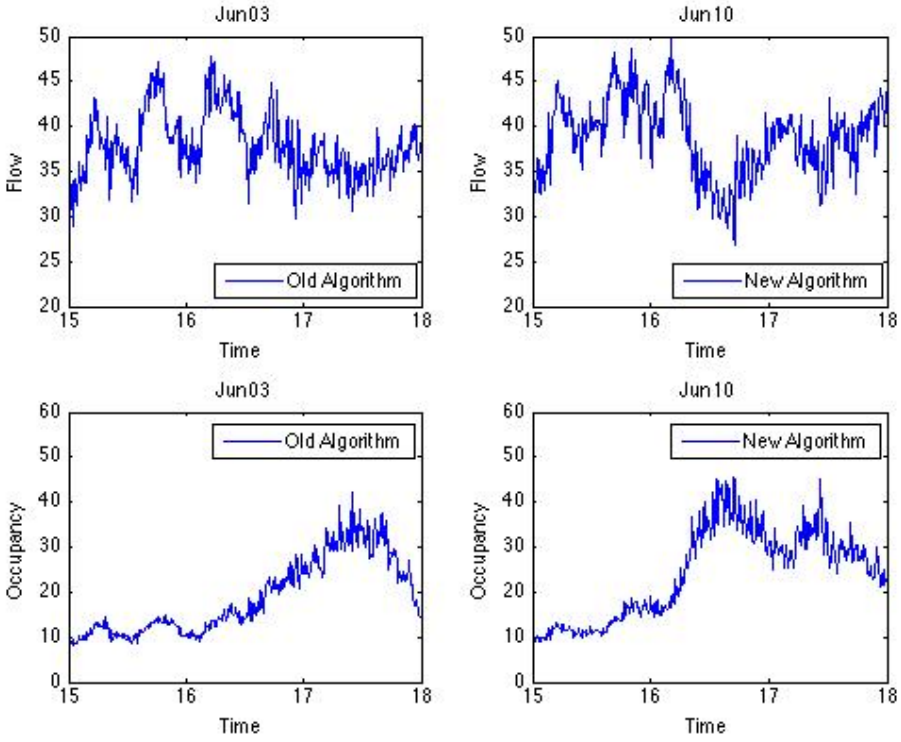

Figure A-40. Average corridor flow and occupancy – afternoons, June 3 and June 10.

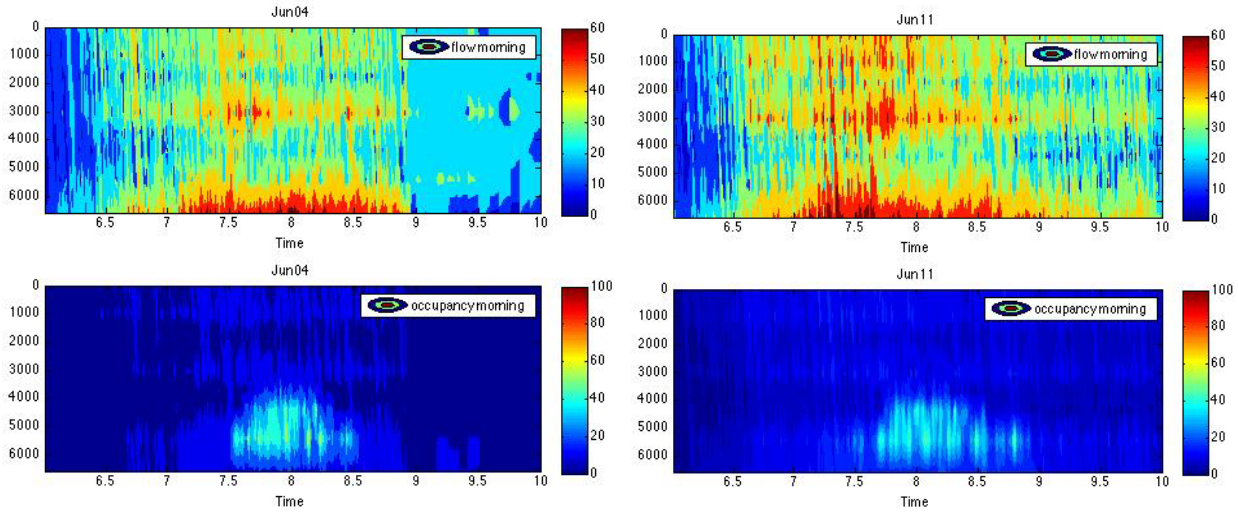

Figure A-41. Flow and occupancy contour plots – mornings, June 4 and June 11.

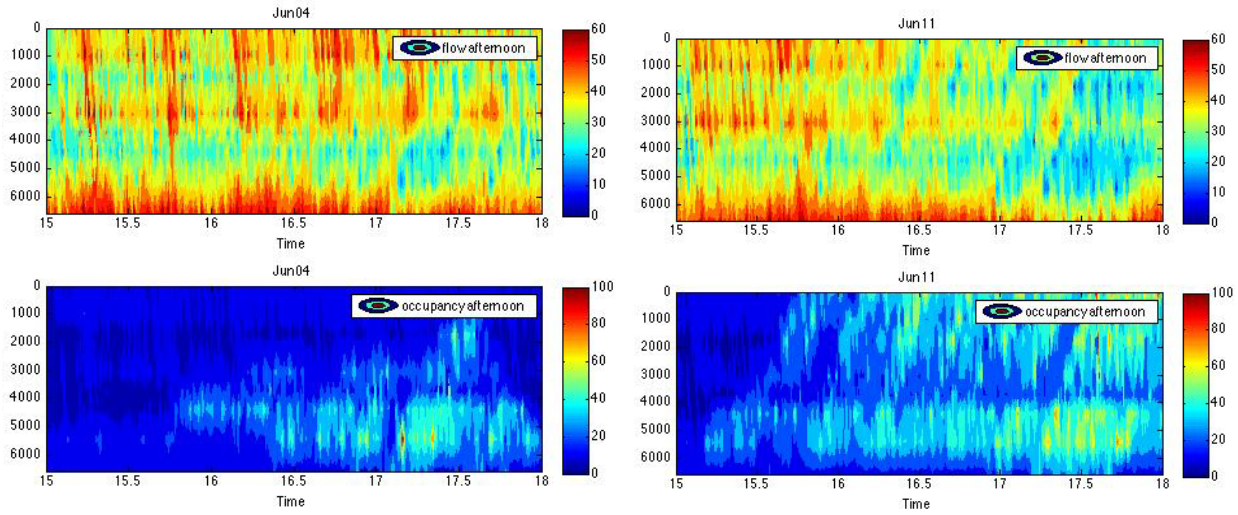

Figure A-42. Flow and occupancy contour plots – afternoons, June 4 and June 11.

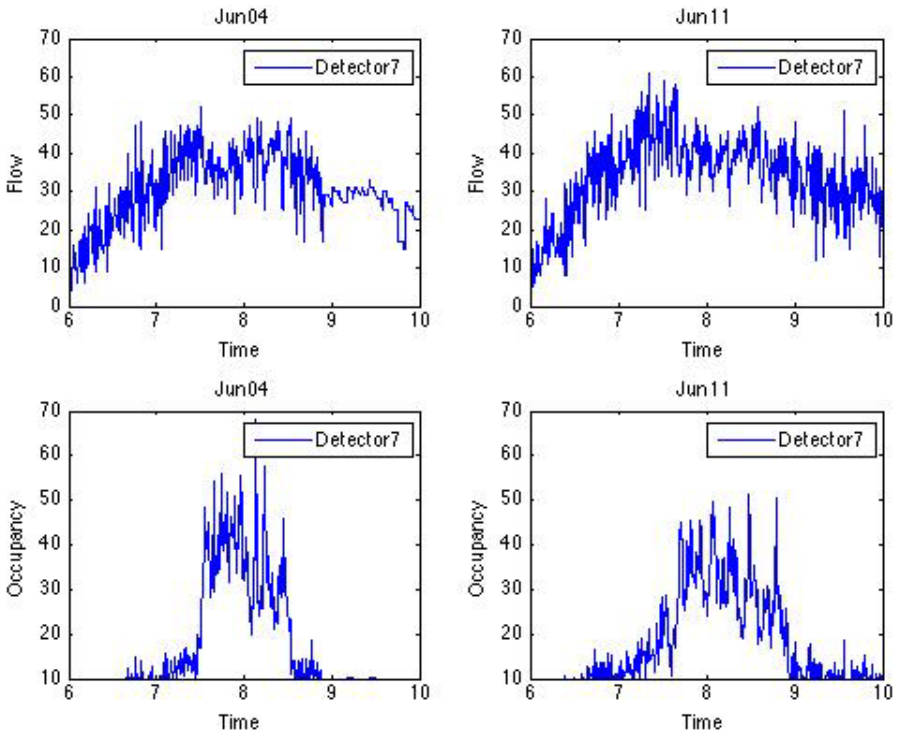

Figure A-43. Mainline flow and occupancy at the active bottleneck – mornings, June 4 and June 11.

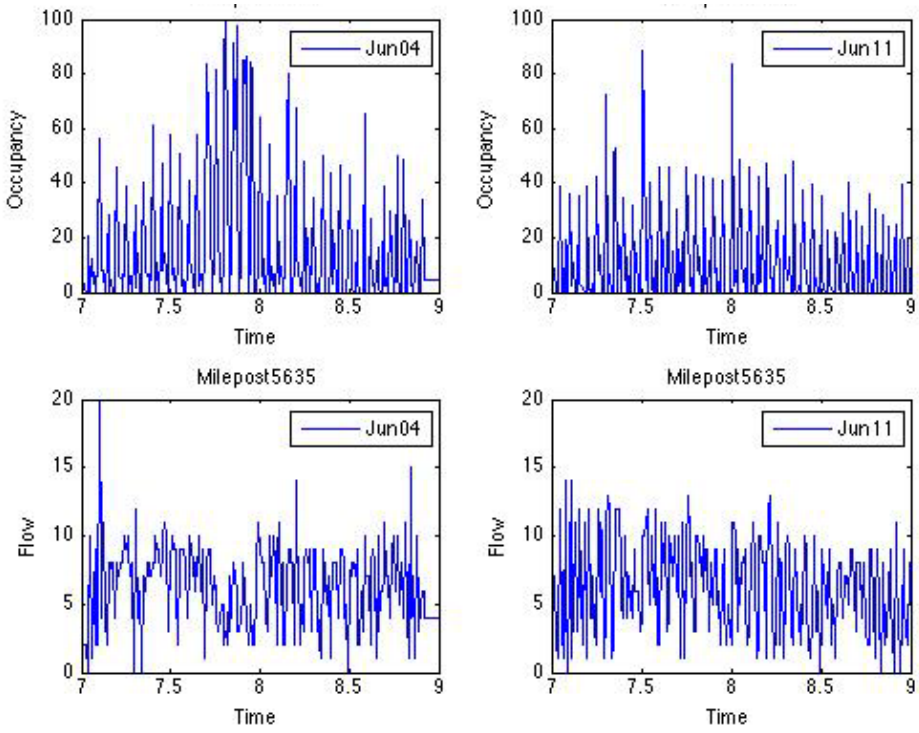

Figure A-44. Flow (passage detector 2022) and occupancy (queue detector 3652) downstream of the active bottleneck – mornings, June 4 and June 11.

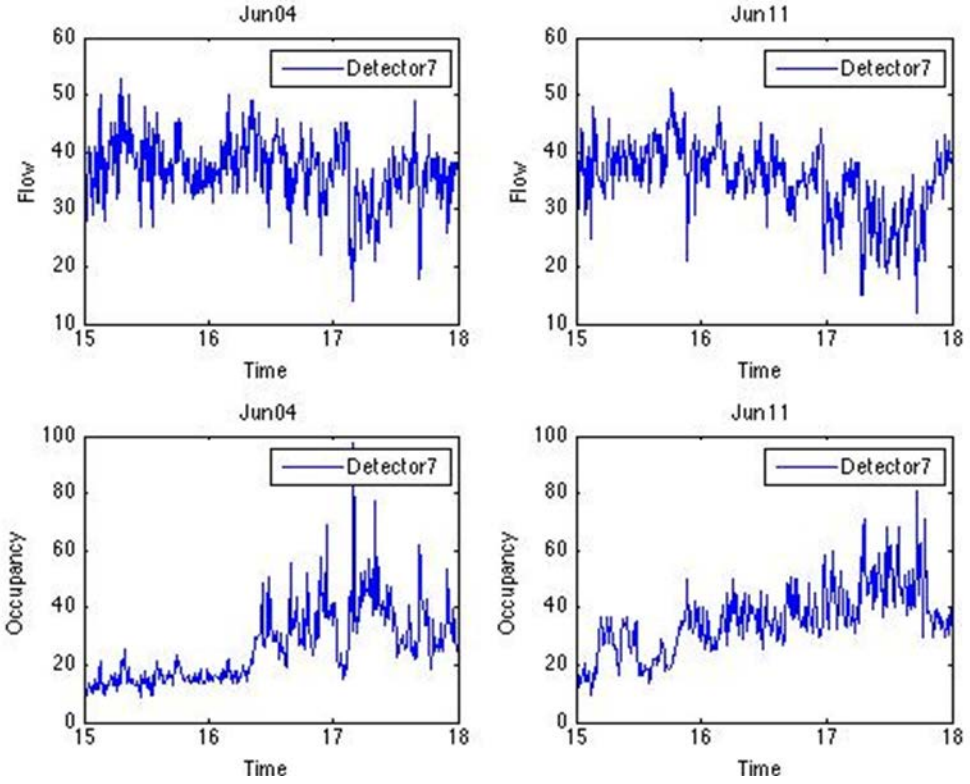

Figure A-45. Mainline flow and occupancy at the active bottleneck – afternoons, June 4 and June 11.

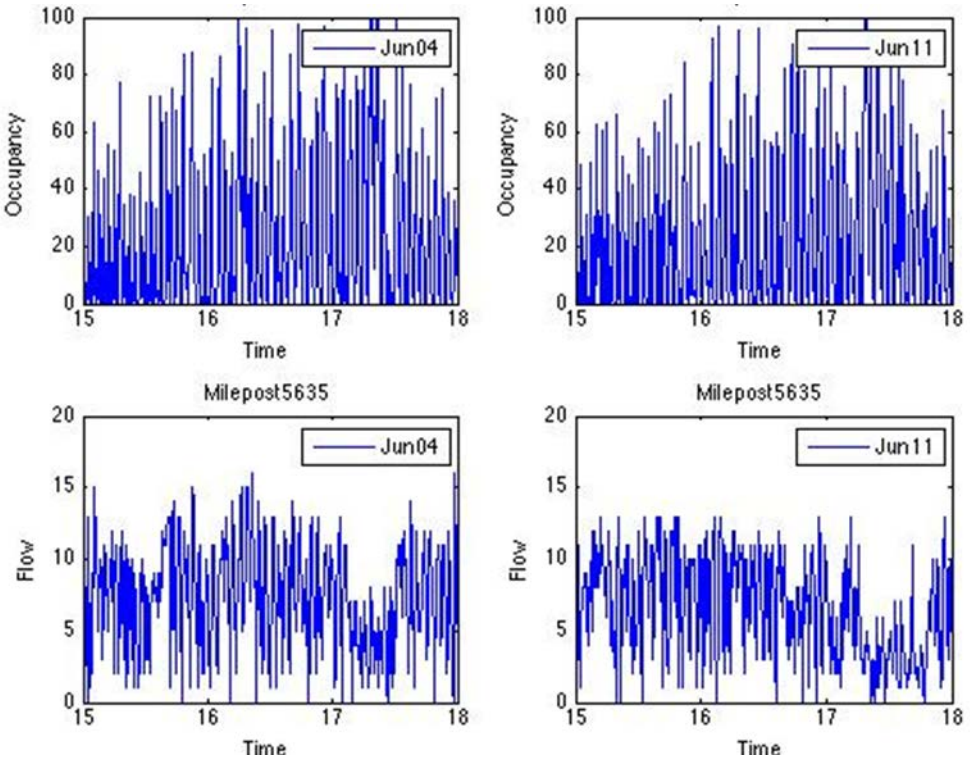

Figure A-46. Flow (passage detector 2022) and occupancy (queue detector 3652) downstream of the active bottleneck – afternoons, June 4 and June 11.

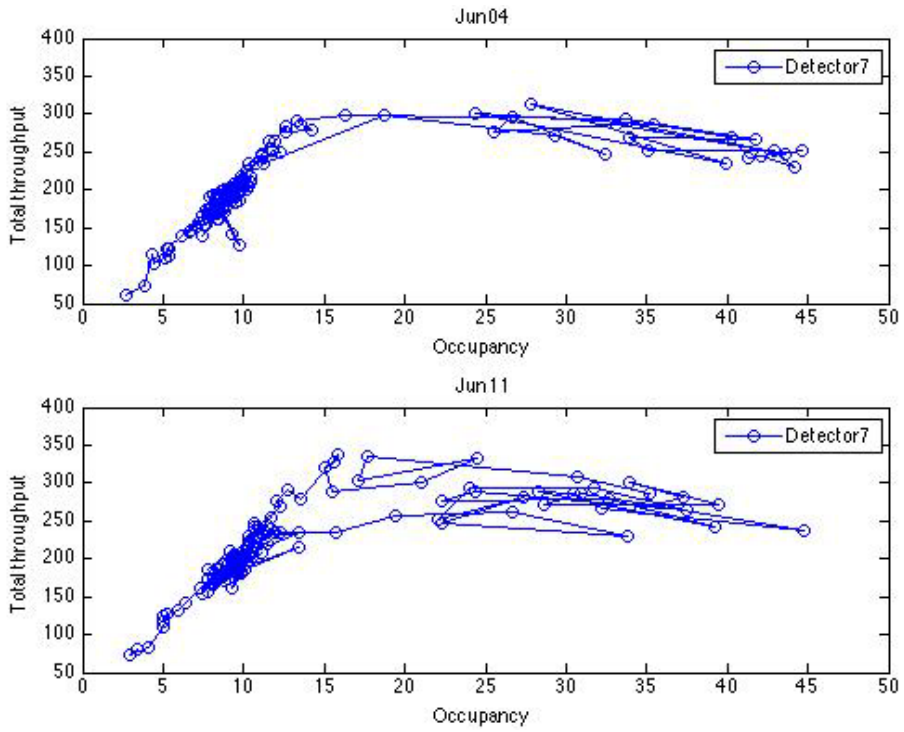

Figure A-47. Total throughput (mainline upstream and ramp) versus occupancy (only mainline upstream) – mornings, June 4 and June 11.

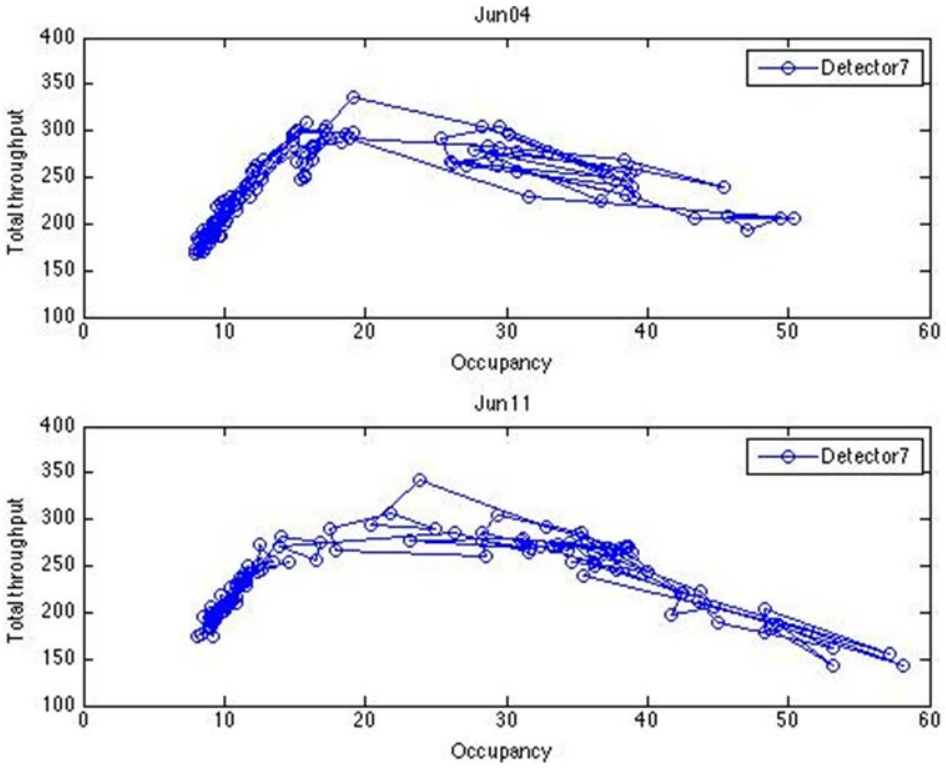

Figure A-48. Total throughput (mainline upstream and ramp) versus occupancy (only mainline upstream) – afternoons, June 4 and June 11.

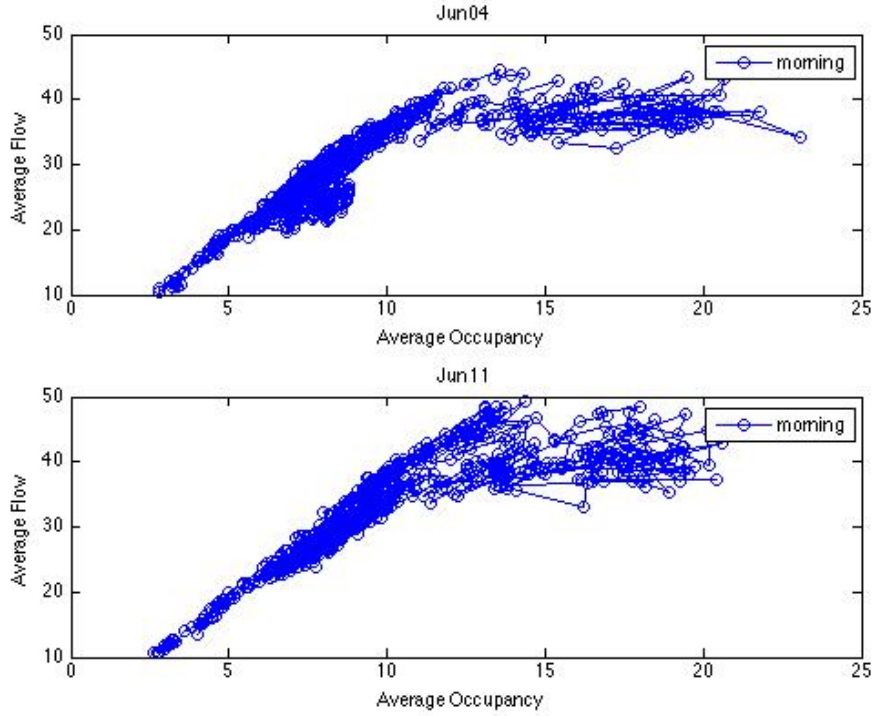

Figure A-49. Macroscopic Fundamental Diagram (MFD) – mornings, June 4 and June 11.

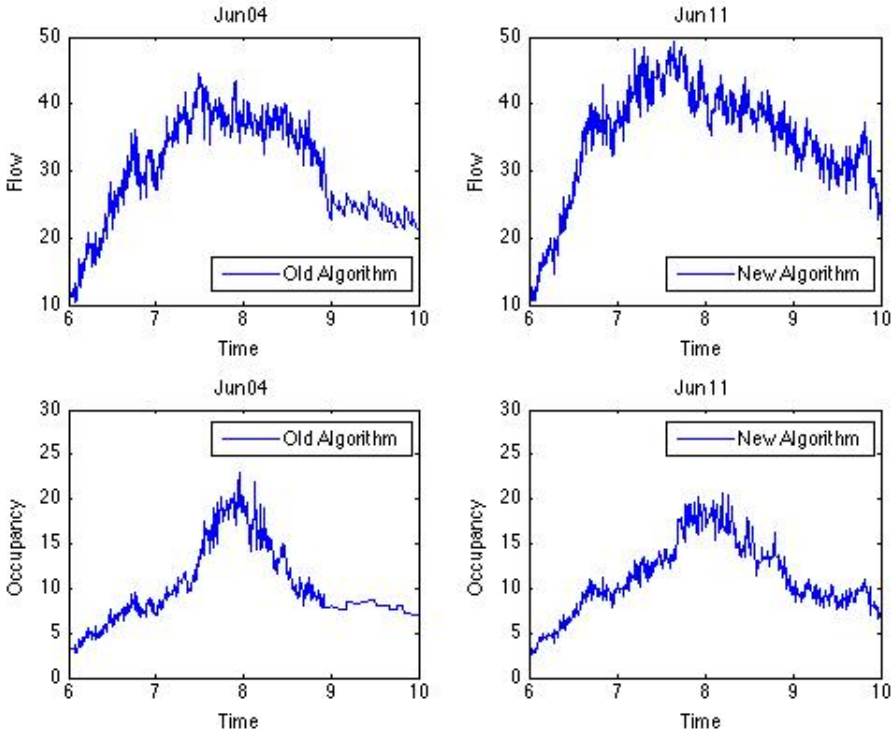

Figure A-50. Average corridor flow and occupancy – mornings, June 4 and June 11.

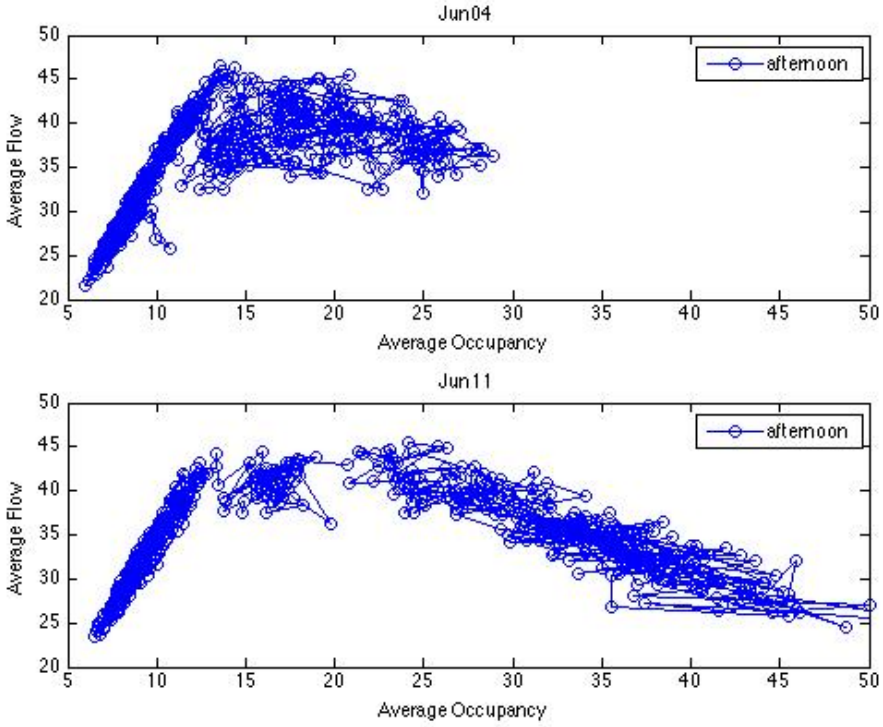

Figure A-51. Macroscopic Fundamental Diagram (MFD) – afternoons, June 4 and June 11.

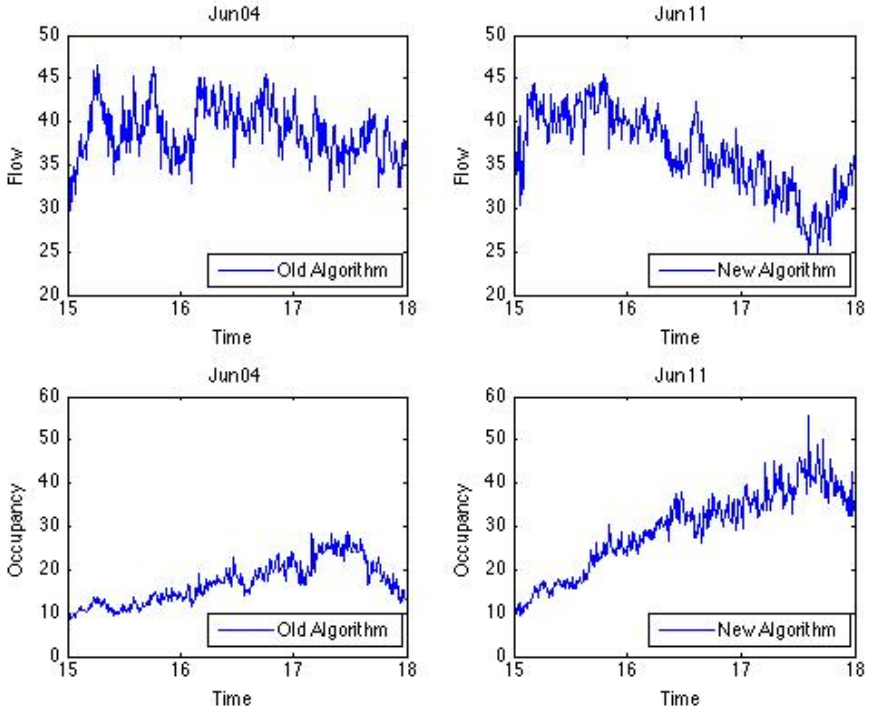

Figure A-52. Average corridor flow and occupancy – afternoons, June 4 and June 11.